

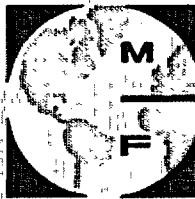
# **VOLUME I - MAIN TEXT, TABLES, AND FIGURES**

## **HYDROGEOLOGICAL AND GEOCHEMICAL SITE CHARACTERIZATION REPORT**

**Prepared For:**

**Sequoyah Fuels Corporation  
I-40 & Highway 10  
Gore, Oklahoma 74435**

**Prepared By:**



**consulting  
scientists and  
engineers**

**3801 Automation Way, Suite 100  
Fort Collins, Colorado 80525**

**October 2002**

## TABLE OF CONTENTS

EXECUTIVE SUMMARY .....	ES-1
1.0 INTRODUCTION .....	1
1.1 Previous Studies and Resources.....	1
1.2 Report Organization and Section Overview .....	4
2.0 FACILITY DESCRIPTION .....	5
2.1 Facility Location and Description.....	5
2.1.1 Main Process Building Area (MPB).....	6
2.1.2 Solvent Extraction (SX) Building.....	7
2.1.3 Initial Lime Neutralization Area.....	7
2.1.4 Solid Waste Burial Area No. 1 (South) .....	8
2.1.5 Emergency Basin .....	8
2.1.6 Sanitary Lagoon.....	9
2.1.7 Pond 1 Spoils Pile.....	9
2.1.8 North Ditch .....	10
2.1.9 Contaminated Equipment Area.....	10
2.1.10 Fluoride Holding Basin No. 1 (South).....	11
2.1.11 Fluoride Holding Basin No. 2 (North).....	11
2.1.12 Fluoride Clarifier and Settling Basins (South).....	12
2.1.13 Fluoride Sludge Burial Area .....	13
2.1.14 South Yellowcake (SYC) Sump .....	13
2.1.15 Clarifier A Basin Area .....	14
2.1.16 Pond 2 .....	15
2.1.17 Area West of Pond No. 2 .....	16
2.1.18 Solid Waste Burial Area No. 2 (North) .....	16
2.1.19 Yellowcake Storage Pad (YSP) .....	17
2.1.20 Fertilizer Pond Area.....	18
2.1.21 Former Raffinate Treatment Area.....	19
2.1.22 Combination Stream .....	19
2.1.23 Present Lime Neutralization Area.....	21
2.1.24 DUF <sub>4</sub> Building Area .....	21
2.1.25 Tank Farm and Cylinder Storage Area .....	22
2.1.26 South Perimeter Area.....	22
2.1.27 Scrap Metal Storage Area .....	23
2.1.28 Drainage/Runoff Areas .....	24
2.2 Operational History.....	24
2.2.1 Fertilizer Program .....	25
2.3 Physical Characteristics of Facility.....	25
2.3.1 Surface Features.....	25
2.3.2 Surface Water Hydrology .....	25
2.3.3 Climatology and Meteorology .....	27
3.0 DECOMMISSIONING PLAN .....	29
4.0 SITE INVESTIGATION .....	31

4.1	Borehole Drilling, Sampling, and Monitoring Well Installation .....	32
4.1.1	Drilling and Construction Methods .....	32
4.1.2	Borehole and Monitoring Well Characteristics and Specifications .....	35
4.2	Hydrologic Testing .....	43
4.3	Resistivity Survey .....	44
4.4	Trenches and Test Pits .....	45
5.0	GEOCHEMICAL TESTING AND ANALYSIS .....	46
5.1	Introduction .....	46
5.2	Methods of Mineralogical Analyses .....	46
5.3	Methods of Chemical Analyses .....	47
5.3.1	Determination of Partition Coefficients ( $K_d$ ) for Uranium and Arsenic .....	47
5.3.2	Laboratory Determination of Partition Coefficients ( $K_d$ ) .....	48
5.3.3	Model Derived $K_d$ Values .....	51
5.3.4	Geochemical Modeling of Groundwater Using PHREEQC .....	52
5.4	Mineralogical Testing Results .....	53
5.5	Test Results and Geochemical Modeling for Partition Coefficients ( $K_d$ and $K_d'$ ) .....	54
5.5.1	Results From Batch Desorption Tests .....	54
5.6	Results of Site Groundwater Geochemical Modeling .....	57
5.7	Distribution of Constituents of Concern .....	59
5.8	Conceptual Geochemical Model .....	61
5.9	Site Complexity and Implications for $K_d$ .....	64
6.0	SITE GEOLOGIC, HYDROGEOLOGIC AND GEOCHEMICAL CONDITIONS .....	67
6.1	Regional Physiographic and Geologic Setting .....	67
6.2	Site Physiography and Geology .....	68
6.2.1	Soils .....	69
6.2.2	Fill Material .....	69
6.2.3	Terrace Deposits .....	70
6.2.4	Alluvium .....	70
6.2.5	Colluvium .....	70
6.2.6	Akota Formation .....	71
6.3	Regional Hydrogeology .....	75
7.0	SITE HYDROGEOLOGIC CONCEPTUAL MODEL .....	75
7.1	Hydrostratigraphic Model .....	76
7.2	Groundwater Occurrence .....	78
7.3	COC Transport .....	80
8.0	HYDROGEOLOGIC NUMERICAL MODEL .....	82
8.1	Groundwater Vistas .....	82
8.2	Groundwater Flow Model .....	82
8.3	Solute Transport Model .....	83
8.4	Groundwater Flow Model Design .....	83
8.4.1	Model Grid .....	84
8.4.2	Boundary Conditions .....	85
8.4.3	Flow Model Parameters .....	89
8.4.4	Flow Model Calibration .....	91
8.4.5	Predictive Scenario .....	93

8.5	Solute Transport Model .....	93
8.5.1	Mathematical Approach.....	94
8.5.2	Transport Model Parameters.....	94
8.5.3	One-Dimensional Transport Analysis.....	95
8.5.4	Transport Model Calibration.....	97
8.5.5	Prediction Simulations.....	101
8.5.6	Transport Model Predictions.....	101
8.5.7	Sensitivity Analysis .....	109
9.0	ANALYSIS AND CONCLUSIONS .....	111
9.1	Appropriate Protective Values.....	111
9.2	Status of Future Protection from Groundwater.....	114
9.2.1	Stream Concentrations and Conditions.....	114
9.2.2	River Loading and Calculated Concentrations .....	116
9.3	Conclusions.....	117
10.0	REFERENCES .....	118

## LIST OF TABLES

Table 2-1	Annual Average Flow
Table 2-2	Stream Flow Calculations
Table 2-3	Location and Description of Seeps and Pools
Table 4-1	Location Summary
Table 4-2	Monitoring Well Survey Information
Table 4-3	Borehole Survey Information
Table 4-4	Borehole Summary
Table 4-5	Monitor Well Completion Data
Table 4-6	Monitor Well Development Data
Table 4-7	Monitor Well Static Water Levels
Table 4-8	Slug Test Results
Table 4-9	Average, Maximum, and Minimum Values of Hydraulic Conductivity
Table 5-1	Core Samples Used in the Mineralogical and Geochemical Testing
Table 5-2	Calculated $K_d$ Values for U and As for all Shale Samples
Table 5-3	Saturation Index Values Calculated Using PHREEQC for Important U, As, and F Solid Phases in Selected Wells
Table 5-4	Important Uranium-Controlling Minerals in Oxidized and Reduced Environments (USEPA, 1999)
Figure 5-5	Partition Coefficient ( $K_d$ ) Values Determined for Arsenic and Uranium in Laboratory Batch Tests
Table 5-6	Analytical Results for the Special Groundwater Sampling of Nine Selected Wells (June 2001) <sup>1</sup>
Table 5-7	Concentrations of Key Analytes Measured from 1991 to 1995



Table 5-8	Percentage Distribution of As(V), F, and U(VI) in the form of Aqueous Species for Selected Wells Calculated Using PHREEQC
Table 5-9	Wells Used for Estimation of Distribution of COCs
Table 5-10	Range of pH Values Recorded from 1991 to 1994
Table 8-1	Model Layer and Corresponding Geologic Layers
Table 8-2	Calibrated Conductive Values
Table 8-3	Computed versus Observed Heads
Table 8-4	Calibrated Uranium $K_d$ Table
Table 8-5a	Summary of Surface Water Modeling Results – Stream Concentrations and Mass Loading
Table 8-5b	Summary of Groundwater Modeling Results – Stream Concentrations and Mass Loading
Table 8-6	Flow Model Sensitivity Parameters
Table 8-7	Transport Model Sensitivity Parameters
Table 9-1	Safe and Toxic Concentrations of Uranium in Water
Table 9-2	Safe and Toxic Concentrations of Nitrate in Water
Table 9-3	Appropriate Protective Standards

## LIST OF FIGURES

Figure 2-1	Location Map
Figure 2-2	Topographic Map
Figure 2-3	Facility Area Designations
Figure 2-4	General Facility Layout
Figure 2-5	Locations of Facility Drainages and Springs
Figure 4-1	SMI Well, Borehole and Geochemical Sampling Locations
Figure 4-2	Slug Test Locations
Figure 5-1	Uranium Concentrations in the $K_d$ Batch Test Solutions
Figure 5-2	Arsenic Concentrations in the $K_d$ Batch Test Solutions
Figure 5-3	X-Ray Diffraction Pattern for Shale 1 (Location 7) Comparing the d(001)-Spacing of Untreated and Ethylene Glycol Solvated Samples
Figure 5-4	Mineral Saturation Indices for the Shale 1 (Location 7) Batch Test Solutions
Figure 5-5	Mineral Saturation Indices for the Shale 2 (Location 8) Batch Test Solutions
Figure 5-6	Mineral Saturation Indices for the Shale 3 (Location 8) Batch Test Solutions
Figure 5-7	Mineral Saturation Indices for the Shale 4 (Location 8) Batch Test Solutions
Figure 5-8	Mineral Saturation Indices for the Shale 3 (Location 9) Batch Test Solutions
Figure 5-9	Mineral Saturation Indices for the Shale 4 (Location 9) Batch Test Solutions
Figure 5-10	Mineral Saturation Indices for the Shale 1 (Location 10) Batch Test Solutions
Figure 5-11	Example of Major Ion Chemistry Changes During the $K_d$ Batch Testing

Figure 5-12 Isopleth of Nitrate Concentrations in Terrace/Shale 1, 2001 Groundwater Sampling

Figure 5-13 Isopleth of Nitrate Concentrations in Shale 2, 2001 Groundwater Sampling

Figure 5-14 Isopleth of Nitrate Concentrations in Shale 3, 2001 Groundwater Sampling

Figure 5-15 Isopleth of Nitrate Concentrations in Shale 4, 2001 Groundwater Sampling

Figure 5-16 Isopleth of Nitrate Concentrations in Shale 5, 2001 Groundwater Sampling

Figure 5-17 Isopleth of Nitrate Concentrations in Alluvium, 2001 Groundwater Sampling

Figure 5-18 Isopleth of Uranium Concentrations in Terrace/Shale 1, 2001 Groundwater Sampling

Figure 5-19 Isopleth of Uranium Concentrations in Shale 2, 2001 Groundwater Sampling

Figure 5-20 Isopleth of Uranium Concentrations in Shale 3, 2001 Groundwater Sampling

Figure 5-21 Isopleth of Uranium Concentrations in Shale 4, 2001 Groundwater Sampling

Figure 5-22 Isopleth of Uranium Concentrations in Shale 5, 2001 Groundwater Sampling

Figure 5-23 Isopleth of Uranium Concentrations in Alluvium, 2001 Groundwater Sampling

Figure 5-24 Isopleth of Arsenic Concentrations in Terrace/Shale 1, 2001 Groundwater Sampling

Figure 5-25 Isopleth of Arsenic Concentrations in Shale 2, 2001 Groundwater Sampling

Figure 5-26 Isopleth of Arsenic Concentrations in Shale 3, 2001 Groundwater Sampling

Figure 5-27 Isopleth of Arsenic Concentrations in Shale 4, 2001 Groundwater Sampling

Figure 5-28 Isopleth of Arsenic Concentrations in Shale 5, 2001 Groundwater Sampling

Figure 5-29 Isopleth of Arsenic Concentrations in Alluvium, 2001 Groundwater Sampling

Figure 5-30 Isopleth of Fluoride Concentrations in Terrace/Shale 1, 2001 Groundwater Sampling

Figure 5-31 Isopleth of Fluoride Concentrations in Shale 2, 2001 Groundwater Sampling

Figure 5-32 Isopleth of Fluoride Concentrations in Shale 3, 2001 Groundwater Sampling

Figure 5-33 Isopleth of Fluoride Concentrations in Shale 4, 2001 Groundwater Sampling

Figure 5-34 Isopleth of Fluoride Concentrations in Shale 5, 2001 Groundwater Sampling

Figure 5-35 Isopleth of Fluoride Concentrations in Alluvium, 2001 Groundwater Sampling

Figure 5-36 Trilinear Diagram for Selected Well Waters

Figure 6-1 Regional Geologic Provinces

Figure 6-2 Regional Geologic Map

Figure 6-2a Explanation of Geologic Map

Figure 6-3 Correlation of Upper Mississippian and Lower Pennsylvanian Formations

Figure 6-4 Locations of Local Faults

Figure 6-5 Site Topographical Surface

Figure 6-6 Regional Hydrological Units

Figure 6-6a Explanation of Regional Hydrological Units

Figure 7-1 Hydrostratigraphic Model Bedrock Geology Map

Figure 7-2 Geologic Cross-Section Locations

Figure 7-3 Layer 1, Hydrostratigraphic Model Cross Section A-A'

Figure 7-4 Layer 2, Hydrostratigraphic Model Cross Section B-B'

Figure 7-5 Layer 3, Hydrostratigraphic Model Cross Section C-C'

Figure 7-6 Layer 4, Hydrostratigraphic Model Cross Section D-D'

Figure 7-7 Layer 5, Hydrostratigraphic Model Cross Section E-E'  
 Figure 7-8 Layer 6, Hydrostratigraphic Model Cross Section F-F'  
 Figure 7-9 Potentiometric Surface Shale 1, June 2001  
 Figure 7-10 Potentiometric Surface Shale 2, June 2001  
 Figure 7-11 Potentiometric Surface Shale 3, June 2001  
 Figure 7-12 Potentiometric Surface Shale 4, June 2001  
 Figure 7-13 Potentiometric Surface Alluvium, June 2001  
 Figure 7-14 Conceptualized Hydrogeology

Figure 8-1 Model Domain  
 Figure 8-2 Model Grid Cross-Section  
 Figure 8-3 Layer 1 Hydrologic Units  
 Figure 8-4 Layer 2 Hydrologic Units  
 Figure 8-5 Layer 3 Hydrologic Units  
 Figure 8-6 Layer 4 Hydrologic Units  
 Figure 8-7 Layer 5 Hydrologic Units  
 Figure 8-8 Layer 6 Hydrologic Units  
 Figure 8-9 Layer 1 Recharge Rates  
 Figure 8-10 Layer 1 Evapotranspiration Rates  
 Figure 8-11 Layer 1 Boundary Conditions  
 Figure 8-12 Layer 2 Boundary Conditions  
 Figure 8-13 Layer 3 Boundary Conditions  
 Figure 8-14 Layer 4 Boundary Conditions  
 Figure 8-15 Layer 5 Boundary Conditions  
 Figure 8-16 Layer 6 Boundary Conditions  
 Figure 8-17 Location of High Conductivity Cells  
 Figure 8-18 Layer 1 Calibrated Heads  
 Figure 8-19 Layer 2 Calibrated Heads  
 Figure 8-20 Layer 3 Calibrated Heads  
 Figure 8-21 Layer 4 Calibrated Heads  
 Figure 8-22 Layer 5 Calibrated Heads  
 Figure 8-23 Layer 6 Calibrated Heads  
 Figure 8-24 Observed vs. Calculated Heads  
 Figure 8-25 Post Decommissioning Topography  
 Figure 8-26 Layer 1 Long-term Heads  
 Figure 8-27 Layer 2 Long-term Heads  
 Figure 8-28 Layer 3 Long-term Heads  
 Figure 8-29 Layer 4 Long-term Heads  
 Figure 8-30 Layer 5 Long-term Heads  
 Figure 8-31 Layer 6 Long-term Heads  
 Figure 8-32 One Dimensional Transport Analysis, Well 2322A  
 Figure 8-33 One Dimensional Transport Analysis, Well 2341  
 Figure 8-34 One Dimensional Transport Analysis, Well 2354  
 Figure 8-35 One Dimensional Transport Analysis, Well 2356  
 Figure 8-36 One Dimensional Transport Analysis, Well MW095A  
 Figure 8-37 Nitrate Calibration Initial Concentrations Layer 1

Figure 8-38	Nitrate Calibration Initial Concentrations Layer 2
Figure 8-39	Nitrate Calibration Initial Concentrations Layer 3
Figure 8-40	Nitrate Calibration Initial Concentrations Layer 4
Figure 8-41	Nitrate Calibration Initial Concentrations Layer 5
Figure 8-42	Uranium Calibration Initial Concentrations Layer 1
Figure 8-43	Uranium Calibration Initial Concentrations Layer 2
Figure 8-44	Uranium Calibration Initial Concentrations Layer 3
Figure 8-45	Uranium Calibration Initial Concentrations Layer 4
Figure 8-46	Uranium Calibration Initial Concentrations Layer 5
Figure 8-47	Arsenic Calibration Initial Concentrations Layer 1
Figure 8-48	Arsenic Calibration Initial Concentrations Layer 2
Figure 8-49	Arsenic Calibration Initial Concentrations Layer 3
Figure 8-50	Arsenic Calibration Initial Concentrations Layer 4
Figure 8-51	Arsenic Calibration Initial Concentrations Layer 5
Figure 8-52	Modeled Nitrate Maximum Initial Concentrations
Figure 8-53	Modeled Nitrate Maximum Concentrations 5 Years
Figure 8-54	Modeled Nitrate Maximum Concentrations 25 Years
Figure 8-55	Modeled Nitrate Maximum Concentration 50 Years
Figure 8-56	Modeled Nitrate Maximum Concentration 100 Years
Figure 8-57	Nitrate Concentrations at Observation Point 1
Figure 8-58	Nitrate Concentrations at Observation Point 2
Figure 8-59	Nitrate Concentrations at Observation Point 3
Figure 8-60	Nitrate Concentrations at Observation Point 4
Figure 8-61	Nitrate Concentrations at Observation Point 5
Figure 8-62	Nitrate Concentrations at Observation Point 6
Figure 8-63	Modeled Arsenic Maximum Initial Concentrations
Figure 8-64	Modeled Arsenic Maximum Concentrations 5 Years
Figure 8-65	Modeled Arsenic Maximum Concentrations 25 Years
Figure 8-66	Modeled Arsenic Maximum Concentrations 50 Years
Figure 8-67	Modeled Arsenic Maximum Concentrations 100 Years
Figure 8-68	Modeled Arsenic Concentration at Observation Point 1
Figure 8-69	Modeled Arsenic Concentration at Observation Point 2
Figure 8-70	Modeled Arsenic Concentration at Observation Point 3
Figure 8-71	Modeled Arsenic Concentration at Observation Point 4
Figure 8-72	Modeled Arsenic Concentration at Observation Point 5
Figure 8-73	Modeled Arsenic Concentration at Observation Point 6
Figure 8-74	Modeled Arsenic Concentration at Observation Point 7
Figure 8-75	Modeled Arsenic Concentration at Observation Point 8
Figure 8-76	Modeled Uranium Maximum Initial Concentrations
Figure 8-77	Modeled Uranium Maximum Concentrations 50 Years
Figure 8-78	Modeled Uranium Maximum Concentrations 100 Years
Figure 8-79	Modeled Uranium Maximum Concentrations 250 Years
Figure 8-80	Modeled Uranium Maximum Concentrations 500 Years
Figure 8-81	Uranium Concentrations at Observation Points 4 and 5
Figure 8-82	Arsenic Concentrations in Streams
Figure 8-83	Nitrate Concentrations in Streams

Figure 8-84	Uranium Concentrations in Streams
Figure 8-85	Nitrate Concentrations in Seeps
Figure 8-86	Modeled Arsenic Concentration at Seeps
Figure 8-87	Uranium Concentrations in Seeps
Figure 8-88	Nitrate Mass Loading to River
Figure 8-89	Arsenic Mass Loading to River
Figure 8-90	Uranium Concentrations at Observation Points 1, 2 and 3
Figure 8-91	Uranium Mass Loading to River
Figure 8-92	Composite Scaled Flow Sensitivity
Figure 8-93	Flow Modeled Scale Sensitivity
Figure 8-94	Composite Scaled Transport Sensitivity

## APPENDICES

Appendix A	Hydrogeological Characterization Work Plan, SOPs and Health and Safety Plan
Appendix B	Supplemental Data Collection Trip Report
Appendix C	Boring Logs and Well Installation Diagrams
Appendix D	Electrical Resistivity Survey
Appendix E	Laboratory Chemical Analysis Report Sheets
Appendix F	Transport Calibration Chemographs
Appendix G	Borehole Data for EVS Model
Appendix H	EVSTRIM.EXE
Appendix I	Vegetation Water Balance Estimates for Sequoyah Site
Appendix J	Hydrologic Test Data
Appendix K	Sufficient Yield Memo

## EXECUTIVE SUMMARY

The Sequoyah Fuels Corporation (SFC) facility (Facility) is a 600-acre parcel of land located in Sequoyah County in mid-eastern Oklahoma. The Facility is bounded on the north by private property, on the east by State Highway 10, on the south by Interstate 40 and on the west by U.S. Government-owned land that is adjacent to the Illinois and Arkansas River tributaries of the Robert S. Kerr Reservoir. The geology at the Facility consists of alluvial and colluvial deposits underlain by an interbedded sequence of well-cemented sandstones, and fissile shales.

SFC conducted uranium conversion operations at the Facility from 1970 to 1993. Operations included conversion of uranium ore concentrates into uranium hexafluoride, and reduction of depleted uranium hexafluoride to depleted uranium tetrafluoride. Additional operations included bulk storage of chemicals, electrolytic production of fluorine from hydrofluoric acid, treatment and storage of liquid waste streams, and a land-treatment program utilizing waste ammonium nitrate solution as fertilizer on SFC property.

In August of 1990, SFC notified the Nuclear Regulatory Commission (NRC) that uranium had been discovered in soils during excavation of underground storage tanks. In late 1990, the NRC issued an Order Modifying License to SFC, which allowed for further investigation and prevention of additional releases of licensed materials. SFC was also charged with the development of a comprehensive Facility Environmental Investigation (FEI) plan. The FEI plan, completed in mid-October 1990, expanded the investigation and monitoring program throughout the Facility area.

In February of 1993, SFC notified the NRC of its intent to discontinue production and submitted to the NRC a preliminary plan for completion of decommissioning the Facility that included the definition of the extent of contamination throughout the Facility and a hydrogeologic transport model to determine future migration of contaminants.

SFC completed a Site Characterization Report to address NRC objectives in December of 1998. In August of 1993, SFC signed a Resource Conservation Recovery Act (RCRA) Section 3008(h) Administrative Order on Consent with the Environmental Protection Agency. As a result, SFC

was required to conduct an RCRA Facility Investigation (RFI) to establish the amount and location of hazardous wastes and constituents at or from the Facility, and to gather information necessary for the Corrective Measures Study. The RFI was completed in 1997.

In February 2001, SFC determined that the hydrogeologic transport model was inadequate, and retained Shepherd Miller, Inc. ([SMI], now MFG, Inc. [MFG]) to re-evaluate the model. The evaluation led to a revised hydrogeologic transport model based on a more robust conceptual model was required to sufficiently predict the long-term migration of constituents of concern (COC). This conclusion was founded on the need to better address the controls of the complex hydrostratigraphy and geochemistry on COC transport.

The objective of the MFG hydrological and geochemical site characterization investigation is to estimate the long-term, post closure chemical conditions of groundwater and surface water surrounding Facility. The investigation consisted of three primary tasks 1) site investigation of geological, hydrological, and geochemical conditions, 2) development of revised conceptual model for the migration of three COCs (uranium, arsenic, and nitrate), and 3) prediction of long-term, post closure COC concentrations in groundwater and surface water with numerical groundwater flow and solute transport models.

The site investigation was developed to more accurately characterize the hydrogeology and geochemistry of individual stratigraphic units underlying the Facility. Specifically, stratigraphic information at various Facility locations was acquired from borehole core logging and bedrock outcroppings. Numerous single well tests were designed to evaluate the hydrogeologic properties of the hydrostratigraphic units. Analyses of groundwater and lithologic samples were performed in order to assess site geochemical conditions in the stratigraphic units. Additionally, specific Facility features were investigated with various methods including electrical resistivity geophysical surveying, trench and test pit excavation, and additional groundwater and lithologic chemical analyses.

The site conceptual model for COC migration was based on data collected from the MFG site investigation, other Facility investigations, and SFC hydrologic and geochemical database. The models have been designed based on the conceptual model framework, and have been calibrated

to observed hydrologic and geochemical conditions. The models simulate 1,000-year predictive scenarios based on steady-state flow conditions and current distributions of COCs dissolved in groundwater. The simulations incorporate post-decommissioning modifications to topography, flow field, and COC source materials to more accurately represent future conditions. Modeling results were evaluated to estimate potential future COC concentrations and mass loading at exposure points, including the 001, 004, 005, and 007 stream drainages, groundwater seeps, and the Robert S. Kerr Reservoir.

The model results indicate that nitrate is the dominant COC at the facility. The nitrate plume appears to be mature and is the result of 20 years of release from activities at the Facility. Nitrate is a conservatively transported COC, i.e., no retardation is applied to solute velocity. Therefore, most of the existing nitrate discharges to the river within 100 years.

Uranium contamination is restricted to the vicinity of the Process Area. Unlike nitrate, uranium transport is retarded by the interaction between the solute and the aquifer matrix. Although significant uranium contamination exists in the terrace materials, uranium has likely reprecipitated as uranium minerals in the unsaturated zone and little additional uranium is assumed to enter the aquifer system. Uranium transport occurs in three primary areas of the Facility. Uranium contamination in the vicinity of the MPB is situated on a local groundwater divide. Migration south follows the gravel/fill area and progresses toward the stormwater pond. This plume disperses to less than 100 mg/L within 500 years. The northern portion of this plume follows the 005 drainage discharges to the river, and is flushed from the Facility within 1,000 years.

The remaining uranium plume emanates from the Solid Waste Burial Areas. This plume is transported down the 007 drainage. This plume is also flushed from the aquifer system within 1,000 years. No modeled discharges to the river from any of the aforementioned plumes exceed the uranium MCL of 30 µg/L after 750 years.

Arsenic is present in the aquifer material in a large portion of the facility. The primary areas of arsenic contamination are Pond 2 and Fluoride Burial Areas. Significant concentration reduction



occurs through dispersion of the plumes. The entire arsenic plume either discharges to the river system or disperses below the 10 µg/L MCL concentration within 200 years.

In order to conduct a screening-level assessment of the potential risk to aquatic biota and to human or other terrestrial receptors, the available Federal and Oklahoma State criteria values for the protection of human health and aquatic life were compiled for nitrate, arsenic, and uranium. If there were not promulgated values, other guidance values and/or values from the scientific literature were compiled and synthesized to derive a protective concentration. The maximum predicted concentrations of nitrate, arsenic, and uranium in the Site streams were compared to these values to determine, on a screening-level basis, if there was any potential risk. Similar comparisons were conducted for loadings of these constituents to the Arkansas and Illinois rivers. In all cases, predicted concentrations of the constituents were below protective criteria for both humans and aquatic life.

## 1.0 INTRODUCTION

### 1.1 Previous Studies and Resources

Sequoyah Fuel Corporation (SFC) conducted uranium conversion operations at its Gore, Oklahoma facility (Facility) from 1970 to 1993. SFC notified the Nuclear Regulatory Commission (NRC) in August of 1990 that uranium had been discovered in soils during excavation of underground storage tanks within the restricted boundary. The NRC initiated an investigation and SFC began an initial characterization of the area surrounding the contaminated soils, retaining Roberts/Schornick and Associates, Inc. (RSA) to assist with the process.

In late 1990, the NRC issued an Order Modifying License (OML) to SFC, which allowed for further investigation and prevention of additional releases of licensed materials from the Main Process Building (MPB) and for the development of a comprehensive Facility Environmental Investigation (FEI) plan. At this point, SFC expanded the characterization investigation to include the MPB and an extensive soil and groundwater monitoring well installation program began (RSA, 1991).

The FEI plan, completed in mid-October 1990, expanded the investigation and monitoring program throughout the SFC Facility area. Implementation of the FEI plan included extensive monitoring of the surface water, groundwater and soils, as well as analysis of possible contamination of underground utility trenches and the Combination Stream Drain (CSD). Only isolated and limited amounts of licensed material were detected throughout the Facility during the investigation. Details of the investigation, its findings, and corrective action taken as a result of the findings are reported in the SFC Facility Environmental Investigation Findings Report (RSA, 1991).

In February of 1993, SFC notified the NRC of its intent to discontinue production and submitted to the NRC a preliminary plan for completion of decommissioning (PPCD) for the Facility. To properly decommission the Facility, SFC determined the extent of contamination throughout the Facility and developed a hydrogeologic transport model to determine future migration of contaminants.

In August of 1993, SFC signed a Resource Conservation Recovery Act (RCRA) Section 3008 (h) Administrative Order on Consent (AOC) with the Environmental Protection Agency (EPA). As a result, SFC was required to conduct an RCRA Facility Investigation (RFI) to establish the amount and location of hazardous wastes and constituents at or from the Facility and to gather information necessary for the Corrective Measures Study (CMS). The RFI, published in 1997, includes detailed information on Facility description and history, local geology and hydrogeology, monitoring activities, extent and concentration of Facility contamination, and the effects of contamination on the surrounding area and its inhabitants (SFC, 1997).

In December of 1998, SFC completed a site Characterization Report (SCR) to address the NRC objectives of:

- Quantifying physical, radiological and non-RCA chemical contamination characteristics and the extent of contaminant distribution
- Quantifying environmental parameters affecting potential human exposure for both existing and possible future contamination
- Supporting evaluation of decommissioning action alternatives and detailed planning of the selected decommissioning and remediation approach

Activities for the SCR were designed to obtain information to characterize the source(s) of contamination, establish the level of contamination in the environment where releases had occurred, and finalize environmental setting characterization to support decommissioning planning.

By February 2001, SFC determined that the site hydrogeologic model was inadequate, and retained Shepherd Miller, Inc. ([SMI], now MFG, Inc. [MFG]) to re-evaluate the conceptual model to assess its deficiencies.

In March 2001, SMI submitted the Database Review and Conceptual Model Revision Report to SFC. In the report, SMI first reviewed the contents of the SFC hydrogeologic and geochemical databases to better understand the hydrogeologic and geochemical transport system at the Facility. Several previous investigations provided a significant amount of hydrogeologic and geochemical data. These investigations included: 1) the SFC Facility Environmental

Investigation Findings Report (RSA, 1991), 2) the SFC Site Characterization Report (SFC, 1998a), and 3) the SFC Final RCRA Facility Investigation (SFC, 1997). Furthermore, groundwater monitoring at the Facility has been ongoing for more than 20 years as part of SFC's Source Materials License. This groundwater monitoring created a large database that SMI used to evaluate the site conceptual model.

Subsequent to the review of the SFC databases, SMI updated the geochemical conceptual model by preparing two-dimensional contour maps of the key constituents (uranium, arsenic, and nitrate) within the key hydrostratigraphic units. As a result of this review, SMI determined that additional site characterization efforts were needed to obtain the data necessary to support groundwater flow and constituent modeling at the Facility, and to refine the geochemical and hydrogeological site conceptual models. These characterization efforts included hydrogeologic, geochemical, and geophysical investigations. The site hydrogeologic investigation was performed to acquire additional data on the extent and depths of the various stratigraphic units, and to acquire data to characterize the hydrologic properties of the various hydrological units. Data collected during the site characterization efforts supplemented data from previous studies to help refine the hydrogeologic physical and conceptual model. The geochemical investigation included the collection of data needed to understand the geochemical processes controlling constituent migration and to determine site-specific distribution coefficients for arsenic and uranium to support geochemical transport modeling. Additional site characterization efforts included a geophysical investigation to determine the existence and location of a suspected paleochannel at the Facility.

This report presents the results of the on-site investigation, the geochemical testing and analysis to date, and the development and results of the hydrogeologic physical and conceptual model. The data and analysis obtained in this study has supported SMI in developing a groundwater flow and transport model, allowing for the delineation of the impact of key constituents on the environment, both in the present and in the future.

## 1.2 Report Organization and Section Overview

This report presents information developed by SFC, including the results of the most recent site characterization, in support of a revised site hydrogeochemical conceptual model. This revised model is the basis for comprehensive site groundwater flow and transport models, which evaluate the potential future concentrations of site-derived constituents at potential exposure points. The results of this predictive modeling provide a technical basis for the groundwater component of the site closure plan.

Section 2.0 presents a summary description of the site Facilities. Operational history and features relevant to the site characterization and modeling effort are presented to set the physical and operations context for the site conceptual model. Section 3.0 presents a summary of the existing site Decommissioning Plan that describes the future site configuration and conditions to set the future physical and operations context for the predictive modeling. Section 4.0 presents a description of the recent site investigation, including descriptions of drilling, well installation and hydrological studies undertaken to more fully characterize the site hydrologic conditions in support of the revised site conceptual model. Section 5.0 presents the geochemical studies undertaken to more fully characterize the site geochemical and constituent transport conditions in support of the site transport model. This section also presents the most current understanding of the distribution of the constituents of concern (COCs) in the groundwater system. Section 6.0 presents the most current understanding of the site geologic and hydrogeologic conditions based on previous studies and the recent site investigation results. Section 7.0 integrates the most current understanding of site conditions into a revised site conceptual model. Section 8.0 presents the design, configuration, calibration and results of the flow and transport models. Section 9.0 summarizes the results of the previous sections, evaluates the modeling results in the context of protective human and ecological standards and provides conclusions regarding the results of the predicted future conditions.

## **2.0 FACILITY DESCRIPTION**

### **2.1 Facility Location and Description**

The SFC facility (Facility) is a 600-acre parcel of land within the SFC Facility containing the Process Area and the Industrial Area. The Facility is located in Sequoyah County in mid-eastern Oklahoma about 150 miles east of Oklahoma City, Oklahoma, 40 miles west of Fort Smith, Arkansas, 25 miles southeast of Muskogee, Oklahoma, and 2.5 miles southeast of Gore, Oklahoma in Section 21 of Township 12 North, Range 21 East. Figure 2-1 shows the location of the Facility. The Facility is bounded on the north by private property, on the east by State Highway 10, on the south by Interstate 40 (I-40) and on the west by U.S. Government-owned land (managed by the U.S. Army Corps of Engineers [COE]) adjacent to the Illinois and Arkansas River tributaries of the Robert S. Kerr Reservoir. Figure 2-2 shows the topography of the Facility and surrounding area.

The Facility lies within the approximately 1,550-acre property owned by SFC. This property extends eastward from Highway 10 north of Interstate 40, and approximately 370 acres south of Interstate 40. Most of the uranium-processing operations were conducted on an 85-acre portion of the Facility that is commonly referred to as the "Process Area." SFC uses an additional 115 acres to manage storm water and store by-product materials. The Process Area and additional management areas are collectively referred to as the "Industrial Area." A location map of Facility designations is included in Figure 2-3. Most of the land outside of the Industrial Area is either used for grazing cattle or forage production, or is forested.

The majority of processing operations were conducted within the Process Area. A general Facility layout is presented in Figure 2-4. The conversion of uranium ore concentrates into uranium hexafluoride ( $UF_6$ ) was conducted in the MPB, the Miscellaneous Digestion Building, and the Solvent Extraction (SX) Building. The reduction of depleted uranium hexafluoride ( $DUF_6$ ) to depleted uranium tetrafluoride ( $DUF_4$ ) was conducted in the  $DUF_4$  building. Feed material for processing was stored on the yellowcake storage pad. Additional facilities at the Facility included bulk storage of chemicals such as ammonia ( $NH_3$ ), hydrofluoric acid (HF), nitric acid ( $HNO_3$ ), and sulfuric acid ( $H_2SO_4$ ), a facility for electrolytic production of fluorine

from HF, treatment systems and storage ponds for liquid waste streams, and a land-treatment program utilizing waste ammonium nitrate solution as fertilizer on SFC property.

The SCR (SFC, 1998a) and FEI (RSA, 1991) provide thorough descriptions of Facility operations, along with the identification of source characteristics associated with various processes. This section summarizes the identification of the sources of potential contamination.

The contamination found at the Facility is a result of uranium processing activities that took place during the operation of the plant (SFC, 1998a). Throughout the operating life of the plant, on-going evaluations of the impact of plant operations, including airborne and liquid discharges, and soil and groundwater sampling, occurred. The FEI (RSA, 1991) was a comprehensive, focused evaluation describing the processing activities and identifying sources of potential contamination.

#### **2.1.1 Main Process Building Area (MPB)**

The MPB is located near the eastern edge of the Process Area. The MPB is the largest building at the Facility and contained the major  $UF_6$  conversion processing operation and fluorine generation facilities, and a chemical process laboratory. Plant operations began in 1970 and ceased in 1992. Numerous leaks and spills occurred throughout the Process Area during operation of the Facility, releasing uranium-bearing materials from process systems or containers (SFC, 1998a). Sources of contamination in the MPB included the gaseous, liquid and solid compounds associated with operation of the Facility. A large amount of  $UF_6$  was released from an overfilled cylinder that ruptured just north of the MPB. The  $UF_4$  ash receivers removed from the MPB were sources of contamination to adjacent areas. Releases of  $UF_4$  ash would have been in a solid powder form.

Soil samples have been collected from locations in and around the MPB with sample depths ranging from the surface to 79 feet. The maximum uranium concentration observed was approximately 7,100 pCi/g (SFC, 1998a), with 92.1 percent of the samples containing less than 110 pCi/g. The soils underlying the MPB area are impacted to depths of 15 feet by uranium, and to a lesser degree, by nitrate and fluoride. The highest concentrations of these contaminants

occur near the western portion of the unit, consistent with known leaks and spills that have occurred in the UF<sub>6</sub> Plant

### **2.1.2 Solvent Extraction (SX) Building**

The Solvent Extraction (SX) Building is located approximately 150 feet west of the MPB. Operations began in 1970 and ceased in 1992. The SX Building operations involved the separation of uranium and impurities such as heavy metals using a hexane solvent and tributylphosphate to float the impurities for easier removal. Numerous leaks and spills occurred during operation of the SX Building, resulting in the release of uranium bearing materials from process systems or containers. During 1990, uranium contaminated water was discovered adjacent to the SX Building in an open excavation. Water samples collected from the excavated area averaged 1.6 g/L uranium, with a maximum concentration of 8.2 g/L (SFC, 1998a). Soil removed from the area had an average uranium concentration of 1,500 pCi/g (SFC, 1998a). A French drain was installed during the excavation of a solvent extraction tank. Contaminated rock from Pond 2 and contaminated limestone were used as backfill in the French drain.

Soil samples have been collected from locations around the SX Building, with sample depths ranging from the surface to 79 feet deep. The maximum uranium concentration observed was approximately 7,500 pCi/g; most samples analyzed contained less than 110 pCi/g. The soils underlying the SX Building are impacted by nitrate, fluoride and uranium, particularly in the northern portion of the unit around the SX Vault, where there are impacts to over 30 feet (SFC, 1998a).

### **2.1.3 Initial Lime Neutralization Area**

The Initial Lime Neutralization Area is located southwest of the Decorative Pond, approximately 150 feet south of the main Facility entrance road. Lime neutralization of scrubber wash water was conducted in this area for a brief time after plant startup until completion of the Fluoride Settling Basins in 1971, when the scrubber wash water was re-routed for neutralization through these settling basins. Hydrogen fluoride scrubber wash water was discharged on top of a large limestone pile. Fluoride and uranium significantly impacted the soils in the Initial Lime



Neutralization Area. In 1992, the majority of the contaminated soil was removed and placed in the Interim Storage Cell, effectively removing the source of contaminants from the area. The maximum uranium concentration observed in soil samples taken from in and around this location was approximately 61 pCi/g.

#### **2.1.4 Solid Waste Burial Area No. 1 (South)**

The Solid Waste Burial Area No. 1 (South) is located within the Process Area north of the Emergency Basin. The burial area operated from September 1970 to January 1981 and was used for disposal of low-level radioactive waste materials such as equipment, drums, and other solids.

Soil samples were collected from locations in and around the Solid Waste Burial Area No. 1 (South) at depths ranging from the surface to 34 feet (SFC, 1998a). The maximum observed uranium concentration of approximately 1,060 pCi/g, with 90.6 percent of samples containing less than 110 pCi/g. Based on plant records, the Solid Waste Burial Area No. 1 (South) contains approximately 43,000 cubic feet of low-level wastes containing about 0.64 Ci (945 kg) of natural uranium (SFC, 1998a). The soil covering the burial area is impacted near the surface by uranium from the materials that were formerly stored on the ground in this area.

#### **2.1.5 Emergency Basin**

The Emergency Basin is located within the Process Area just west of the North Ditch (see Section 2.1.8). The Emergency Basin is unlined and has an estimated capacity of 133,300 cubic feet. The Emergency Basin was constructed in 1969 to provide temporary storage of surface water runoff from controlled areas in the plant. The basin has also been used for the containment of accidental spills, wash-down of surrounding pads, and the contents of sump and pits, including the North Yellowcake Sump and the North Ditch.

Soil samples from around the basin to depths of 4.5 feet contain a maximum uranium concentration of 3,500 pCi/g. Sediment at the bottom of the pond has uranium concentrations between 1,600 and 6,000 pCi/g. Soils underlying the basin are assumed to be impacted from exposure to the sediment in the basin and from liquids seeping down from the basin. Full extent of contamination will not be known until sediments at the bottom of the basin are removed.

### **2.1.6 Sanitary Lagoon**

The Sanitary Lagoon is located in the Process Area west of the MPB and SX Building. It was built in 1971 and was used for microbiological oxidation of wastewater from toilets, lavatories, showers, and laundry facilities. The lagoon water was discharged via the Combination Stream (Section 2.1.22). The lagoon was drained after production ceased and a synthetic liner was installed to eliminate any potential hydraulic head caused by impounded rainwater. The lagoon has a capacity of approximately 129,000 cubic feet. During 1990, uranium contaminated water was discovered adjacent to the SX Building in an open excavation and potentially contributed uranium to the Sanitary Lagoon. The sludges in the Sanitary Lagoon are comprised primarily of solids derived from microbial oxidation of domestic wastewater. Concentrations in these sludges ranged from approximately 2,300 pCi/g to 26,000 pCi/g uranium, 7 to 440 µg/g nitrate and 160 to 5,200 µg/g fluoride.

Soil samples have been collected from several locations around the Sanitary Lagoon with sample depths ranging from the surface to 29 feet. The maximum uranium concentration observed was approximately 6,200 pCi/g, 92 percent of samples collected had uranium concentrations less than 110 pCi/g. The soils underlying the Sanitary Lagoon are impacted from exposure to the sludge and liquid contained in the Sanitary Lagoon. The extent of the impact will be determined once the sludges are removed. Soils surrounding the unit are impacted, primarily by uranium, generally at depths of less than 5 feet.

### **2.1.7 Pond 1 Spoils Pile**

The Pond 1 Spoils Pile is located west of the Emergency Basin and Sanitary Lagoon. This area consists of residual clays removed from the old raffinate Pond 1 during construction of Clarifier A Basin in May 1980. The spoils pile consists of approximately 437,000 cubic feet of residual material from Pond 1 and cover soil. Soil samples were collected from locations in and around the Spoils Pile at depths ranging from the surface to 38 feet. The maximum uranium concentration observed was approximately 15 pCi/g. Fluoride, nitrate, and uranium impact the soils in the area surrounding the Pond 1 Spoils Pile. The impact is generally less than a depth of 5 feet.

### **2.1.8 North Ditch**

The North Ditch is located within the Process Area, immediately east of the Emergency Basin. The North Ditch was constructed in 1972 when an additional berm was added to the north end of the Emergency Basin retaining dike and has an estimated capacity of 12,500 cubic feet. The North Ditch is primarily utilized to contain storm water runoff. Historically storm water runoff was pumped to the Combination Stream, water presently in the North Ditch gravity drains to the Emergency Basin. In 1979, SFC concluded that a drain tile from the new tank farm was a source of uranium in the North Ditch. The drain tile that was suspected of containing uranium was subsequently removed. In February 1982, a pipeline ruptured and resulted in the release of approximately 3,000 gallons of raffinate into the North Ditch. A significant amount of uranyl fluoride washed into the North Ditch following the 1986 UF<sub>6</sub> release (see section 2.2.1). Much of this material remains in the North Ditch and probably contributes to soil and groundwater contamination in the area. During 1992, a leak of dilute HF from the HF Off-gas Scrubber system occurred, draining approximately 300 gallons of fluid to the surrounding area. The fluids and wash water drained to the North Ditch.

Soil samples have been collected from several locations around the North Ditch, with sample depths ranging from the surface to 5 feet. The maximum uranium concentration observed was approximately 510 pCi/g, with 77.4 percent of samples analyzed containing less than 110 pCi/g. The soils underlying the basin are assumed to be impacted from exposure to the sediment and liquid contained in the North Ditch. The extent of the impact will not be known until sediment from the basin bottom has been removed. Soils surrounding the unit are impacted, primarily by uranium, generally at depths of less than 5 feet.

### **2.1.9 Contaminated Equipment Area**

The Contaminated Equipment Area is located to the east of the North Ditch and the Solid Waste Burial Area No. 1 within the Process Area. The Contaminated Equipment Area includes an incinerator and the Solid Waste Management Building. Contaminated scrap materials were previously stored in this unit. The Solid Waste Management Building was constructed in 1989

and is approximately 30 feet by 50 feet. The building provides an enclosed area to sort trash and compact low-level radioactive waste. No sources are currently contained in this area.

Soil samples have been collected in and around this unit at depths ranging from the surface to 40 feet. The maximum uranium concentration observed was approximately 12,200 pCi/g, with 83.2 percent of analyses containing less than 110 pCi/g. The soils in the Contaminated Equipment Area are impacted by uranium and fluoride generally to depths of less than 3 feet. Soils surrounding the unit are impacted, primarily by uranium, generally at depths of less than 5 feet. Significant soil impacts are present southeast of the Solid Waste Management Building (SFC, 1998a).

#### **2.1.10 Fluoride Holding Basin No. 1 (South)**

The Fluoride Sludge Holding Basin No.1 is located south of the Fluoride Settling Basins. The holding basin was constructed in 1981 to hold calcium fluoride ( $\text{CaF}_2$ ) sludge generated from the Lime Neutralization Area. Fluoride Holding Basin No. 1 (South) is constructed of clay and as an estimated capacity of 186,800 cubic feet. The sludges in Fluoride Holding Basin No. 1 (South) are comprised of  $\text{CaF}_2$  solids derived from the neutralization of HF off-gas scrubber water with calcium oxide (lime). The underlying soils are probably impacted from exposure to the sludge and liquid contained in Fluoride Sludge Holding Basin No.1 (South). The extent of the impact will be determined by the sludges have been removed from the basin bottom.

Soil samples have been collected in and around this unit, with sample depths ranging from the surface to 28 feet. The maximum uranium concentration observed was approximately 320 pCi/g, with 78.8 percent of analyses containing less than 35 pCi/g. Fluoride Holding Basin No. 1 (South) contains an estimated 171,400 cubic feet of calcium fluoride sludge with a uranium content of about 0.82 Ci (1,224 kg) of natural uranium. Soils surrounding the basin are slightly impacted by fluoride and uranium in the surface layer.

#### **2.1.11 Fluoride Holding Basin No. 2 (North)**

The Fluoride Sludge Holding Basin No. 2 is located in the northwest corner of the Facility west of Solid Waste Burial Area No. 2 and north of the Pond 1 Spoils Pile. The basin is clay-lined

basin and has an estimated capacity of 201,000 cubic feet. The basin was built in 1985 to store  $\text{CaF}_2$  sludge from the lime neutralization process. The basin was originally hypalon-lined and temporarily used upon completion for storing treated raffinate. The treated raffinate was transferred to the Clarifier Basins and the liner was removed. The basin has since been used for storage of calcium fluoride sludge.

Soil samples have been collected around the basin, with sample depths ranging from the surface to 30 feet. All of the samples analyzed contained less than 110 pCi/g of uranium. Fluoride Holding Basin No. 2 contains an estimated 186,000 cubic feet of calcium fluoride sludge with a uranium content of about 1.02 Ci (1,522 kg) of natural uranium. Soils surrounding the basin are slightly impacted by fluoride and uranium in the surface layer.

#### **2.1.12 Fluoride Clarifier and Settling Basins (South)**

The Fluoride Clarifier and Settling Basins (South) is located south of Clarifier A Basin Area and west/northwest of Fluoride Sludge Burial Area. The unit consists of three separate basins, a fluoride clarifier and two settling basins, which were built in 1971. Estimated capacities are 102,100 cubic feet and 46,800 cubic feet for the fluoride clarifier and each settling basin, respectively. None of these basins have synthetic liners. The settling basins were designed to allow  $\text{CaF}_2$  solids from the lime neutralization process to settle. After the solids settle, the liquid was decanted and flowed to the fluoride clarifier. Liquid from the fluoride clarifier was routed to the Combination Stream (see Section 2.1.22).

Soil samples have been collected from three locations around the Fluoride Clarifier and Settling Basins. Sample depths ranged from the surface to 32 feet deep. The maximum uranium concentration observed was approximately 54 pCi/g. The Fluoride Settling Basins No. 1 and No. 2 and the Fluoride Clarifier contain an estimated 114,300 cubic feet of calcium fluoride sludge with a uranium content of about 0.92 Ci (1365 kg) of natural uranium. Soils surrounding the basin are slightly impacted by fluoride and uranium in the surface layer.

### 2.1.13 Fluoride Sludge Burial Area

The Fluoride Sludge Burial Area is located directly east and south of the Fluoride Settling Basins and, prior to 1981, was used for the burial of  $\text{CaF}_2$  sludge. This area consists of three distinct sections. The northern section measures approximately 100 feet by 200 feet. The second section is located directly south of the East and West Pits and measures approximately 50 feet by 275 feet. The third section is located at the southwest corner of the area and contains  $\text{CaF}_2$  sludge that has not been buried and is currently used for the retention of sludge. None of these areas are lined. Materials other than  $\text{CaF}_2$ , such as  $\text{UF}_4$  ash and drums of hardened yellowcake, are probably buried in these areas. A total of 96,830 cubic feet of fluoride sludge was buried, with a total activity of 1.5 curies of natural uranium.

Soil samples have been collected near or around this unit with sample depths ranging from the surface to 26 feet deep. The maximum uranium concentration observed was approximately 7.7 pCi/g. Based on plant records, the Fluoride Sludge Burial Area contains approximately 96,380 cubic feet of buried  $\text{CaF}_2$  sludge with a uranium content of 1.52 Ci (2,268 kg) of natural uranium, with an additional 57,200 cubic feet of  $\text{CaF}_2$  sludge containing 1.55 Ci (2,300 kg) of natural uranium.

### 2.1.14 South Yellowcake (SYC) Sump

The South Yellowcake (SYC) Sump is located inside the Process Area directly south of the Yellowcake Storage Pad. It was built in 1980 to receive surface water runoff from the Yellowcake Pad. The sediments contained in the SYC Sump are comprised of soils and debris collected from surface water runoff from the Yellowcake Pad.

Soil samples have been collected from locations in and around this unit with sample depths ranging from the surface to 25 feet. The maximum uranium concentration observed was approximately 160 pCi/g, and 95.2 percent of the samples analyzed had less than 110 pCi/g. The soils underlying the sump may be impacted by leakage from the sump, however, the extent of any impacts will not be determined until the sump structure has been removed. The soils surrounding the sump have been impacted by uranium.

### 2.1.15 Clarifier A Basin Area

The Clarifier Basin Area is located directly north of the Fluoride Settling Basins and east of Pond 2. It consists of the Clarifier A Basins, the New Barium Chloride (BaCl) Mixing Area (WPC Building), and the Centrifuge Building. The Clarifier A Basins consist of four clay and hypalon-lined ponds. The basins received raffinate from the solvent extraction process. The raffinate was treated with ammonia and barium chloride to precipitate metals and radionuclides within these ponds. A pipeline then transferred the treated ammonium nitrate solution to the fertilizer ponds. Raffinate sludge accumulated in the bottom of the basins. The raffinate sludge was shipped off-site for additional uranium recovery until 1992. The remainder of the sludge is stored in the clarifier area. The WPC Building is located south of the Clarifier Basins. It was built in 1982 to house a research project that attempted to solidify raffinate sludge in asphalt (WPC Project). The experiment lasted for less than one year and afterwards the building was used for storage until 1992. In 1992, the building was used for mixing and storing BaCl, and was utilized for raffinate treatment until 1995. The Centrifuge Building is located south of the Clarifier basins and was built in 1989. The metal building housed four de-watering tanks that were used in a centrifuge process that attempted to de-water the raffinate sludge by-product prior to disposition. Prior to construction of Clarifier A in 1980, one surface impoundment, Pond 1, existed in this area. As with the Clarifier A Basins, Pond 1 was utilized to treat raffinate from the SX Building. Raffinate was transferred to Pond 1 via a trough. Spills or leaks that occurred from the trough would have flowed toward the 005 Stream pathway. A valve in a raffinate sludge transfer line located on top of the centrifuge building failed and released material outside the building. The ground near the northeast corner of the building was impacted.

Soil samples have been collected from locations in and around this unit with sampling depths ranging from the surface to 44 feet deep. The maximum uranium concentration observed was approximately 210 pCi/g, with 98.1 percent of the samples analyzed containing less than 110 pCi/g. The sludge in Clarifier A Basin currently contains about 37.1 Ci (54,861 kg) of natural uranium. The synthetic liners in the Clarifier Basins have been damaged in the past, impacting the clay liner and possibly some of the underlying soil. Fluoride, nitrate, and uranium impact the soils surrounding the Clarifier basins.

### 2.1.16 Pond 2

Pond 2 is located west of the Clarifier Basins and the Fluoride Settling Basins. The pond was constructed in 1971 and has an estimated total capacity of 2,963,000 cubic feet. Pond 2 contained raffinate and sludge by-products until it was taken out of service in the early 1980s due to historically documented leaks. Also discarded into Pond 2 were contaminated rock, yellowcake drums, soda ash, anode blades, drum liners, electrolyte sludge, and laboratory waste. After 1991 sludge and residual clays from Pond 2 were removed and transferred to the hypalon-lined Pond 4. Pond 2 was then covered with a synthetic liner and the southwest corner of the berm was breached to allow rainfall to drain. This action was intended to help eliminate any potential hydraulic head caused by impounded rainwater.

Leakage from Pond 2 was first noted in an adjacent monitor well in May 1974. Continuous monitoring of Pond 2 subsequently began, which included installation of additional monitoring wells, implementing revised sampling techniques and conducting geophysical surveys. In March 1984, Facility personnel discovered the presence of nitrates in concentrations up to 1,000 mg/L in seeps approximately 500 feet south of Pond 2. Based on the location of the seeps and the magnitude of nitrate contamination in the area, two collection trenches and flow barrier slurry walls were constructed to intercept contaminated groundwater. All recovered groundwater was pumped back into Pond 2. In 1985, a french drain system was installed on the southern end of Pond 2. This system was designed with an automatic pumping system to keep the area dewatered. The French drain system was constructed with a gravel-filled trench connected to a buried concrete tank installed approximately 4 feet below ground level. Groundwater collected from the trench gravity flowed into the tank and was subsequently pumped back to Pond 2. Pumping was discontinued prior to 1990 after the area failed to yield enough water to pump. In 1991, liquids in the pond were removed and the pond sludges were removed to levels that exhibited uranium levels less than 2,000 pCi/g. Intermittent pumping was resumed during 1995 and automated pumping began in 1997. A high-density polyethylene (HDPE) liner was then placed over the remaining sludges. In addition, a portion of the west pond embankment was breached to facilitate gravity drainage of rainwater.



Soil samples have been collected from locations in and around Pond 2, with sample depths ranging from the surface to 40 feet. The maximum uranium concentration observed was approximately 49 pCi/g. The impacted clay liner and residual sludge in the bottom and sides of Pond 2 is estimated to be 749,000 cubic feet, which contains approximately 10.8 Ci (16,074 kg) of natural uranium. The soils surrounding the basin do not appear to be impacted by uranium, but have probably been impacted by nitrate.

#### **2.1.17 Area West of Pond No. 2**

A natural drainage ditch was previously located west of Pond 2 outside of the restricted area boundary. This drainage was designated as permitted 004 Outfall and was used for storm water drainage that discharged from the Facility via a concrete culvert. The drainage area was backfilled during the storm water collection trench project in 1989 and a French drain type recovery system was simultaneously installed within the natural drainage area. The French drain consisted of a gravel-filled east to west trench connected to a concrete tank buried approximately 30 feet below the present ground elevation. An automatic pumping system was installed in the tank and pumping from the recovery system, Ditch West of Pond 2 (DWP2), began that same year. Water recovered from the collection system typically averages less than 3.4 pCi/L of uranium and 250 mg/L of nitrate.

Soil samples have been collected from locations in and around the area west of Pond 2 with sample depths ranging from the surface to 46 feet. The maximum uranium concentration observed was approximately 3.9 pCi/g. A gamma scan was performed west of Pond 2 in 1996. The soils in the area west of Pond 2 are not impacted based on the sampling conducted to date.

#### **2.1.18 Solid Waste Burial Area No. 2 (North)**

The Solid Waste Burial Area No. 2 (North) is a fenced area approximately 250 by 300 feet in size located north of Solid Waste Burial Area No. 1 and east of Fluoride Holding Basin No. 2. The Burial Area operated for a brief time between late 1979 and early 1980. Only a small area (75 feet by 75 feet) in the southeast corner of the entire fenced area is believed to contain buried material. An incident occurred during February 1984 where approximately 15,000 gallons of

surface water from the excavated portion of the Burial Area was released to the northwest. An estimate was made that between 8 and 10 pounds of uranium were released during this event. Equipment stored in this unit has also contributed to contamination of surface soils.

Soil samples have been collected from locations in and around the Burial Area unit, with sample depths ranging from the surface to 40 feet. The maximum uranium concentration observed was approximately 5,060 pCi/g. About 89 percent of the uranium analyses were less than 110 pCi/g. Based on plant records, Solid Waste Burial Area No. 2 (North) contains approximately 8,100 cubic feet of low-level wastes with a natural uranium content of about 0.04 Ci (60 kg). The soil near the surface was impacted by uranium from the materials that were formerly stored on the ground in this area. This soil was removed and placed in the Interim Storage Cell. Clean soil was spread over the burial area to limit impacts to storm water runoff.

#### **2.1.19 Yellowcake Storage Pad (YSP)**

The Yellowcake Storage Pad (YSP) lies within the Process Area north of the Decorative Pond and west of the MPB. The YSP has existed since plant start-up in 1970 and was primarily used for storage of uranium yellowcake contained in 55-gallon drums. A portion of the YSP is presently used for storage of contaminated equipment.

Located just north of the YSP is the ADU/Miscellaneous Digestion Building. The ADU/Miscellaneous Digestion Building was built in 1977 to handle uranium slurry. Modifications to the building in 1978 and 1983 allowed room for drum handling equipment along with the uranium slurry unloading station and the miscellaneous digestion equipment. Acidic or corrosive liquids used in the process deteriorated concrete floors in the ADU/Miscellaneous Digestion Building and provided pathways for process materials to enter the soils beneath the floor of this building.

The North Yellowcake (NYC) Sump is located immediately east of the ADU/Miscellaneous Digestion Building. The sump is constructed of concrete and measures approximately 28 feet square by 5 feet deep. It receives surface water runoff from the YSP. The sludges in the NYC Sump were deposited in the basin during storm water runoff from the YSP.

Soil samples have been collected from locations in and around the YSP, with sample depths ranging from the surface to 44 feet. The maximum uranium concentration observed was approximately 1,070 pCi/g. 94.9 percent of samples analyzed, however, had uranium concentrations less than 110 pCi/g. The YSP Area is currently being used as an interim storage location for an estimate 100,000 cubic feet of miscellaneous scrap metal and failed equipment containing an estimated 0.15 Ci (220 kg) of natural uranium. The NYC Sump has historically contained uranium-impacted sediments. The soils under the YSP are impacted by uranium since drummed yellowcake was stored directly on the ground for some period of time. Samples collected to date indicate some impacts are present. Additionally, the soils under the ADU/Miscellaneous Digest Building and the North Yellowcake Sump are expected to be impacted by leakage from these and adjacent facilities such as SX Building and the MPB.

#### **2.1.20 Fertilizer Pond Area**

The Fertilizer Pond Area is located several hundred yards south of the MPB, and consists of five ponds each with a capacity of approximately two million cubic feet. All the ponds are clay and hypalon-lined with leak detection underdrains under the hypalon liner, and were constructed between 1978 and 1985. Four ponds (Ponds 3E, 3W, 5 and 6) were used to store ammonium nitrate fertilizer that was transferred from the Clarifier basins. Pond 4 was utilized for storage of raffinate sludge from Pond 2. The fertilizer loadout area is also located within this unit. Pond 3E was the first in the series of ponds to receive treated liquid from the clarification process. Sediment that collected on the bottom contained residual amounts of uranium. Pond 3E was posted as a radioactive materials area until the sediment was removed and placed into Pond 4. Pond 4 was also posted as a radioactive materials area. Currently Ponds 3W, 4 and 6 are empty. Storm water that accumulates in these ponds is transferred to Pond 3E where the water is sampled and eventually discharged through a permitted outfall. Pond 5 is still used for storing small quantities of dilute ammonium nitrate fertilizer where it is land applied during growing season.

Soil samples have been collected from locations in and around this the pond area, with sample depths ranging from the surface to 6 feet. The maximum uranium concentration observed was

approximately 39 pCi/g. A gamma scan completed between 1995 and 1998 indicates impacted soils exist outside of Pond 4. Soils around the Fertilizer Pond Area are also impacted by nitrate.

#### **2.1.21 Former Raffinate Treatment Area**

The Former Raffinate Treatment Area is located between the Clarifier A and the YSP. The raffinate treatment area was operated from 1970 to the mid-1980s, and consisted of several large tanks which were used for pilot studies and processing of various raffinate solutions and ammonium nitrate solutions. The Former BaCl Mixing area is located northeast of the former raffinate treatment area and east of the Clarifier Basins. Leaks and spills of raffinate were reported to have occurred in this area. In 1982, an estimated 3,000 gallons of raffinate were released when a transfer pipeline that extends from the solvent extraction area to the raffinate storage area ruptured. The material was released to 005 Stream located northwest of the Facility. Uranium concentrations of the released material were reported to be 74,470 pCi/L.

Soil samples have been collected from locations in and around this the raffinate storage area, with sample depths ranging from the surface to 4.5 feet. The maximum uranium concentration observed was approximately 215 pCi/g, with 95.0 percent of the samples analyzed containing less than 110 pCi/g uranium. Soils in the Former Raffinate Treatment Area have been impacted by fluoride, nitrate and uranium from the former operations and from nearby units.

#### **2.1.22 Combination Stream**

The Combination Stream is a gravity-flow reinforced concrete pipe ranging in size from 12 to 30 inches nominal diameter, at depths ranging from 5 to 30 feet below the ground surface. The Combination Stream was used to transport various discharges to permitted 001 Outfall. These discharges included contact and non-contact over-flow water from the re-circulating cooling water system, cooling water emergency system effluent, MPB roof drain storm water, fire water drains, steam boiler blow-down, decanted water softener blowdown, Yellowcake Pad storm water runoff, treated sanitary wastewater, excess raw water, fluoride treatment effluent, and other miscellaneous storm water from the Process Area. Contributions to the Combination Stream are made at 10 junction manholes at various locations along the Combination Stream. A major flow

contribution occurs at the equalization basin overflow weir into the main sump located on the southeast side of the cooling water tower. Smaller flow contributors are plumbed directly into portions of the Combination Stream. The discharge from 001 Outfall, located at the south edge of the Process Area, is routed by pipeline southwest to the headwaters of the Robert S. Kerr Reservoir. The pipeline was installed in 1989 to convey the Combination Stream discharge to an unnamed tributary that flowed to the receiving waters, and in 1996 the pipeline was extended to the east bank of the headwaters of the Robert S. Kerr Reservoir. Prior to construction of the pipeline the Combination Stream, discharge from 001 Outfall was originally a surface flow that meandered to the west and eventually to the headwaters of the Robert S. Kerr Reservoir. The Storm Water Reservoir covers part of this historical drainage outfall.

Two Combination Stream investigations, one internal and one external, were performed during the FEI. The internal investigation identified all contributing waste streams to the Combination Stream and clarified the operational dynamics of the Combination Stream. The Combination Stream characterization investigation determined that the major uranium loading is from the cooling tower equalization basin. Other potential sources of inflow with the greatest uranium concentration include the sanitary sump and cooling water hot side basin sump. The internal investigation also determined that no measurable infiltration or exfiltration was occurring into or out of the Combination Stream, respectively. The external investigation of the Combination Stream studied and monitored trench backfill. The external investigation identified the SX Building area as the probable major contributor of uranium to the Combination Stream trench. Results of the soil samples collected from boreholes completed into the Combination Stream trench backfill show concentrations are at or near background from the surface to the top of the Combination Stream pipe, and vary from less than 34 to 510 pCi/g uranium.

Soil samples have been collected from locations in and around the Combination Stream, with sample depths ranging from the surface to 32.5 feet. The maximum uranium concentration observed was approximately 510 pCi/g, 93.7 percent of samples analyzed, however, contained less than 110 pCi/g. A gamma scan for the Combination Stream was completed during 1995. The scan determined that impacted soils are present in the Combination Stream above the Storm Water Reservoir. Fluoride and uranium impact the Combination Stream trench backfill in the

Process Area. The historical pathway downstream of the outfall station also has been impacted as indicated by sample results and the gamma scan.

#### **2.1.23 Present Lime Neutralization Area**

The Present Lime Neutralization Area is located in the far northeast corner of the Yellowcake Storage Area. The Area was constructed in 1970 and is a curbed area originally consisting of four tanks used to neutralize both raffinate and HF through the use of lime. The original tanks in the Lime Neutralization Area included a 2,200-gallon lime storage tank, a 1,000-gallon lime slurry tank, a 450-gallon raffinate neutralization tank, and a 3,000-gallon HF neutralization tank. No records of releases or remedial actions were discovered in the research of the Area.

Soil samples have been collected from locations in and around the Area, with sample depths ranging from the surface to 2 feet deep. The maximum uranium concentration observed was approximately 350 pCi/g. Fluoride and uranium impact the soil in the Present Lime Neutralization Area.

#### **2.1.24 DUF<sub>4</sub> Building Area**

The DUF<sub>4</sub> building and adjacent concrete storage pad area are located near the northeast corner of the Process Area. The DUF<sub>4</sub> building was built in 1984 and housed the process equipment to chemically react DUF<sub>6</sub> with hydrogen (H<sub>2</sub>) to produce DUF<sub>4</sub> and anhydrous hydrofluoric acid (AHF). The dry product was placed in 55-gallon drums and the recovered AHF was condensed to a liquid and sent to a holding tank south of the DUF<sub>4</sub> building. The steam condensate from the DUF<sub>4</sub> plant discharged to the sanitary lagoon through an underground sanitary sewer pipeline. Review of information on file indicates that uranium-bearing materials were released from process systems or containers, with some of the incidents resulting in extensive contamination.

Soil samples have been collected from locations in and around the DUF<sub>4</sub> building, with sample depths ranging from the surface to 45 feet. The maximum uranium concentration observed was approximately 68 pCi/g. Fluoride and uranium impact the soils in the areas around the DUF<sub>4</sub> Building. Based on historical use of the area prior to construction of the DUF<sub>4</sub> building, there may be some limited uranium impact under the concrete pad areas and the floor of the building.

### 2.1.25 Tank Farm and Cylinder Storage Area

The South Tank Farm is located immediately north of the MPB and was part of the original construction completed in 1969. The South Tank Farm area is lined with a limestone rock curb for neutralization in case of a spill or upset. Rainfall collected in the curbed area is discharged to the North Ditch. The tank farm consisted of two anhydrous HF storage tanks, two NH<sub>3</sub> storage tanks, and three HNO<sub>3</sub> storage tanks. All of these tanks except for one had a capacity of 15,000 gallons. One of the HNO<sub>3</sub> tanks had a capacity of 18,000 gallons. All of the tanks within the South Tank Farm have been emptied. The North Tank Farm is located north of the South Tank Farm and was built in 1975. The area consists of chemical tanks, a diesel fuel tank and an emergency water supply tank. The North Tank Farm Area is lined with a limestone rock curb for neutralization in case of a spill or upset. The North Tank Farm consisted of two 15,000 gallon 40 percent HNO<sub>3</sub> tanks, one 15,000-gallon anhydrous HF, and one 15,000-gallon aqueous HF tank. Accumulated rainwater drains into the North Ditch. The diesel fuel tank has an earthen berm and rainfall is discharged to the North Ditch. The remainder of the area drains naturally to the North Ditch. Review of information on file indicates that there were incidents in which uranium-bearing materials were released from process systems or containers. The HNO<sub>3</sub> tanks were occasionally overfilled, resulting in HNO<sub>3</sub> running over into the limestone containment.

Soil samples have been collected from locations in and around the Tank Farm and Cylinder Storage Area, with sample depths ranging from the surface to 46 feet. The maximum uranium concentration observed was approximately 650 pCi/g. Of the samples analyzed, 96.5 percent contained less than less than 110 pCi/g of uranium. The soils in the Tank Farm and Cylinder Storage Area are impacted by uranium, primarily in the area just north of the MPB. Additional near surface impact is expected under the concrete pads.

### 2.1.26 South Perimeter Area

The primary feature of the South Perimeter Area is a storm water reservoir that was completed in 1991. The Storm Water Reservoir has a capacity of 8,960,000 cubic feet and covers 16 acres. The reservoir was constructed to control nitrate and ammonia exceedances through the storm water outfalls. The reservoir was designed to collect storm water from the Process Area to

facilitate a reduction of nutrient levels by biological processes prior to discharge. In 1990, SFC constructed a collection trench around the Process Area to divert surface water runoff from the northern and western portions of the Process Area through 008 Outfall. Currently the storm water reservoir collects water from non-Process Areas only.

Soil samples have been collected from locations in and around the storm water reservoir, with sample depths ranging from the surface to 30 feet. The maximum uranium concentration observed was approximately 120 pCi/g, and 99.4 percent of samples analyzed contained less than 110 pCi/g. A gamma scan around the storm water reservoir was completed between 1995 and 1998. The results indicate the potential for impacted soils associated with intermittent drainages and identified an area with slightly elevated readings in the just north of Pond 4 and west of Pond 6. Soils in the South Perimeter Area just south of the Initial Lime Neutralization Area have limited impact from fluoride and uranium.

#### **2.1.27 Scrap Metal Storage Area**

The Scrap Metal Storage Area and the Interim Storage Cell are located north of the DUF<sub>4</sub> Building Area. The area was used to store leftover construction materials such as pipe, beams, and siding that were previously stored near the North Tank Farm, as well as some radiologically contaminated equipment. In 1991, SFC began plans to consolidate, stabilize and store contaminated soils on-site on an interim basis, pending future treatment or disposal. The selected interim storage method was an above-ground containment cell. The Interim Storage Cell was constructed on an existing concrete pad (north cylinder pad) at the north end of the Process Area. The wall structure of the cell is formed from concrete inverted-tee sections. A 38-mil thick liner was placed on the bottom of the storage cell. A geotextile fabric was used for added strength and physical protection of the liner. Several drums of dirt and gravel containing uranium-bearing materials leaked on the north cylinder pad. Soil samples collected from the impacted area indicate a maximum uranium concentration of 765 pCi/g. Soils were placed into the Interim Storage Cell in the fall of 1991.

Soil samples have been collected from locations in and around the Scrap Metal Storage Area, with sample depths ranging from the surface to 36 feet. The maximum uranium concentration



observed was approximately 1,560 pCi/g, 93.3 percent of the uranium analyses, however, were less than 110 pCi/g. The Interim Storage Cell contains approximately 154,800 cubic feet of contaminated soils and other materials with an estimated 2.84 Ci of natural uranium.

#### **2.1.28 Drainage/Runoff Areas**

There are several drainage areas that historically originated in or near the Process Area and flow towards the headwaters of the Robert S. Kerr Reservoir. These drainage pathways consist of permitted 004, 005, 007 and 008 outfalls. 004, 005, and 007 outfalls have been inactive since the construction of a surface water runoff collection trench in June 1990. The collection trench conveys the storm water that previously exited the Process Area via these outfalls to permitted 008 Outfall. Sediment samples have been collected from several locations from the 004 Stream, with sample depths ranging from the surface to 0.3 feet. The maximum uranium concentration observed was approximately 6.1 pCi/g. Sediment samples have been collected from locations from the 005 Stream, with sample depths ranging from the surface to 0.3 feet. The maximum uranium concentration observed was approximately 520 pCi/g, with 75 percent of the samples analyzed containing less than 110 pCi/g. Sediment samples were collected from the 007 Stream, with sample depths ranging from the surface to 0.3 feet. The maximum uranium concentration observed was approximately 80 pCi/g, with 72.7 percent of the samples analyzed containing less than 35 pCi/g. Sediment samples were collected from the 008 Stream, with sample depths ranging from the surface to 0.2 feet. The maximum uranium concentration observed was approximately 7 pCi/g. A gamma scan for the various streams was completed during 1995. The results of the scan are consistent with the historical assessment and soil samples from this unit; i.e. indicative of impacted soils in 005 Outfall and possibly the upper portion of 007 Outfall.

### **2.2 Operational History**

In 1986, a shipping container containing heated UF<sub>6</sub> ruptured, releasing several tons of gaseous UF<sub>6</sub> into the air (SFC, 1998a). The gaseous UF<sub>6</sub> reacted with water vapor in the air, forming a uranyl fluoride precipitate that quickly settled to the ground. Building surfaces, including the MPB, and several acres of ground were contaminated with uranium by this release. Some of the contamination was cleaned up immediately following the accident, however impacts still exist in

some areas between the MPB and the Facility Boundary near Highway 10. A significant amount of uranyl fluoride precipitate washed into the North Ditch and Emergency Basin. Most of this material remains there and contributes to the soil and groundwater contamination in the area.

### **2.2.1 Fertilizer Program**

A byproduct of the  $UF_6$  processing at the Facility was a dilute aqueous solution of ammonium nitrate. After treatment to reduce radionuclide concentrations, this solution was applied as a fertilizer primarily to grasslands.

The fertilizer solution used in the program had lower concentrations of trace elements than commercially available nitrogen fertilizer, with the exception of copper, nickel and molybdenum. The contributions of trace elements from fertilizer to the soil and forage were small in relation to inputs from other necessary fertilizers and soil amendments. No increases in concentration of trace metals or radionuclides over background soils, surface waters, or groundwater could be attributed to fertilizer program

## **2.3 Physical Characteristics of Facility**

### **2.3.1 Surface Features**

The Facility is situated on gently rolling to level land with several steep slopes to the northwest and wooded lands to the north and south. Elevations on or near the Facility range from 460 feet above mean sea level (amsl) for the normal pool elevation of the Robert S. Kerr Reservoir to nearly 700 feet amsl (Figure 2-2). Slopes over most of the upland areas of the Facility are less than seven percent. Steeper slopes in creek ravines and on hillsides average roughly 28 percent. Near the Robert S. Kerr Reservoir, slopes are very steep. This area is owned by the federal government and is administrated by the COE. Most of the 600 acres occupied by the Facility are used as pasture land and for forage production in conjunction with the fertilizer program.

### **2.3.2 Surface Water Hydrology**

The Facility is located on the east bank of the Illinois River tributary of the Robert S. Kerr Reservoir. Southwest of the Facility the Illinois River joins with the Arkansas River tributary of

the Robert S. Kerr Reservoir. Flow in the Illinois River arm of the Robert S. Kerr Reservoir is regulated by releases from the Tenkiller River Reservoir, which is located on the Illinois River approximately seven miles upstream from the Facility. As shown in Table 2-1, the annual average flow of the Illinois River at the gauging station between the Tenkiller Reservoir and the Facility is 1,610 cubic feet per second (cfs).

Significant differences occur in water quality between the Illinois and Arkansas Rivers. The Illinois River flows through a rugged, rocky watershed throughout much of its course in northeastern Oklahoma and is fed largely by releases from Lake Tenkiller Ferry Reservoir and from steep, spring-fed streams. This results in relatively clear waters, with an average specific conductance of 170 microsiemen per centimeter ( $\mu\text{S}/\text{cm}$ ). In contrast, the Arkansas River, which acquires sediment from farming areas along its course in Colorado, Kansas, and Oklahoma, resulting in relatively turbid waters. Specific conductance values from the Robert S. Kerr Reservoir dam are about 600  $\mu\text{S}/\text{cm}$  (SFC, 1998a).

The Process Area is located on an upland area approximately 100 feet in elevation higher than the surface elevation of the Robert S. Kerr Reservoir. Relatively steep (40 percent average) surface gradients occur between the Process Area and the Robert S. Kerr Reservoir or between the floodplain area to in the southwest portion of the SFC property. Several small ephemeral streams drain the Industrial Area to the Robert S. Kerr Reservoir, including the 001, 004, 005, 007, 008, and 009 streams (Figure 2-5), and the drainage associated with the Storm Water Reservoir. Several other drainages affect the SFC property. One stream, hereafter referred to as Creek A, drains the area south of the Fertilizer Ponds, this stream bends northwestward and follows along the eastern edge of the Agland area, and eventually joins with water from the Storm Water Reservoir drainage. A small, northeast flowing stream occurs east of Highway 10, this stream closely parallels the Carlile School Fault and drains much of the eastern portions of the SFC property (Figure 2-2). This small stream empties into Salt Branch (Figure 2-2), a northwestward flowing drainage that closely parallels the SFC northernmost property boundary.

Some discharge monitoring has been conducted in the drainages, however insufficient data is available to establish a representative value of annual mean discharge for each stream. Stream

flow for selected site drainages has been estimated by applying an empirical stream flow model (Harlin, 2001). The model calculates mean annual stream flow based on drainage area, and is expressed as:

$$Q_U = A_D 0.89 \text{ cfs/mi}^2$$

Where:

$Q_U$  = mean annual stream flow  
 $A_D$  = Drainage Area

Stream flow has been calculated for 001, 004, 005, and 007 streams based on drainage areas digitized from surface topography data provided by SFC. The results are presented in Table 2-2.

A facility inspection on August 27, 2001 conducted by Craig Harlin and Scott Munson of SFC identified and located three seeps in the drainage areas of the Facility. These seeps were identified by a seep and associated pool in the 005 and 008 outfalls, and with a pool in the 007 Outfall. The locations of the seeps are presented in Figure 2-5 and descriptions of the seeps are included in Table 2-3.

### 2.3.3 Climatology and Meteorology

Sequoyah County has a warm, temperate, continental climate. Storms bring ample precipitation when moisture-laden air from the Gulf of Mexico meets cooler, dryer air from the western and northern regions. The most variable weather occurs in the spring, when local storms can be severe and bring large amounts of precipitation. The mean annual temperature is 61.5° F. The monthly average ranges from 40° F in January to 82° F in July. The average daily range in temperature is 24° F. The lowest temperature on record was -19° F in January 1930 and the highest was 115° F in August 1936. The mean annual precipitation ranges from 42.9 inches in the town of Sallisaw, to approximately 44.1 inches in the northeastern part of Sequoyah County. The seasonal distribution of rainfall is fairly even, with 31 percent in spring, 26 percent in summer, 23 percent in fall and 20 percent in winter.

The average amount of snowfall from November through April is about 5.2 inches. Lake evaporation averages about 47.5 inches annually. Of this, 72 percent occurs from May through October. Based on the precipitation and lake evaporation values, there is a net annual evaporation rate of about 4 inches in the SFC area.

The most severe storms occur in the spring, although thunderstorms are also frequent during the summer months. Strong winds, heavy precipitation, and intense lightning may be associated with these storms.

The nearest Sequoyah County weather station is in the town of Sallisaw, Oklahoma. There is no national weather station in the immediate vicinity. Meteorological data may be obtained from the national weather station at Tulsa, Oklahoma, about 70 miles northwest, and at Fort Smith, Arkansas, about 40 miles east. Fort Smith, Arkansas is the closest data station having similar topographic and climatological characteristics as the Facility.

### 3.0 DECOMMISSIONING PLAN

In 1996, a study of remediation alternatives was submitted in the Final Decommissioning Alternatives Study Report [FDASR] (SFC, 1998b). This study identified an on-site disposal cell as the preferred decommissioning and waste management alternative. As part of the closure process for the SFC Facility, several site characterization studies, briefly summarized in Section 1.1 of this report, also have been performed. The most recent of these studies, submitted to NRC in 1998 (SFC, 1998a), included technical analysis and description of the Facility's radiological contamination. In 1999, SFC resubmitted the Decommissioning Plan (SFC, 1999) that incorporated the technical specifications of the selected reclamation alternative screened in the FDASR.

Based on current site characterization data, it is expected that approximately 5.1 million cubic feet of radiologically and/or chemically impacted materials will be addressed during the decommissioning of the SFC Facility (SFC, 1999). This material is to be placed in an on-site engineered disposal cell.

The conceptual design of the engineered disposal cell includes excavation of Facility soils above the site-specific derived concentration guideline levels (DCGLs) ( $>110$  pCi/g natural uranium, 12 pCi/g Th-230, 1.8 pCi/g Ra-226), solidification and stabilization (S/S) of highly impacted soils ( $>440$  pCi/g) with fly ash and cement and placement in a 10-acre monolithic cell with an engineered cover. The engineered cover consists of a 48-inch thick rock layer successively underlain by a 6-inch bedding layer, a 6-inch sand filter layer, a 6-inch gravel drainage layer and a 48-inch thick compacted clay infiltration and radon barrier. The clay barrier is designed to have a hydraulic conductivity of  $1 \times 10^{-7}$  cm/sec or less while the S/S materials are expected to have hydraulic conductivities on the order of  $1.9 \times 10^{-6}$  cm/sec to  $5 \times 10^{-5}$  cm/sec (SFC, 1998b). The proposed design does not include an engineered liner but rather relies on evapotranspiration, the low permeability and high drainage characteristics of the engineered cover and the low permeability characteristics of the S/S wastes and underlying geologic materials to reduce infiltration and seepage. The estimated annual average steady-state seepage through the infiltration/radon barrier and out the bottom of the disposal cell is estimated to be 1.18 inches or slightly more than 317,000 gallons. The gravel drainage layer is anticipated to intercept

approximately 19 inches of infiltration per year. This intercepted water will be collected in a drainage ditch on the east side of the cell or will flow away from the cell as sheet flow on the cell north, west and south aspects.

A treatability study evaluated the leaching characteristics of the S/S materials using a modified version of the American National Standard for the Measurement of the Leachability of Solidified Low-Level Radioactive Wastes by a Short Term Procedure (ANSI/ANS-16.1) (Earth Sciences Consultants, 1998). This study, performed on a variety of S/S feedstock samples of the various decommissioning materials, indicated that there is essentially no significant leaching of uranium or arsenic from the S/S materials. This is an expected result given the high pH buffering capacity and the high cation exchange capacity of the fly ash and cement matrix associated with the S/S materials as well as the low mobility of these constituents in the natural environment. The S/S materials are not anticipated to have high nitrate concentrations and therefore are not anticipated to contribute significant amounts of nitrate to the seepage waters from the disposal cell.

The NRC is currently conducting an environmental review of the proposed decommissioning alternative and will develop an environmental impact statement (EIS) to determine whether the alternative proposed by the company for remediation of the Facility is acceptable. The EIS will evaluate the potential impacts of the licensee's proposal, including the effects on water resources, air quality, ecological resources, socioeconomic and community resources, human health, noise, and environmental justice. The EIS will also discuss the option of disposing of the contaminated material off-site in a licensed disposal facility.

#### 4.0 SITE INVESTIGATION

SMI performed a site characterization investigation to more accurately characterize the hydrogeology and geochemistry of the Facility. Specifically, SMI acquired stratigraphic information at various site locations, data to characterize the hydrologic properties of the various hydrological units on the site, and rock samples for geochemical testing and analysis. The primary field investigation, included borehole core logging, rock sampling, hydrological unit testing, and groundwater sampling, and was conducted at SFC from May 14, 2001 to June 6, 2001. Furthermore, SMI contracted Hasbrouck Geophysics, Inc, of Montrose, Colorado, to perform an electrical resistivity geophysical survey at selected Facility locations. This work was performed pursuant to the Hydrogeochemical Characterization Work Plan for the Sequoyah Fuels Company site, Gore, Oklahoma, (SMI, 2001). The work plan, along with the Health and Safety Plan used during the field study, is included in Appendix A.

A supplemental field investigation was conducted from February 7 through February 13, 2002 to address specific issues raised by the NRC. The objectives of the supplemental investigations were to investigate 1) increasing arsenic concentrations in well MW095A, 2) anomalous uranium and arsenic water chemistry data in 005 Stream, and 3) the delineation and characterization of the hydrogeologic and geochemical conditions associated with the subsurface swale near well MW010. The investigation consisted of hydrologic testing of stratigraphic units, geochemical testing of groundwater samples and lithologic materials, and trench/test pit excavation. A complete discussion of the conduct and findings of the supplemental investigation are presented in the Supplemental Data Investigation Trip Report in Appendix B.

The following sections address the specific components of the field investigation including drilling and sampling of boreholes, the installation and hydrologic testing of monitoring wells, and the electrical resistivity testing. Discussion of the geochemical sampling and analysis of borehole materials, test pits, and groundwater is presented in Section 5.0.



## **4.1 Borehole Drilling, Sampling, and Monitoring Well Installation**

Fourteen boreholes and 11 monitoring wells were installed between May 14, 2001 and June 6, 2001 to facilitate site hydrogeologic and geochemical characterization. The borehole and well locations, the specific stratigraphic units targeted, and specific objectives for the boring locations proposed in the original work plan are included in Appendix A. The locations of the borehole and monitoring wells are shown on Figure 4-1. Boreholes and monitoring wells were numbered sequentially in the order they were drilled starting at borehole 327 (BH-327) and monitoring well 110A (MW110A). Table 4-1 summarizes the borehole and monitoring well location information. The coordinates and elevations of the monitoring wells, determined by survey following completion of the monitoring wells, are presented in Table 4-2. Borehole survey information is presented in Table 4-3. A summary of borehole depths and the intervals of geologic units encountered in the boreholes are presented in Table 4-4.

### **4.1.1 Drilling and Construction Methods**

#### **4.1.1.1 Monitoring Well Drilling, Construction, and Development Methods**

Borehole and monitoring well drilling, monitoring well construction, and well development were performed in accordance with the following standard operating procedures (SOP) specified in the Work Plan (see Appendix A), except where deviations were required due to specific field conditions:

SOP No. 1	Groundwater Monitoring Well Installation
SOP No. 2	Monitoring Well Development
SOP No. 3	Equipment Decontamination

Specific deviations from the methods specified in the SOPs are described under the applicable monitoring well subsection. SOPs are included in Appendix A.

#### **4.1.1.2 Borehole/Monitoring Well Drilling Methods**

Drilling was performed according to SOP No. 1 (Groundwater Monitoring Well Installation) by Peterson Drilling and Testing, Inc. of Amarillo, Texas. The lithologic boreholes were drilled

using a Mobile B-61 drill rig with hollow stem augers and wireline coring. An Ingersoll Rand T3W drill rig with an air rotary drilling method was used to install monitoring wells.

Fourteen boreholes were drilled with the Mobile B-61 using hollow stem augers and continuously sampled with a 2-foot long Moss split spoon sampler and wireline coring. Continuous soil samples or rock cores were collected with either split spoon samplers or a 10-foot core barrel. Soil samples collected during hollow stem auger drilling were double bagged in 1-gallon Ziploc<sup>®</sup> plastic bags. Rock core was placed in core boxes. Coring initially utilized air-coring methods but water inflow prevented proper circulation and subsequent coring was done with water. Selected core samples from boreholes BH-330, BH-332, BH-333, BH-334, and BH-339 were double bagged and preserved with dry ice for geochemical testing (see Sections 4.1.2.11 through 4.1.2.14).

The Ingersoll Rand T3W rig used air rotary drilling and casing advance drilling methods to install all monitoring wells, except MW117 and MW120. MW117 and MW120 were installed utilizing the Mobil B-61 and the hollow stem auger method.

#### **4.1.1.3 Monitoring Well Construction Methods**

Monitoring wells were constructed according to the methods specified in SOP No. 1. Well completion diagrams that include documentation of the materials used, and dimensions of the well screen, well casing, sand pack, seals, etc., are provided in Appendix C. Table 4-5 presents monitoring well completion details of installed wells. Monitoring wells were constructed in open boreholes or within the hollow stem augers or temporary steel casing advanced during the air rotary drilling. The augers/steel casing was removed incrementally as the monitoring wells were constructed.

Two-inch nominal diameter flush-threaded Schedule 40 PVC blank well casing, slotted well screen, and threaded end caps were installed in the boreholes. The screen slot size for the 2-inch screens was 0.020 inch. All well screen and blank casing were kept in the manufacturer's plastic protective wrapping and stored off the ground until the time of use. Clean gloves were used when handling the screen and casing. The lengths of the blank casing, screen, and bottom caps

were measured to the nearest 0.1-foot before installation. Centralizers were installed to ensure proper filterpack installation, except for wells constructed in hollow stem auger boreholes (MW117 and MW120).

Oglebay Norton Sand Company's 10-20 silica sand was installed as the filter pack by gravity placement into the annular space between the PVC casing and the borehole to above the top of the screen. The filter pack was installed through either the hollow stem augers or the temporary steel casing when present. The hollow stem augers or the temporary steel casing were removed incrementally as the filter pack was installed. Filter pack depths and volumes were verified by measuring with a weighted tape. Sand pack depths and volumes were monitored to ensure that any bridging would be detected.

A bentonite seal was installed on top of the filter pack. The bentonite seal was constructed from either bentonite pellets and/or medium chip bentonite. The bentonite pellets consisted of Cetco Coated Tablets 3/8 inch coated bentonite pellets. The depth of the bottom (Top of Sand Depth, Table 4-5) and top of bentonite seal for each monitoring well are provided in Table 4-5. Both bentonite chips and pellets were gravity placed by pouring from the surface. After bentonite installation, water was added if the borehole was dry and the bentonite was allowed to hydrate before proceeding with grout placement. The temporary steel casing/augers were removed incrementally as the bentonite was installed. Bentonite depths were verified using a weighted tape. Bentonite depths and volumes above the filter pack were monitored to ensure that any bridging would be detected.

A cement/bentonite grout surface seal was installed in each monitoring well from the top of the bentonite to the ground surface. The cement/bentonite grout consisted of Class C oil well cement, three to five percent bentonite powder by weight, and approximately eight gallons of water per bag of cement. The grout was installed by pumping through a 2-inch nominal diameter hose that was installed above the top of the bentonite. The temporary steel casing/augers were removed incrementally as the cement/bentonite grout was installed.

Protective steel casings with lockable caps were installed above ground surface after completing each monitoring well. Cement/bentonite grout was installed inside the protective casing to above

ground surface and a weep hole was drilled through the protective casing above the top of the grout. The weep hole was drilled to prevent the accumulation of water in the annulus between the PVC well casing and the protective steel casing. A 3-foot diameter cement surface pad was constructed around the protective casing.

#### **4.1.1.4 Monitoring Well Development Methods**

Development of the monitoring wells was performed according to SOP No. 2 (Monitoring Well Development). Each well was initially surged with a bailer. The entire length of the screen was surged with a bailer starting at the top of the screen and working toward the bottom. After surging, any accumulated sediment at the bottom of the screen was removed using a bailer. The monitoring wells were surged and bailed until sediment production had stabilized or ceased. An electric submersible pump was installed in monitoring wells with sufficient production rate (MW110A and MW120) after bailing. The monitoring wells were surged again by alternately turning the pump on to lower the water level and then off to allow partial or full recovery of the water level. After surging, the well was pumped until the turbidity stabilized. A summary of pertinent well development data is provided in Table 4-6. Table 4-7 presents static water level data measured after development. Minimal water production combined with the drilling method (air rotary) resulted in monitoring wells that will continue to yield silt if strongly surged. Great care should be exercised when purging and collecting groundwater samples not to surge the well to minimize silt production.

#### **4.1.2 Borehole and Monitoring Well Characteristics and Specifications**

Individual monitoring well characteristics and specifications are presented in this section in chronological order of installation. In addition, any deviations from the SOPs are noted. Table 4-5 summarizes as-built data for the installed monitoring wells. Appendix C presents monitoring well completion diagrams. Figure 4-1 shows the borehole/well locations as proposed in the work plan, and the actual locations of the completed monitoring wells and boreholes.

#### **4.1.2.1 Monitoring Well MW110A and Borehole BH-327**

Borehole BH-327 was drilled to 50 feet below ground surface (bgs) at Location No. 4 on May 16, 2001. The borehole log for BH-327 is included in Appendix C. Monitoring well MW110A was drilled on May 19, 2001 to a depth of 45 feet bgs with an 8.5-inch nominal outside diameter (OD) air hammer.

Following completion, MW110A was developed by bailing/surging with a bailer followed by surging/purging with a RediFlo2 pump. A total of 80 gallons was purged during development. Although recovery rates are slow, MW110A could not be bailed completely dry. Static water level measured in MW110A on June 13, 2001 was 19.4 feet below the top of PVC casing, or 533.19 feet amsl.

Monitoring well MW110A was completed as a background monitoring well within the Unit 4 Shale. The Unit 4 Shale was encountered from 24.2 to 40.6 feet bgs in BH-327. The filter pack interval for monitoring well MW110A was 32.0 to 45.0 feet bgs. Monitoring wells were originally to be completed in both the Unit 2 and Unit 3 shales. Due to the limited thickness and lack of water in the Unit 2 Shale and the Unit 3 Shale, monitoring wells were not completed in those units at Location No. 4.

#### **4.1.2.2 Monitoring Well MW111A and Borehole BH-328**

Borehole BH-328 was drilled to 48 feet bgs at Location No. 2 on May 17, 2001. The borehole log for BH-328 is included in Appendix C. There was no recovery between 20 and 26 feet bgs in BH-328 due to a clayey gravel and excessive water inflow. Monitoring well MW111A was drilled on May 19, 2001 at Location No. 2 to a depth of 38 feet bgs with an 8.5-inch nominal OD air hammer. The borehole would not remain open for well completion due to water inflow from the alluvium. On May 21, 2001, 8 5/8-inch OD threaded steel casing was installed with a casing hammer to 38.5 feet bgs. Monitoring well MW111A was then completed within the steel casing, incrementally removing the steel casing as the monitoring well was constructed.

Following completion, MW111A was developed by bailing/surging with a bailer. A total of 24.75 gallons was purged during development. Although recovery rates are slow, MW111A

could not be bailed completely dry. Static water level measured in MW111A on June 15, 2001 was 15.17 feet below the top of PVC casing or 465.03 feet amsl.

Monitoring well MW111A was completed within the Unit 4 Shale. The Unit 4 Shale was encountered from about 26 feet to 39.4 feet bgs in BH-328. The filter pack interval for Monitoring Well MW111A was located 28.9 to 38.5 feet bgs.

#### **4.1.2.3 Monitoring Well MW112A and Borehole BH-329**

Borehole BH-329 was drilled to 41 feet bgs at Location No. 6 on May 17, 2001. The borehole log for BH-327 is included in Appendix C. Monitoring well MW112A was drilled on May 20, 2001 at Location No. 6 to a depth of 32.4 feet bgs with an 8.5-inch nominal OD air hammer.

Following completion, MW112A was developed by bailing/surging with a bailer. A total of 41 gallons was purged during development. Although recovery rates are slow, MW112A could not be bailed completely dry. Static water level measured in MW112A on June 12, 2001 was 17.11 feet below the top of PVC casing or 465.77 feet amsl.

Monitoring well MW112A was completed as a monitoring well within the Unit 4 Shale. The Unit 4 Shale was encountered from 15.2 to 33.0 feet bgs in BH-329. The filter pack interval for Monitoring well MW112A was located 18.9 to 32.4 feet bgs. The alluvium at Location No. 6 was found to be dry and an alluvial monitoring well was not installed.

#### **4.1.2.4 Monitoring Well MW113A and Borehole BH- 331**

Borehole BH-331 was drilled to 42 feet bgs at Location No. 5 on May 20, 2001. The borehole log for BH-331 is included in Appendix C. Monitor well MW113A was drilled on May 21, 2001 at Location No. 5 to a depth of 42.5 feet bgs with an 8.5-inch nominal OD air hammer.

Following completion, MW113A was developed by bailing/surging with a bailer. A total of 32.5 gallons was purged during development. Although recovery rates are slow, MW113A could not be bailed completely dry. Static water level measured in MW113A on June 12, 2001 was 2.8 feet below the top of PVC casing or 498.80 feet amsl.

Monitoring well MW113A was completed as a monitoring well within the Unit 4 Shale. The Unit 4 Shale was encountered from 20.0 to 42.0 feet bgs in BH-331. The filter pack interval for Monitoring well MW113A was located 22.4 to 41.2 feet bgs. The alluvium at Location No. 5 was found to be dry and an alluvial monitoring well was not installed.

#### **4.1.2.5 Monitoring Well MW114A**

Monitoring well MW114A was the second Unit 4 Shale monitoring well at Location No. 2 (see Section 4.1.2.2). MW114A was drilled on May 23, 2001 at Location No. 2 to a depth of 38.95 feet bgs with a 9-inch nominal OD casing hammer. Monitoring well MW114A was drilled using 8 5/8-inch OD threaded steel casing and a casing hammer to 38.95 feet bgs, and was then completed within the steel casing. The casing was removed incrementally as the monitoring well was constructed.

Following completion, MW114A was developed by bailing/surging with a bailer. A total of 15.5 gallons was purged during development. Monitoring well MW114A was easily bailed dry. Static water level measured in MW114A on June 15, 2001 was 15.34 feet below the top of PVC casing or 464.749 feet amsl.

Monitoring well MW114A was completed within the Unit 4 Shale. The Unit 4 Shale was encountered from about 26 feet to 39.4 feet bgs in BH-328. The filter pack interval for monitoring well MW114A was located 29.0 to 38.95 feet bgs.

#### **4.1.2.6 Monitoring Well MW115A and Borehole BH-335**

Borehole BH-335 was drilled to 18 feet bgs at Location No. 11 on May 31, 2001. The borehole log for BH-335 is included in Appendix C. Monitor well MW115A was drilled on June 1, 2001 at Location No. 11 to a depth of 15.0 feet bgs with an 8.5-inch nominal OD air hammer. A bentonite chip seal was installed from 13.0 to 15.0 feet bgs due to overdrilling.

Following completion, MW115A was developed by bailing/surging with a bailer. A total of 0.6 gallons was purged during development. Although there was initially some recovery during

development, the purged water was water added during monitoring well completion. Monitoring well MW115A was dry when measured on June 16, 2001.

Monitoring well MW115A was completed within the Unit 3 Shale. The Unit 3 Shale was encountered from 5.9 to 13.0 feet bgs in BH-335. The filter pack interval for monitoring well MW115A was located 6.0 to 13.0 feet bgs.

#### **4.1.2.7 Monitoring Well MW116A and Borehole BH-336**

Borehole BH-336 was drilled to 20.2 feet bgs at Location No. 14 on June 1, 2001. The borehole log for BH-336 is included in Appendix C. Monitoring well MW116A was drilled on June 2, 2001 at Location No. 14 to a depth of 14.2 feet bgs with an 8.5-inch nominal OD air hammer.

Following completion, MW116A was developed by bailing/surging with a bailer. A total of 4.5 gallons was purged during development. The purged water was the water added during monitoring well completion. Monitoring well MW116A was dry when measured on June 13, 2001.

Monitoring well MW116A was completed as a monitoring well within the Unit 2 Shale. The Unit 2 Shale was encountered from 7.5 to 11.0 feet bgs in BH-336. The filter pack interval for Monitoring well MW116A was located 7.0 to 14.34 feet bgs. Due to the length of the screen (5 feet) and the limited Unit 2 Shale thickness (3.5 feet), the filter pack extends above Unit 2 Shale into the Unit 1 Sandstone and below the Unit 2 Shale into the Unit 2 Sandstone.

#### **4.1.2.8 Monitoring Well MW117 and Borehole BH-338**

Monitoring well MW117 was placed at Location No. 12 on June 2, 2001. Heaving sands at 6 feet precluded ready well installation. This initial location for MW117 was abandoned and designated BH-338. The borehole log for BH-338 is included in Appendix C. MW117 was installed on approximately 120 feet north of BH-338 to a depth of 15.53 feet bgs on June 2, 2001. MW117 was drilled with hollow stem augers with an 8-inch nominal outside diameter. A bentonite chip seal was placed from 14.6 to 15.53 feet bgs due to overdrilling.



Following completion, MW117 was developed by bailing/surging with a bailer. A total of 6 gallons was purged during development. Monitoring well MW117 was bailed dry. Static water level measured in MW117 on June 12, 2001 was 12.14 feet below the top of PVC casing or 475.97 feet amsl.

MW-117 was completed as a monitoring well within the alluvium. Drilling proceeded until bedrock was encountered, and the well was placed in the overlying alluvium. The filter pack interval for monitoring well MW117 was located 7.59 to 14.6 feet bgs.

#### **4.1.2.8 Monitoring Well MW118**

Monitoring well MW118 was installed on June 2, 2001 at Location No. 1 to a depth of 7.34 feet bgs within the open borehole. Monitoring well MW118 was drilled with an 8.5-inch nominal OD air hammer.

MW118 was dry following completion and when the static water level was measured in on June 13, 2001.

Monitoring well MW118 was completed within the alluvium. Drilling proceeded until bedrock was encountered, and the well was placed in the overlying alluvium. The filter pack interval for monitoring well MW118 was located at 1.5 to 7.34 feet bgs.

#### **4.1.2.9 Monitoring Well MW119A and BH-337**

Borehole BH-337 was drilled to 14 feet bgs at Location No. 13 on June 1, 2001. The borehole log for BH-337 is included in Appendix C. Monitor well MW119A was drilled on June 2, 2001 at Location No. 13 to a depth of 14.5 feet bgs with an 8.5-inch nominal OD air hammer. Monitor well MW119A is approximately 100 feet west of BH-337.

Following completion, MW119A was developed by bailing/surging with a bailer. A total of four gallons was purged during development. The purged water was the water added during monitoring well completion. Monitoring well MW119A was dry when measured on June 16, 2001.

Monitoring well MW119A was completed within the Unit 2 Shale. The Unit 2 Shale was encountered from 7.0 to 10.0 feet bgs in BH-337. Drilling indicated that the Unit 2 Shale was encountered from 7 to 10.9 feet bgs at the MW119A location, consequently the filter pack was located 7.0 to 14.0 feet bgs.

#### **4.1.2.10 Monitoring Well MW120**

Monitoring well MW120 was the third well installed at Location No. 2. See BH-328 (Appendix C) for the borehole log for Location No. 2. Monitoring well MW120 was drilled to 24.0 feet bgs on June 4, 2001 within the 8¼-inch outside diameter hollow stem augers. MW120 was completed with alluvium. Heaving sands and filterpack bridging were encountered during well completion.

Following completion, MW120 was developed by bailing/surging with a bailer followed by surging/purging with a RediFlo2 pump. A total of 270 gallons was purged during development. Static water level measured in MW120 on June 15, 2001 was 14.99 feet below the top of PVC casing or 465.18 feet amsl.

#### **4.1.2.11 BH-330**

Borehole BH-330 was drilled to 53.5 feet bgs at Location No. 9 on May 18 and 19, 2001. The borehole log for BH-330 is included in Appendix C. Unit 3 Shale was encountered from 20.4 to 23 feet and Unit 4 Shale was encountered between 29.7 and 46.1 feet. Core samples of Unit 3 Shale and Unit 4 Shale were recovered for geochemical testing.

#### **4.1.2.12 BH-332**

Borehole BH-332 was drilled to 16 feet bgs at Location No. 10 on May 19 and 21, 2001. The borehole log for BH-332 is included in Appendix C. Unit 1 Shale was encountered from 10 to 16 feet, and core samples of Unit 1 Shale were recovered for geochemical testing.

#### **4.1.2.13 BH-333 and BH-334**

Borehole BH-333 was drilled to 28 feet bgs at Location No. 7 on May 20 and 21, 2001. The borehole log for BH-333 is included in Appendix C. Unit 1 Shale was encountered from 4.4 to 19 feet. Split spoon samples of Unit 1 Shale were recovered for geochemical testing. Refusal occurred at 19 feet. Unit 2 Shale was encountered between 25.8 and 27.1 feet, and core samples of Unit 2 Shale were recovered for geochemical testing. The low recovery rates and high degree of difficulty of drilling prompted abandonment of BH-333. Drilling of borehole BH-334 occurred on May 22, 2001. BH-334 is located approximately 15 feet south of BH-333. BH-334 was blind drilled to refusal at 21 feet, when core sampling began. Core sampling occurred from 21 to 23.5 feet, until drilling circulation within the hole was lost. Unit 2 Shale was encountered between 23.0 and 23.5 feet. Core samples of Unit 2 Shale were recovered for geochemical testing. The coring tool was replaced with driving split spoons, but encountered immediate refusal. BH-334 was subsequently abandoned, and no further core sampling occurred at Location No. 7.

#### **4.1.2.14 BH-339 and BH-340**

Borehole BH-339 was drilled to 49 feet bgs at Location No. 8 on June 2 and 3, 2001. The borehole log for BH-339 is included in Appendix C. Unit 2 Shale was encountered from 12.5 to 21 feet bgs. Core samples of Unit 2 Shale (1.8 feet) were recovered for geochemical testing. Unit 3 Shale was encountered between 26.9 and 30 feet. Unit 4 Shale was encountered between 36.5 feet and the bottom of the boring. Core samples of Unit 3 Shale and Unit 4 Shale were recovered for geochemical testing. In an attempt to obtain more core sample from the Unit 2 Shale, Borehole BH-340 was drilled approximately three feet west of BH-339 on June 3, 2001. BH-340 was blind drilled to refusal at 12 feet, when core sampling began. Sandstone with approximately 0.05 feet of highly weathered, clayey shale (at the bottom of the core) was encountered from 12 to 14 feet. No rock was recovered from 14-15.5 feet and BH-340 was subsequently abandoned without recovery from Unit 2 Shale for geochemical testing.

## 4.2 Hydrologic Testing

The hydrologic testing program was conducted in June 2001 in order to evaluate the hydrologic properties and conditions in the shallow geology across the Facility. The work consisted of slug tests and the water level measurements conducted in wells screened in only a single hydrologic unit. Other methods to evaluate hydrologic properties (pumping, tracer tests) were not conducted due the inability to obtain sustainable discharge rates from the majority of the wells at the Facility. Four additional slug tests were performed in wells completed in a single unit as part of the supplemental field investigation. Based on the SMI borehole drilling program and review of previous hydrologic investigations (RSA, 1991), five primary hydrologic units have been identified in the shallow geology at the Facility. These primary hydrologic units are Arkansas/Illinois River alluvium (alluvium), terrace/Unit 1 Shale, Unit 2 Shale, Unit 3 Shale, and Unit 4 Shale. The objective of the SMI hydrologic testing program is to individually evaluate properties and conditions of each of the five primary hydrologic units.

Slug tests were performed on a total of 24 existing and newly installed wells in order to develop representative estimates of horizontal hydraulic conductivity for each of the hydrologic units. Location of the slug tests is presented in Figure 4-2. Discussion of the field procedures and analytical methodology is presented in Appendices B and C.

Slug tests were also conducted at the Facility by SFC in 1991 (RSA, 1991). Although a total of 35 slug tests were conducted during this investigation, only seven tests were performed in wells that are screened in a single hydrologic unit. Therefore, only these seven wells are included in the evaluation of hydraulic conductivity of the five primary hydrologic units.

Table 4-8 presents the slug test results from each well. Estimates of hydraulic conductivity range from 19.9 ft/day to 0.0042 ft/day. Table 4-9 presents the average, maximum, and minimum calculated conductivity value from each hydrologic unit. The results indicate that the hydrologic units are highly heterogeneous, as the conductivity ranges by as much as three orders of magnitude in a single unit. The variability in conductivity does not appear to represent any geospatial patterns, nor do values appear to relate to any geological features at the Facility. The

variability in conductivity can be attributed to heterogeneous (clay, sand, silt) alluvial deposits, and to small-scale fracture patterns in the shale units.

### 4.3 Resistivity Survey

A previous study (RSA, 1991) indicated that high concentrations of uranium existed in wells near the southwest corner of the main process building, mainly in MW010. SFC proposed that the primary cause of the high uranium concentrations might be due to movement from the vicinity of the solvent extraction building through a shallow (less than 30 feet deep), southward trending paleochannel (RSA, 1991). In order to further evaluate this potential transport mechanism, SMI contracted Hasbrouck Geophysics, Inc of Montrose, Colorado, to perform a series of electrical resistivity surveys to aid in locating any possible paleochannels.

The electrical resistivity survey was completed along five east-west trending survey lines from south of the yellowcake storage pad (Line 4, see Line Location Map, Appendix D) to east of the Fertilizer Pond Area (Line 1, see Line Location Map, Appendix D). An additional survey was performed along a line west of Pond 1 (Line 6, see Line Location Map, Appendix D) to constrain any possible eastern extension of the 005 Stream. Complete results of the resistivity survey are included in Appendix D. The survey detected high electrical resistivity at several subsurface locations south of the Process Area. These resistivity anomalies were interpreted as sands or sands with gravel, fluvial-type deposits typically found in paleochannels. SMI completed boreholes BH-336 and BH-337 along resistivity survey lines 1 and 3, respectively, to determine if the high resistivity at these locations represented fluvial-type deposits. No fluvial-type deposits were found at either borehole, therefore it is unlikely that the high resistivity represent paleochannels. It is possible that the high resistivity found may represent well-cemented sandstones (see Appendix D). Furthermore, no groundwater was encountered in these boreholes, therefore no contaminant transport can occur there. The results of the resistivity survey along two survey lines within the Process Area (Lines 4 and 5, Line Location Map, Appendix D) show no evidence of higher resistivity at depth, indicating no paleochannel exists within the Industrial Area downgradient of the restricted area.

#### 4.4 Trenches and Test Pits

Trenches and test pits were excavated in the 005 Stream and MW010 swale areas in order to estimate local stratigraphy and collect groundwater and lithologic samples. In the 005 Stream area a trench was excavated in the fill materials at the head of the 005 Stream between the Emergency Basin and the existing 005 Sump, south of Fluoride Holding Basin No. 2. The buried channel bottom was encountered at approximately six to eight feet deep. Stratigraphy observed in the trench consisted of a hard sandstone unit overlain by one to two feet of clay. Based on its elevation and lateral occurrence, the sandstone is believed to be Unit 3 Sandstone and the overlying clay is interpreted to be weathered remnants of Unit 3 Shale. Overlying the clay/weathered shale unit is a one-foot thick layer of gravel with clay. This unit is interpreted to be the basal gravel on which fill or gravelly fill material was placed in the old 005 Stream bottom. Small pits were also excavated down to sandstone bedrock along the margins of the 005 stream. Soil and groundwater samples were collected from the trench and the pits.

The excavation of a trench and several test pits was also conducted in the MW010 swale area. The swale is essentially a small surface drainage channel that was covered with local fill materials at the time of facility construction and is suspected of significantly influencing groundwater flow. The trench and pit were excavated down to sandstone bedrock or refusal. Geologic mapping of the material encountered in each pit was conducted. In particular, a lens of well-rounded, well-sorted river gravel was encountered just above sandstone bedrock. Soil and groundwater samples were collected from the gravel and the overlying fill. The potentiometric head in the gravel and overlying fill were also estimated.

Two pits were excavated into un-impacted terrace materials east of Highway 10. Soil and water samples from these locations were collected to develop  $K_d$  values for the terrace materials using batch tests. Detailed discussion of results and findings of the supplemental investigation is presented in Appendix B.

## **5.0 GEOCHEMICAL TESTING AND ANALYSIS**

### **5.1 Introduction**

Detailed geochemical analyses of shale and colluvial samples, terrace material and groundwater from the SFC Facility were undertaken to: (1) characterize the sedimentary mineralogy and aqueous geochemistry of the groundwater system, and (2) determine partition coefficients ( $K_d$ ) for uranium (U) and arsenic (As) that can be used in the hydrologic transport model. These detailed analyses are used in conjunction with the geochemical equilibrium speciation model PHREEQC (Parkhurst and Appelo, 1999) to improve our understanding of the factors controlling the concentrations and transport of U and As in the groundwater system. The mineralogical analyses, geochemical groundwater characterization, and geochemical modeling are integrated to better understand factors controlling fluoride (F), U, As, and nitrate ( $\text{NO}_3$ ) concentrations in groundwater.

### **5.2 Methods of Mineralogical Analyses**

Mineralogical analyses were carried out on selected core samples collected from Unit 1, 2, 3, and 4 shales during the May 2001 drilling program (Table 5-1). The SOPs used to collect the samples are outlined in Appendix A. The objectives of these analyses were to characterize the bulk mineralogy of the samples to understand potential mineral-water interactions that might control the concentrations and transport of U and As. The mineralogical analyses were used in conjunction with detailed groundwater analyses and geochemical speciation modeling to improve the conceptual geochemical model for the hydrologic system and to support the basis for predictive constituent transport modeling.

The bulk mineralogical characterization of the shale samples was made using X-ray diffraction (XRD) analysis. The XRD analyses were carried out by SMI personnel at the Department of Geology and Geological Engineering at the Colorado School of Mines (Golden, Colorado). The samples were prepared as oriented mounts and analyzed using an automated Scintag diffractometer, Cu-K $\alpha$  radiation, and a curved graphite monochromator on the diffracted beam path. Ethylene glycol solvation was carried out to identify possible interstratification of phyllosilicate minerals. The samples were routinely run from 5.0 to 60.0 degrees  $2\theta$  at 2.0° per

minute. Mineral phases were identified with XRD by comparing distances between diffraction planes to those of reference standards based on International Centre for Diffraction Data (1993).

### 5.3 Methods of Chemical Analyses

Chemical analyses were carried out on solid and water samples collected from the SFC Facility to: (1) determine partition coefficients ( $K_d$ ) for U and As for use in the hydrologic transport model, and (2) perform geochemical speciation calculations using data collected from groundwater wells to understand potential geochemical controls on U, As, F and  $\text{NO}_3$  migration through the hydrologic units. Partition coefficients were determined experimentally in the laboratory using two methodologies. Geochemical speciation modeling was carried out using data collected from selected groundwater wells during the SMI field investigation in June 2001.

#### 5.3.1 Determination of Partition Coefficients ( $K_d$ ) for Uranium and Arsenic

The transport of any contaminant in a groundwater system is dependent on hydrological parameters such as advection and dispersion, as well as numerous physiochemical and biological processes, including sorption/desorption, precipitation/dissolution and oxidation/reduction. In sum, these processes determine the rate and extent of contaminant transport within a given system. The simplest and most common method of estimating contaminant retardation ( $R_f$ ) is based on  $K_d$  values (EPA, 1999).  $K_d$  is a measure of the partitioning of a contaminant between the solid and aqueous phases and is defined as the ratio of the contaminant concentration associated with the solid phase to the concentration of the contaminant in the aqueous phase at equilibrium as described by equation [1]. The  $K_d$  parameter is often used in predicting the potential for contaminant retardation due to adsorption of the dissolved contaminant to the soil matrix.

$$K_d (\text{mL} / \text{gm}) = \frac{\text{Mass of adsorbate sorbed} / \text{gram}}{\text{Mass of adsorbate in solution}} = \frac{\mu\text{g} / \text{gm}}{\mu\text{g} / \text{mL}} \quad [1]$$

There are certain inherent assumptions associated with the  $K_d$  models, many of which are violated in the common procedures used to measure  $K_d$  values for use in contaminant transport codes. In addition, there are numerous issues such as chemical nonequilibrium, field variability,



and the “gravel” and “colloid” issues that make the determination of an appropriate  $K_d$  difficult (EPA, 1999). Despite the many problems associated with determining an appropriate  $K_d$ , the partition coefficient is widely used in contaminant transport codes for predicting the rate and extent of contaminant migration.

During the development of the transport model, several methods were used to determine appropriate  $K_d$  values that could be used to reasonably model arsenic and uranium transport at the Facility. Sections 5.3.2 and 5.3.3 discuss the methodology used during these studies to define a  $K_d$ . Sections 5.8 and 5.9 discuss specific conditions present at this site that made the use of a constant, experimentally derived  $K_d$  value impractical at this Facility.

### **5.3.2 Laboratory Determination of Partition Coefficients ( $K_d$ )**

#### **5.3.2.1 Batch Desorption Tests**

During the course of the geochemical characterization, two laboratory methods were used to arrive at  $K_d$  values. In the initial site characterization study, laboratory batch tests were used to determine  $K_d$  values for U and As for use in the hydrologic transport model. Laboratory batch tests are commonly used to measure  $K_d$  values because they can be completed quickly for a wide variety of elements and chemical environments (EPA, 1999). Typically, the laboratory batch test consists of equilibrating a known mass of solid with a solution containing a known mass of contaminant ( $\mu\text{g/ml}$ ) and determining the quantity of the contaminant sorbed onto the solid phase. One disadvantage of the batch  $K_d$  determination is that the method, as described by the EPA (1999), does not accurately simulate desorption of constituents from contaminated soils. Therefore, the batch test procedure was modified during some experiments to simulate long-term rinsing, or desorption, of U and As from contaminated shales and soils below the SFC Facility as clean upgradient water moves through the hydrologic unit. The  $K_d$  values determined with the batch desorption procedure will be denoted as  $K_d'$  in this report. No  $K_d$  determinations were made for  $\text{NO}_3$  since this constituent is assumed to exhibit conservative behavior during transport; this is a highly conservative assumption because  $\text{NO}_3$  can be degraded by biological reduction. Fluoride typically also exhibits conservative behavior, unless its solubility is controlled by  $\text{CaF}_2$ .

The batch testing in the initial characterization study utilized contaminated shale samples collected from Unit 1 Shale (Locations 7 and 10), Unit 2 Shale (Location 8), Unit 3 Shale (Locations 8 and 9), and Unit 4 Shale (Locations 8 and 9) (see Table 5-1 and Drawing 4-1). These locations were chosen because they typically contain the highest groundwater concentrations of U and As based on examination of preliminary plume maps. The samples were shipped to Energy Laboratories, Inc. (ELI, Casper, Wyoming), an analytical testing laboratory licensed to handle and store 11e.(2) by-product material. The shale samples were prepared by ELI for use in the batch testing by air-drying, followed by gentle crushing to pass a 10-mesh (2-mm) screen. Groundwater that is representative of background conditions was obtained from an upgradient well screened in Unit 4 Shale (MW110) and was used as the liquid phase in the  $K_d'$  batch testing. The water was filtered (0.45  $\mu$ m pore-size filter), shipped at 4°C directly from the Facility to ELI, and analyzed for dissolved concentrations of major cations, anions, selected trace metals, and pH. Analytical testing results of the water from MW110 are included in Appendix E.

The  $K_d'$  batch tests were carried out using a solution to solid ratio of 2:1 (100 mL:50 g). Each shale sample was reacted with six consecutive 100-mL volumes of clean groundwater. Assuming a shale porosity of 0.33, this equates to 6 pore volumes of flow through the sediment per batch experiment. After the addition of each 100-mL aliquot, the samples were agitated for 16 hours and the solutions filtered through a 0.45  $\mu$ m pore-size filter. The supernatant from each batch rinse was analyzed for major anions, cations, and dissolved aluminum (Al), iron (Fe), U, and As. After the sixth 100-mL rinse, the solid was analyzed for total U and As (EPA method 3050). The  $K_d$  values (in units of mL/g = L/kg) were then calculated according to the equation [1].

The chemical compositions of the supernatants were input into the geochemical equilibrium model PHREEQC (Parkhurst and Appelo, 1999) for chemical speciation and calculation of ion activities and saturation indices (SI) for solid phases. Evaluating the SI values calculated using PHREEQC for various mineral phases is used to test if any solubility limits have been exceeded. In those cases where discrete U and/or As-bearing solid phases are predicted to precipitate, the

empirically determined  $K_d$  values are a mixture of both solubility and adsorption processes. The SI value for a given mineral is defined as:

$$SI = \frac{IAP}{K_{sp}}$$

Where:

IAP = ion activity product in solution

$K_{sp}$  = the solubility constant

Therefore, when  $SI = 0$  (equilibrium), or when  $SI$  greater than 0, there is a potential for solid phase control. In other words, the determined  $K_d$  value under these conditions would represent elemental partitioning based on both precipitation and adsorption, but the empirical value would be valid for the mixed process.

The procedure described above used in the original characterization studies were repeated during the SDCP with minor exceptions. First, each soil/shale sample was rinsed with three consecutive 100-mL volumes of uncontaminated groundwater versus six rinses in the initial investigation. It was shown during the initial characterization studies that uranium and arsenic concentrations reached relatively constant values quickly and that there was very little change from rinse No. 3 to rinse No. 6 (Figures 5-1 and 5-2), so the number of extraction steps was reduced to three for the SDCP. Secondly, uncontaminated water obtained from Facility E-2 was used in the rinses instead of groundwater collected at well MW110. In addition, at the conclusion of the rinses, the solid phase was first digested with 0.04 M Hydroxylamine hydrochloride ( $NH_2OH \cdot HCl$ ) in 25 percent acetic acid (V/V) equilibrated for 6 hours at 96 °C, with occasional agitation. Following the hydroxylamine hydrochloride (Ha-HCl) extraction, the solids were analyzed for total metals using the EPA 3050 digestions as was done in the initial geochemical characterization studies. The Ha-HCl extraction is designed to provide information on those constituents that are released upon the dissolution of the iron and manganese (hydr)oxide fraction of the solid phase. It is expected that most of the arsenic and uranium, which is removed from solution through sorption, is bound in the hydroxide fraction. Therefore, this additional step was added to determine the amount of arsenic and uranium that was likely to be sorbed versus that which was incorporated

into the mineral matrix or is present as a distinct mineral species. Following each digestion, the aqueous phase was analyzed for arsenic, iron, manganese, and uranium.

#### **5.3.2.2 Batch Adsorption Tests**

Analysis of groundwater samples collected at the SFC Facility suggest that the  $K_d'$  values determined from batch desorption tests during the initial investigation and used in the initial stages of transport modeling did not accurately predict the migration of uranium and arsenic at certain locations within the SFC Facility. In particular, the increasing arsenic levels at MW095A could not be predicted using the  $K_d'$  values used in the original model. In addition, uranium concentrations observed at MW005A were also not predicted by the original model. Therefore, traditional batch adsorption test methods for determining  $K_d$  values were used during the SDCP for the revised transport modeling. The supplemental geochemical analysis also included determination of  $K_d$  values for colluvial and terrace material that were not determined in the initial characterization studies. The  $K_d$  values determined for terrace material would be important for modeling contaminant migration potentially leaching from a storage cell placed on top of this material and for arriving at appropriate clean up levels.

Batch adsorption  $K_d$  tests were carried out using a solution to solid ratio of 2:1 (100 ml to 50 g) as was done in the previous desorption tests. Soil samples were wet sieved through 10 mesh (<2.0 mm) screen and the sieved fraction added to reaction vessels to provide approximately 50 g of soil on a dry weight basis. Background groundwater obtained from trench E-2 was spiked with uranium and/or arsenic to give a final concentration of 0.01, 0.1, and 1.0 mg/L of each of the constituents to be tested. Reactions were allowed to equilibrate for three days. At the end of the equilibration period the aqueous phase was removed, filtered through a 0.45  $\mu$ m poresize membrane filter and analyzed for uranium and/or arsenic. Following the adsorption tests the soil phase was digested and analyzed as described above.

#### **5.3.3 Model Derived $K_d$ Values**

As discussed in the introduction to this section, at least some of the impetus for the additional tests done during the SDCP was to experimentally determine  $K_d$  values that could more

realistically describe the migration of arsenic and uranium as measured in the field. Uranium  $K_d$  values determined during the SDCP studies were generally higher than those initially determined in the batch desorption experiments. In addition, while the  $K_d$  values for arsenic from the batch adsorption tests were somewhat lower than those obtained in the desorption studies, they still did not adequately predict the migration of arsenic observed in the field.

An alternative to experimental determination of  $K_d$  values is to use a transport model to derive a  $K_d$  by fitting model predicted migration of various constituents to historical data. Because the values for  $K_d$  arrived at via laboratory experimentation were not completely satisfactory for describing the transport of constituents as observed in the field, this approach was ultimately used to develop a "modeled  $K_d$  parameter." It should be noted that, while these model-derived values are often referred to as a  $K_d$ , it is more appropriate to label them as a transport parameter (TP). The partition coefficient is by definition the ratio of the contaminant concentration associated with the solid to the contaminant concentration in the aqueous phase when the system is at equilibrium. Laboratory methods for determining constant  $K_d$  values describe the partitioning of a molecule between the solid and aqueous phases due to reversible sorptive reactions. Fitting field data does not provide an equivalent parameter. The subsurface processes, which account for changes in analyte concentration in the field, are not well defined and the systems are unlikely to be in equilibrium. Thus, the modeled  $K_d$  ( $K_{d-mod}$ ), arrived at via model fitting, is essentially a bulk transport parameter that incorporates numerous geochemical reactions such as reversible and irreversible sorption/desorption, precipitation/dissolution, coprecipitation, sequestration within organic phases and oxidation/reduction. In addition, hydrogeological parameters not accounted for in the initial model design, such as flow through fractured media, are incorporated into  $K_{d-mod}$ . Values determined for  $K_{d-mod}$  and used in the transport model to describe the migration of arsenic and uranium range between 0.1 to 1.5 mL/g and 0.25 to 0.6 mL/g respectively. A complete description of how these were determined with the model is discussed in Transport Model Calibration (Section 8.5.4).

### 5.3.4 Geochemical Modeling of Groundwater Using PHREEQC

Geochemical modeling of selected Facility groundwaters wells was undertaken to: (1) further assess the validity of the  $K_d$ ' values by comparing U and As speciation in site groundwater to the

laboratory conditions under which the values were determined, and (2) understand the mechanism controlling U and As migration through the shales. Nine groundwater monitoring wells were sampled and analyzed for a detailed list of constituents to provide input to the geochemical equilibrium speciation model PHREEQC (Parkhurst and Appelo, 1999).

Preliminary maps of the U, As, and NO<sub>3</sub> concentrations in the groundwater were used to select wells where high concentrations of contaminants might exist, so that representative samples of groundwater from different shale units could be obtained. The nine wells selected for detailed geochemical sampling and analyses were: MW064A (Unit 4 Shale), MW059A (Unit 4 Shale), MW042A (Unit 2 Shale), MW075 (Unit 1 Shale), MW067A (Unit 4 Shale), MW025 (Unit 1 Shale), MW025A (Unit 2 Shale), MW12A (Unit 3 Shale), and MW012B (Unit 5 Shale) (see Drawing 4-1). The wells were purged using standard procedures (Appendix A) and the temperature, electrical conductivity, and pH were recorded. Oxidation-reduction potential (ORP) measurements were also recorded using a Pt electrode with a Ag/AgCl reference electrode. The accuracy of the electrode was confirmed using ZoBell's Solution prior to sample measurement, and the ORP measurements were converted to Eh (American Public Health Association [APHA], 1992).

Filtered samples (using 0.45 µm pore-size filters) were preserved according to standard procedures (APHA, 1992) in the field and delivered to Outreach Laboratory (Broken Arrow, Oklahoma). The water samples were analyzed for cations (Ca, Mg, Na, K), anions (Cl, F, SO<sub>4</sub>), metals (Al, As, Si, V, Mn, ferrous iron [Fe(II)], total dissolved Fe), radionuclides (U, Ra-226), alkalinity, NO<sub>3</sub>, NO<sub>2</sub>, NH<sub>3</sub>-N, P, S<sup>2-</sup>, total suspended solids (TSS), and organic carbon. Unfiltered samples were also collected and analyzed to assess the potential for colloidal transport of U and As through the hydrologic units. The unfiltered samples were analyzed for TSS, as well as the same suite of metals plus U as for the filtered samples.

#### 5.4 Mineralogical Testing Results

X-ray diffraction analyses indicate that the shale samples are composed primarily of quartz (α-SiO<sub>2</sub>), illite (e.g., mica), and 2:1 expanding and non-expanding layer phyllosilicates. Solvation of the sample with ethylene glycol indicates that the phyllosilicates are mainly composed of

interstratified chlorite-smectite. The shift in the d-spacing from 14.3 Å to 15.6 Å upon ethylene glycol solvation is characteristic of interstratified chlorite-smectite (Sawhney, 1989). The XRD patterns for shale samples from Unit 1, 2, 3, and 4 shales indicated that all samples contained the same bulk mineralogical composition. A representative diffraction pattern for Unit 1 Shale from Location 7 (See Drawing 4-1) is shown on Figure 5-3.

## **5.5 Test Results and Geochemical Modeling for Partition Coefficients ( $K_d$ and $K_d'$ )**

### **5.5.1 Results From Batch Desorption Tests**

The results of the  $K_d'$  batch desorption testing indicate that an adequate number of rinses was performed to simulate the long-term rinsing (desorption) of U and As from the solid. The concentrations of U (Figure 5-1) and As (Figure 5-2) reached relatively constant values by the 3<sup>rd</sup> rinse of the batch testing. Therefore,  $K_d'$  values calculated during the initial studies using elemental concentrations of the solid and the liquid from the final rinse are representative of long-term desorption equilibrium conditions, and were considered to be valid measurements for use in the hydrologic transport model. The original laboratory data sheets and quality assurance report are presented in Appendix E. The calculated U and As  $K_d'$  values for all shale samples are given in Table 5-2.

Results of the geochemical modeling using PHREEQC show that solubility limits for the common U and As phases were not exceeded, further validating the calculated  $K_d'$  values as being representative of desorption processes (Table 5-2). The SI values for the common U minerals given in Table 5-3 were calculated by the model for the batch test solutions for all shale samples. For elements that were below detection in the batch solutions, their detection limits were input into PHREEQC so that conservatively high SI values could be calculated.

The resulting negative SI values (Figures 5-4 through 5-10) show that the solutions were undersaturated with respect to the common U minerals, indicating that adsorption/desorption reactions, rather than precipitation/dissolution reactions, controlled U concentrations during the batch desorption testing. The U(IV) minerals that occur in reduced environments (Table 5-4) are not expected to form under the oxidized conditions encountered during the batch testing;

however, these U(IV) minerals were included in Table 5-4 and in the analysis of SI values for completeness. Field measurements of Eh show that the groundwater generally has an oxidizing potential. Positive SI values were calculated for tyuyamunite  $[\text{Ca}(\text{UO}_2)_2(\text{VO}_4)_2]$  (Table 5-3) in the Unit 1 Shale (Location 7) batch test solution (Figure 5-4); however this high value results from artificially using the detection limit value (0.10 mg/L) for V in the SI calculation; V was below detection in this solution, and the relatively low  $K_d'$  value for this sample (Table 5-2) does not indicate that tyuyamunite precipitated during the test. The constant near-equilibrium values for gypsum ( $\text{CaSO}_4 \cdot 2\text{H}_2\text{O}$ ) indicate that gypsum is the controlling mineral phase for  $\text{SO}_4$ , the dominant anion in the system.

Similarly for As, geochemical modeling of SI values shows that there were no mineral solubility controls on As concentrations during the initial desorption  $K_d'$  testing. In oxidizing waters, such as those encountered in the batch test solutions, As concentrations are typically controlled by adsorption to and/or co-precipitation with iron oxides (Welch and others, 2000), although in some cases metal arsenates such as scorodite ( $\text{FeAsO}_4 \cdot 2\text{H}_2\text{O}$ ) or calcium arsenate  $[\text{Ca}_3(\text{AsO}_4)_2 \cdot 6\text{H}_2\text{O}]$  may act to control aqueous As concentrations. The negative SI values calculated for various metal arsenates and arsenic oxides (Figures 5-4 through 5-10) show that the test solutions were undersaturated with respect to these As minerals.

The chemistry of the major ions during the batch testing was consistent with the known mineralogy of the shales, and indicates that ion exchange is the important process controlling major cation concentrations. Figure 5-11 compares the concentrations of Ca, Na, Mg and K in the initial solution (Rinse 0, from upgradient well MW-110) to those in the six batch test solutions. The results show that as clean water from upgradient reacts with shales at the Facility, there is an ion exchange of Na for Ca and Mg (Figure 5-11). As the chemistry of the exchange sites reaches equilibrium with the clean water, the Ca, Na, and Mg concentrations approach background conditions.

Samples used during the SDCP for  $K_d$  analysis were obtained from surface trenches and are listed in Table 5-5. The locations where the samples were collected along with the associated aqueous and solid phase geochemistry of the samples are provided in Appendix G.



During the initial site characterization studies,  $K_d'$  values were determined for samples consisting of shales from the various layers. During the SDCP investigation, adsorption and desorption  $K_d$  and  $K_d'$  values were determined for shale samples as well as for selected soil materials. During the initial studies it was also assumed that the amount of arsenic contained in the mineralogical fraction of the samples would be small and that the majority of arsenic in the samples would be sorbed to the shale matrix. During the subsequent desorption tests two extraction methods were employed in the analysis of the solid phase in order to validate this assumption. If a large fraction of the arsenic in a sample is present as a distinct mineral phase and therefore not available for desorption, then desorption experiments followed by a total digest could give artificially elevated values for  $K_d'$ . Data presented in Table 5-5 suggest that this may be the case. Values for  $K_d'$  determined using the hydroxylamine hydrochloride extraction, which targets iron and manganese (hydr)oxides are between 10 and 100 time lower than those determined with the 3050 digestions. Since it is likely that the majority of sorbed arsenic would partition with the oxide fraction, these data suggest that a large portion of the arsenic in these samples is not sorbed, but rather is present as a distinct mineral phase. This was true for both shale and soil samples and thus also indicates that arsenic  $K_d'$  values used in the original transport modeling were not representative of actual site conditions. Greater  $K_d'$  values observed in the initial desorption studies suggest that there may have been a significant amount of arsenic associated with the mineral fraction. Therefore the values used previously were likely to have been unrealistically high and would not accurately describe arsenic migration under site conditions.

Uranium  $K_d'$  values determined varied considerably less between those determined with the Ha-HCl and the 3050 extractions. This suggests that a greater portion of the U present in the solids was actually sorbed versus present as a distinct mineral phase or sequestered within the organic fraction, or if a secondary U-mineral phase is present it was also released with the oxide fraction. In general,  $K_d'$  values determined for uranium during the SDCP studies, which range from 258 to 4,212 and 108 to 2,176 for Ha-HCL and 3050 extractions respectively, were higher than those determined in the initial tests using only shale samples.

### 5.5.2 Results From Batch Adsorption Tests

$K_d$  values determined for arsenic using traditional batch adsorption tests ranged from 331 to 817 mL/g for the samples tested (Table 5-5). In general this is lower than the  $K_d'$  values determined in the previous study using shale materials and about an order of magnitude greater than those determined on similar samples during this study with the Ha-HCl extraction procedure. Even when comparing results from a single sample (005-04S-1) the  $K_d$  and  $K_d'$  values determined with the batch adsorption and desorption procedures varied over two orders of magnitude.

Uranium  $K_d$  values from adsorption studies varied less from values determined in desorption tests than did the arsenic partition coefficients derived from the two procedures.  $K_d$  values for uranium determined from adsorption tests varied from 572 to 2,340 mL/g, which compares closely with those determined on like samples in desorption tests (Table 5-5). In general, they are slightly higher than those determined for shale samples during the initial characterizations studies, which ranged from 11 to 286 mL/g (Table 5-2).

### 5.6 Results of Site Groundwater Geochemical Modeling

Geochemical modeling of selected site groundwater was undertaken to further assess the validity of the  $K_d'$  values by comparing U and As speciation in site groundwater to the laboratory conditions under which the  $K_d'$  values were determined. In addition, geochemical modeling can provide insight into the potential mechanisms that may be controlling U and As migration through the shales. The results of the detailed groundwater sampling conducted on the nine wells in June 2001 are given in Table 5-6. Examination of filtered (dissolved) versus unfiltered (total) concentrations of Fe, Al, and Mn, indicate that, in most cases, the unfiltered values are substantially higher than those from filtered samples, for these elements. This indicates that there are suspended colloids in the groundwater that have the potential to aid in the movement of adsorbed metals, such as As and U. The presence of suspended colloids of Al, Fe, and Mn (presumably occurring in their oxide and/or hydroxide forms) are an indicator of relatively oxidizing conditions in the groundwater. However, comparison of the filtered versus unfiltered values for As and U do not indicate that colloidal transport is a significant mechanism for migration of these constituents through the hydrologic unit. The inability to detect  $S^{2-}$ , Fe(II), and

$\text{NH}_3\text{-N}$  in most samples is consistent with measured Eh values of those samples and are indicative of oxidizing conditions. Based on Eh-pH stability diagrams (Brookins, 1988) both U and As are expected to exist in their oxidized aqueous forms, uranyl ( $\text{UO}_2^{2+}$ ) and arsenate ( $\text{AsO}_4^{3-}$ ) for U and As, respectively. However, historical data (Table 5-7) shows that at some locations reducing conditions exist where elevated concentrations of iron and manganese can be found. Reducing conditions should tend to increase the mobility of arsenic via the reduction of Fe and Mn (hydr)oxides to which the arsenic is presumably sorbed. In contrast, reducing conditions will tend to limit the migration of uranium as U(VI) is reduced to U(IV) and precipitated as uraninite ( $\text{UO}_2$ ) (Lovley and others, 1991).

The results from the detailed groundwater sampling that occurred in June 2001 (Table 5-6) were input into the geochemical speciation model PHREEQC. The resulting SI values indicate that common potential minerals controlling U, As, Ra, and F solubility are undersaturated in the site groundwater (Table 5-3). The results from PHREEQC using groundwater quality data from the June 2001 sampling also indicate that virtually 100 percent of the U in groundwater at the locations sampled exists in the oxidized form, U(VI). Undersaturation was also observed for  $\text{RaSO}_4$ , eliminating this solid as a control on Ra-226 mobility. This observation is consistent with those of Langmuir and Riese (1985), who point out that concentrations of Ra in waters affected by U milling are usually not high enough to reach saturation with respect to  $\text{RaSO}_4$ ; rather, Ra concentrations in solution are limited to adsorption to mineral surfaces or co-precipitation with other solid phases.

Similarly for As, the selected groundwater is calculated to be undersaturated with respect to the common As minerals, such as the Al-, Fe-, and Ca-arsenates (Table 5-3). Therefore, bulk groundwater conditions as measured at these nine sites are similar to the conditions under which the  $K_d$  values for As were derived in the laboratory. The PHREEQC modeling results (Table 5-8) also indicate that virtually 100 percent of the total As in solution exists in the oxidized aqueous arsenate form ( $\text{AsO}_4^{3-}$ ). Arsenic, present as arsenate in groundwater and during determination of  $K_d$  values, is controlled by adsorption to mineral surfaces, and not generally controlled through precipitation of discrete As-bearing solid phases. However, subsequent tests conducted during the SDCP in 2002 indicate that a significant fraction of As in the solid phase is

not amenable to extraction by hydroxylamine hydrochloride and therefore not likely to be associated with the Fe and Mn oxide fraction. This would suggest that while current site conditions do not support As mineral precipitation that a substantial fraction of the As incorporated in the shales is present as a discrete mineral phase or associated with a non-oxide fraction. The SI values in Table 5-3 also show that most of the bulk groundwater is undersaturated with respect to  $\text{CaF}_2$  and therefore generally conservative behavior for F, similar to  $\text{NO}_3$ , is expected.

The calculated aqueous distributions of the dominant U(VI) and As(V) solution species are presented in Table 5-8. The results indicate that the aqueous speciation of As is dominated by  $\text{H}_2\text{AsO}_4^-$ . Dissolved  $\text{F}^-$  tends to be associated with Al in the lower pH waters (below  $\text{pH} = 5.5$ ); in higher pH waters, where dissolved Al is low, F exists as the mobile  $\text{F}^-$  anion. Aqueous U(VI) indicates that U(VI) exists predominantly as negatively-charged carbonate complexes (Table 5-8). In the presence of P, U may also exist as negatively charged phosphate complexes. Only in areas of low pH (below a pH of approximately 5.0) is the dissolved U species expected to be dominated by  $\text{UO}_2^{+2}$  (Table 5-8; Langmuir, 1997).

## 5.7 Distribution of Constituents of Concern

The key COCs identified by SFC for this study are arsenic, natural uranium, nitrate and fluoride. The current distributions of these COCs were estimated for each hydrostratigraphic unit using the data collected as part of this geochemical study as well as sample data collected in April, June, and August 2001. Isopleth contour maps showing distribution of COCs is provided in Figures 5-12 through 5-35. Ninety-five monitoring wells have been constructed appropriately to monitor a single hydrostratigraphic unit. Sample data from these wells were primarily used to determine the distribution of the COCs. All other Facility wells have been determined to be constructed such that the well screen and/or filter pack connect more than one hydrostratigraphic unit and, therefore, are not representative of any one unit. Because of the sparse amount of appropriately constructed wells in the hydrostratigraphic units, most notably Unit 3 and 4 shales, data from 46 wells not completed in a single hydrostratigraphic unit were used to supplement the estimation of the distribution of COCs. Table 5-9 presents the wells used to estimate the distribution of the COCs, including wells that were completed in a single hydrostratigraphic unit

(Primary Wells), along with other monitoring wells used for estimation of distribution of COCs (Secondary Wells). Table 5-9 summarizes the hydrostratigraphic units used in the distribution estimate (Completion), sample dates, and the water quality data from wells used in the distribution estimate. Original analytical data is available through SFC upon request.

Figures 5-12 through 5-17 show that nitrate exceeds the maximum contaminant level (MCL) of 10 mg/L in Unit 1 through 4 shales. Nitrate concentration in groundwater is especially high (between 1,000 and 10,000 mg/L in Unit 2, 3, and 4 shales centered on the southwest corner of Pond 2, and in Unit 3 and 4 shales in the Fertilizer Pond Area. Nitrate in the Fertilizer Ponds have probably significantly impacted groundwater in Unit 1 and 2 shales, however a lack of any appropriately completed wells in Unit 1 and 2 shales preclude an estimation of the distribution of nitrate in those units in the Fertilizer Pond Area. Nitrate concentrations exceeded the MCL in five alluvium wells.

Figures 5-18 through 5-23 show that uranium exceeds the site-specific DCGL of 100 µg/L (U.S Department of Defense and others, 2000) in Unit 1, 2, and 3 shales. In Unit 1 and 2 shales, uranium exceeds the DCGL in three relatively small areas, one centered just northeast of the SX Building, one centered on the southeast corner of the MPB, and one centered on Solid Waste Burial Area No. 2. In Unit 3 Shale, uranium exceeds the DCGL in two very small areas, one just east of the SX Building and one just northeast of Solid Waste Burial Area No. 2. The highest uranium concentrations are found in groundwater near the SX Building. Uranium concentrations exceeding the DCGL were not recorded in any area outside of the Process Area.

Figures 5-24 through 5-29 show that arsenic exceeds the MCL of 0.05 mg/L in Unit 1 through 4 shales. In Unit 1 Shale, arsenic exceeds the MCL in two broad areas, one crescent-shaped area centered on the Emergency Basin, and another in the southern portions of the Process Area. In Unit 2, 3, and 4 shales, arsenic exceeds the MCL broad areas centered on the southwest corner of Pond 2. Highest arsenic concentration recorded was 3.35 mg/L, in MW-057A, near the southwest corner of Pond 2. Arsenic concentrations exceeding the MCL was not recorded in any well completed in Unit 4 Shale west of the Process Area, nor in the alluvium in the southwest portions of the Facility.

Figures 5-30 through 5-35 show that fluoride exceeds the MCL of 4 mg/L in only a few relatively small, isolated locations in Unit 1 through 4 shales. In Unit 1 Shale, fluoride exceeds 4 mg/L near the southeast corner of the North Ditch and also just north of Clarifier A Basin 1. In Unit 2 and 3 shales, fluoride exceeds 4 mg/L in a small area centered on the southwest corner of Pond 2. In Unit 4 Shale, fluoride exceeds the MCL in a small area just east of Fluoride Holding Basin No. 1. Maximum fluoride concentration recorded was 7.6 mg/L.

Fluoride concentrations only slightly exceed the MCL in very limited, small areas of the shale units in the Industrial Area. Fluoride also behaves conservatively and is relatively mobile in groundwater, therefore the fluoride derived from any available higher concentration source will tend to be readily diluted with groundwater concentrations below the MCL. From the sources available, fluoride will not impact any surface water exposure point with concentrations above the MCL, therefore fluoride will be removed from any further consideration as a COC.

## 5.8 Conceptual Geochemical Model

Processing operations at the SFC Facility utilized yellowcake ( $U_3O_8$ ) in the stepwise production of  $UF_6$ . Intermediate solid compounds such as  $UO_2(NO_3)_2$ ,  $UO_3$ ,  $UO_2$ , and  $UF_4$ , were produced. Various chemicals, such as  $H_2SO_4$ ,  $HNO_3$ ,  $HF$ ,  $NH_3$ ,  $BaCl_2$ ,  $CaO$ , and limestone were stored on-site and used in the process. Major by-products of the operation were  $NH_4NO_3$ ,  $CaF_2$ , and raffinate sludge. During the operative years, known releases of  $UO_2(NO_3)_2$ ,  $NH_3$ ,  $NH_4NO_3$ , and As occurred from corrosion of storage containers, overflows, on-site burial of wastes, and leakage from unlined ditches and storage ponds. Neutralization of scrubber water with limestone was another source of aqueous F, U, and elevated in Ca and Mg. The U, As, F, and N released were predominantly in their oxidized, mobile forms and a portion of these constituents migrated into shale units of the terrace and shallow bedrock groundwater system beneath the Facility.

Mineralogical analyses of the shale units indicate that the reactive minerals present are largely phyllosilicate clays. Phyllosilicates exhibit negatively-charged edge surfaces that are capable of retaining cations through electrostatic forces (Bohn and others, 1985). Based on the predominance of phyllosilicate clays in the shale, ion exchange is likely an important process controlling constituent migration through the hydrologic units. Hydrrous ferric oxide is

undoubtedly present in the shales (as indicated by brown and yellow colors), but was not identified in the mineralogical analysis due to the low concentrations. However, extractions performed on samples during the SDCP using hydroxylamine hydrochloride indicate that there is a significant amount of Fe and Mn in the oxide fraction. Hydrous ferric oxide is a naturally dominant adsorbent because of its tendency to be finely dispersed and to exist as both ubiquitous coatings on mineral particles and as discrete oxide particles (Jenne, 1968; Dzombak and Morel, 1990).

Due to the high influx of Ca-rich and Mg-rich waters (Mg most likely being present as an impurity in limestone) into the shale units, groundwater at the site exhibits a distinctly different ionic composition compared to upgradient water. Figure 5-36 shows that the upgradient water (MW-110) is a Na-SO<sub>4</sub> type water, and hydrological unit materials upgradient are in equilibrium with this water. Site groundwater, however, is Ca-Mg-SO<sub>4</sub> type water, with a few waters having a high percentage of Cl as the anion component (Figure 5-36). The results of the batch tests indicate that as upgradient water moves through the hydrological unit, exchange of Na will occur for Ca (and to a lesser extent, Mg), removing Na from solution and releasing Ca + Mg (Figure 5-11). As the exchange sites on the clays continue to equilibrate with fresh upgradient water, the water will trend back toward Na-SO<sub>4</sub>-type water. Sulfate concentrations remain relatively constant due to their control by gypsum solubility.

Of the contaminants of concern, U, As, F, and N were released primarily in their oxidized forms during process operations. Nitrogen, primarily as NO<sub>3</sub>, may be biologically reduced but in the absence of organic carbon, tends to behave conservatively in groundwater. Analytical results for NO<sub>2</sub><sup>-</sup> and NH<sub>3</sub>-N at the nine wells examined in the 2001 sampling indicate, however, that only very limited N reduction occurs (Table 5-6). Similarly, F is not strongly adsorbed, and is very mobile in groundwater when not controlled by CaF<sub>2</sub> precipitation, as shown in Table 5-3.

During the initial characterization studies modeling of groundwater collected from a limited set of wells suggested that arsenic exists primarily in various protonated forms of arsenate [As(V)] (Table 5-8). The adsorptive capacity of hydrous ferric oxide and of functional groups on surfaces of other oxide minerals is high (Pierce and Moore, 1982) and therefore high K<sub>d</sub>' values were measured for As during the initial study (Table 5-2). However, as described above,

elevated levels of As associated with the mineral fraction of the samples likely resulted in artificially high  $K_d'$  values during the initial studies. As previously noted, these high  $K_d'$  values did not appear to accurately reflect As transport at some locations at the site. Specifically, this was true for elevated levels of As observed at well MW095A. One possible explanation for this anomaly was the formation and migration of organic-arsenic complexes. SFC personnel have indicated that significant amounts of the organic compounds tributylphosphate ( $C_{12}H_{27}PO_4$ ) and hexane ( $C_6H_{14}$ ), which were associated with the solvent extraction process, were deposited in Pond 2. This has led to speculation that the arsenic in Pond 2 may have formed organic-arsenic complexes or possibly ammonium-arsenic complexes that could migrate at a less retarded rate than the uncomplexed arsenic. Therefore, analytical testing of water samples for arsenic speciation (As III, As V, monomethylarsonic acid [MMAs], dimethylarsinic acid [DMAs], thioarsenates, and other organoarsenicals) was undertaken. Results from these studies proved inconclusive, however, due to analytical problems encountered during attempts to quantify the As species present. Details of these studies and results are provided in Appendix G. A second possibility is that organic compounds entering the aquifer produced reducing conditions. Naturally occurring arsenic compounds, such as, scoridite and As sorbed to Fe and Mn (hydr)oxides within the shales would be mobilized under these conditions. Data presented in Table 5-7 suggests that in some areas of the site, reductive dissolution of iron and manganese oxides has resulted in increases in As concentrations. For example, wells MW042, MW059A, MW061A, MW064A, MW087, and MW102A have elevated levels of As, Fe, and Mn but concentrations of U that is below the detection limit. This is what would be expected in reducing environments as As adsorbed onto Fe and Mn (hydr)oxides is liberated by reductive dissolution reactions and U(VI) is reduced to U(IV) and precipitated as  $UO_2$ .

Geochemical modeling done during the initial investigation indicated that uranium tends to exist primarily as carbonate species, or sometimes complexed with phosphate (Table 5-8). These negatively charged species are not as strongly adsorbed and are highly soluble (Duff and Amrhein, 1996). The two primary controls on the transport of the uranyl ion are pH and carbonate concentration (Langmuir, 1997). However, in addition to ion exchange reactions, precipitation of secondary uranium mineral phases may contribute substantially to the control on U transport. A recent report published by the NRC suggests that precipitation of uranium



minerals is the primary sink for U, followed by adsorption (Jove Colon and others, 2001). These studies examined migration of uranium plumes associated with both natural U deposits and U mining and mill-tailings sites. Uranium concentrations greater than about  $10^{-6}$  molar fall within the stability fields of schoepite  $[(\text{UO}_2)_8(\text{OH})_{12}(\text{H}_2\text{O})_{12}]$  and bequerilite  $[\text{Ca}(\text{UO}_2)_6\text{O}_4(\text{OH})_6(\text{H}_2\text{O})_8]$ , which are thought to be primary controls on U migration under near neutral, oxidizing conditions. Under reducing conditions where U(IV) becomes the stable U species, uraninite ( $\text{UO}_2$ ) becomes the dominant mineral phase controlling U solubility and transport.

### 5.9 Site Complexity and Implications for $K_d$

Nearly all reaction transport models have used the partition coefficient or “constant  $K_d$ ” approach to describe the effects of sorption processes on solute transport. However, more sophisticated treatments such as Langmuir and Freundlich isotherms and surface complexation models are available that can more accurately describe these reactions (Davis and Kent, 1990; Zachara and Smith, 1994). The  $K_d$  approach is reported to work best for trace amounts of non-ionized, hydrophobic organic molecules (Stumm and Morgan, 1996) and is often too simplistic to represent sorption of ionic species within soil and sedimentary environments (Domenico and Schwartz, 1998; Reardon, 1981).  $K_d$  values for metal ions typically vary over many orders of magnitude, depending on solution pH and composition as well as the nature of the solid matrix (Davis and Kent, 1990). Thus, in complex, highly heterogeneous environments, the incorporation of a laboratory-derived  $K_d$  that can accurately reflect solute transport is problematic. Under these conditions a model-derived “transport factor” may be more appropriate. However, it should be realized that such transport factors describe the movement of contaminants under historical conditions when they are determined using historical data. As Facility conditions change (e.g. pH, saturation conditions), the transport factors will likely also change.

The Sequoyah Fuels Facility is geologically and geochemically complex and highly heterogeneous. In addition, the complex geochemical environment has evolved with time and with changes in site activity. For example, pH values measured at various locations at the Facility from 1991 to 1994 vary over seven orders of magnitude from 4.3 to 11.9 with an average

value of 7.2 (Table 5-10). These wide variations in pH dramatically affect the physiochemical properties of solid and aqueous phase constituents. Arsenate ( $\text{As}^{5+}$ ) is strongly sorbed to iron hydroxides and many clay minerals at pH values below about 7.5 but is desorbed as pH values greater than 7.5. In contrast, arsenite ( $\text{As}^{3+}$ ) while tending to adsorb less strongly at low pH values, tends to remain adsorbed under more alkaline conditions (Raven and others, 1998; Pierce and Moore, 1980). Likewise, uranium also shows the greatest adsorption in the near neutral pH range, from about 6.0 to 7.5, and is sorbed to a much lesser extent outside this range (Langmuir, 1997). Thus, determination of a single  $K_d$  with laboratory experiments performed over a limited pH range cannot adequately represent a Facility with this complexity.

While somewhat limited with respect to certain parameters, historical water quality data suggest that redox conditions also change significantly across the Facility. Changing redox chemistry is also likely to affect the mobility of arsenic and uranium. Under oxidizing conditions, As(V) and U(VI) are expected to be the predominant species present, whereas under reducing conditions As(III) and U(IV) should be the stable species. As previously noted, the adsorptive properties of arsenic vary considerably for the oxidized and reduced forms due to the ionic species each forms. The oxidized and reduced forms of uranium also exhibit dramatically different geochemical properties. The oxidized uranyl ion forms numerous aqueous complexes with carbonate, phosphate, fluoride and sulfate. The uranyl carbonate complexes are responsible for much of the observed uranium transport in oxidized neutral pH environments (Langmuir, 1997). In contrast, the reduced uranous ion, while also capable of forming aqueous complexes tends to form solid phase products with limited solubility (e.g. uraninite [ $\text{UO}_2$ ]). Thus, mildly reducing conditions, which is typical of metal reduction (e.g. manganese, iron, and uranium) will tend to cause the precipitation and sequestration of uranium. In contrast, the reduction of manganese and iron (hydr)oxides under these conditions would tend to release arsenic that is sorbed to these manganese and iron phases. Under more strongly reducing conditions (e.g. sulfidogenic) arsenic can also be expected to form highly insoluble arsenic sulfide and be removed from the aqueous phase.

An additional complication is the potential for mineral precipitation reactions to take place under field conditions with changes in soil moisture content (e.g. as conditions go from saturated to

unsaturated), which cannot be duplicated in the lab. Localized interfacial precipitation of secondary uranyl minerals in undersaturated fluid conditions is thought to be a plausible mechanism for explaining the formation of these phases associated with natural ore deposits (Jove Colon and others, 2001). Analysis of numerous uranium plumes has lead to the conclusion that U migration over the short-term is limited by sorption and precipitation reactions along with dilution. Over the long-term, weathering processes and formation of secondary uranyl mineral phases appears to limit the extent of uranium transport. These control factors are unlikely to be duplicated with laboratory experimentation.

From the above-described geochemical considerations, it should be evident that describing the transport of an ionic species with a laboratory derived  $K_d$  is difficult, if not impossible. Thus, a more appropriate method to describe the transport of arsenic and uranium for a site as complex as the SFC Facility is via a model-derived transport factor, which incorporates numerous geochemical and hydrodynamic processes.

## **6.0 SITE GEOLOGIC, HYDROGEOLOGIC AND GEOCHEMICAL CONDITIONS**

Based on data from this recent site investigation and previous studies, the following describes the current understanding of the geologic, hydrogeologic and geochemical conditions at the SFC Facility.

### **6.1 Regional Physiographic and Geologic Setting**

The Sequoyah Fuels Corporation property is located near the northern edge of the Arkoma Basin, on the southwest flank of the Ozark Uplift (Figure 6-1). The Arkoma Basin is an arcuate structural depression that extends from the Gulf coastal plain in central Arkansas westward to the Arbuckle Mountains in south central Oklahoma. The Ozark Uplift is a large structural feature extending from east central Missouri to northeast Arkansas and northeast Oklahoma. For geographic reference, the Ouachita Mountains are about 50 miles south of the site. Bedrock formations underlying the area consist of Ordovician, Silurian, Devonian, Mississippian, and Pennsylvanian- aged rocks, mostly limestones, shales, and sandstones. A regional geologic map is presented in Figure 6-2. A regional stratigraphic column correlating upper Mississippian and lower Pennsylvanian formations and members in Arkansas and Oklahoma is presented in Figure 6-3. The Facility lies in an area of facies transition from the southwestern Ozark region to the Arkoma Basin. A passive, continental margin existed in the area of the Facility between the Cambrian through Mississippian, and rocks deposited during that time represent shallow continental shelf sediments, mostly limestones and dolomites with some terrestrial clastic sediments derived from the Ozark region to the north. By Pennsylvanian time, a northward-advancing continental terrain to the south created a convergent plate margin, and the region was warped, creating a foreland basin above the stable continental craton. Sandstones, siltstones, and shales accumulated in fluvial, delta, and tidal flat systems that prograded southwestward from sources to the north and the northeast (the Ozark region).

Geological formations regionally dip southwest to southeast (SFC, 1997, Miller and others, 1989), at dips of less 20°, and commonly at only one or four degrees. The most prominent structural feature in the immediate area of the Facility is the Carlile School Fault (CSF), which trends northeast to southwest and is located approximately 5,000 feet southeast of the MPB

(Figure 6-4). The CSF is a nearly vertical normal fault, downdropped to the south. The fault is less than one mile in length, and has a displacement of less than 100 feet. The plane of the fault is not exposed, but it is revealed as a series of low, hummocky, parallel erosional ridges, consisting of nearly vertical beds of sandstone. The fault lies hydrologically upgradient and geologically up-dip from the Process Area. There is no surface evidence that the CSF connects with any other faults. The Marble City Fault, located approximately 2.5 miles south of the MPB (Figure 6-4), is in the area of the Mulberry Fault, one of the primary structural features identified by the Oklahoma Geological Survey. Both structures were developed in early Pennsylvanian time, and are not considered to be capable faults (NRC, 1998). The most recent documented subsurface movement in the region has occurred within the last 2,000 years along the Meers Fault System in southwest Oklahoma. This fault system is consistent with measured seismic events, and is approximately 200 miles from the Facility. Measured seismic activity is concentrated in south-central Oklahoma corresponding with the Meers Fault System and the central Oklahoma Fault Zone, over 150 miles from the Facility. The most significant recent regional tectonic movement occurred in the New Madrid area of Missouri, during the first half of the 19<sup>th</sup> century. Based on general seismicity information, the Facility is within a region of low seismicity, classified as a Zone 1 area by COE (1982).

## **6.2 Site Physiography and Geology**

The Facility is situated on gently rolling to level land, bounded on the west by the Arkansas and Illinois Rivers and to the north by the Salt Branch. Elevations on or near the Facility range from 460 feet amsl at the Illinois River to about 585 feet amsl near the northeast corner of the property (Figure 6-5). The Process Area is situated on a broad, local topographic high that extends eastward from the Process Area and has elevations of greater than 540 feet. The land surface drops steeply to the north, west, and southwest of the Process Area. Slopes on upland areas are generally less than about seven percent. The steeper slopes in the creek ravines and on hillsides surrounding the Industrial Area average about 28 percent. Several small, intermittent streams that flow outward from the Process Area bisect the property. Most of the streams that flow westward from the Industrial Area are relatively short and incise deep ravines before reaching the Robert S. Kerr Reservoir. Streams that trend southward from the Facility tend to form

relatively shallow channels before turning westward towards the Robert S. Kerr Reservoir. Relatively low-lying and level land occurs south and west of the Fertilizer Pond Area.

The bedrock immediately underlying the site includes the sandstones, siltstones, and shales of the Pennsylvanian-age Atoka Formation (Figure 6-2). The Pennsylvanian-age Wapanuka Limestone underlies the Atoka Formation. The Atoka Formation is overlain by Quaternary-age unconsolidated sediments, including terrace deposits, which occur primarily in the Process Area, colluvium on the slopes extending outward from the Process Area, and alluvial deposits adjacent to the Arkansas River. Soils are ubiquitous throughout the site, consisting mostly of loams and silty loams up to about six feet thick. Man-made fill material is present in various areas, mostly in the Process Area and as surface impoundment material south of the Process Area.

#### **6.2.1 Soils**

Soils on the site consist mostly of loams and silty loams. Soil thickness range from zero to approximately six feet, and are commonly about one to two feet thick (SFC, 1997; this study). A detailed description of Facility soils is given in the Final RFI (SFC, 1997). The soils consist mostly of clay and silt, and are similar lithologically to underlying terrace, alluvium, or colluvium deposits. Because of this similar lithology, the hydrologic properties of the soils are believed to be similar to the underlying terrace, alluvium, or colluvium deposits, and the soils were not differentiated from the underlying deposits.

#### **6.2.2 Fill Material**

Small amounts of fill material are found in various locations on the Facility (SFC, 1997). Fill material within the Process Area is found within buried utility lines, and as a sub-base to concrete floors, concrete and asphalt roads, and concrete storage pads. The fill material within buried trenches ranges from 0 to 20 feet thick, and consists mostly of silty sand and silty gravel, overlain by silty clays and/or weathered shale fill. Fill material beneath concrete floors, concrete pads, and roadways have a maximum thickness of about 1.5 feet, and consists mostly of silty sand, sandy clay, sandy gravel, silty clays, and weathered shale. Fill material is also found in surface impoundment dikes throughout the property. Impoundment dikes reach a thickness of up

to 20 feet and consist mostly of clayey silts with minor amounts of gravel in some impoundments. The fill material consists mostly of clay and silt, and is similar lithologically to underlying terrace, alluvium, or colluvium deposits.

### **6.2.3 Terrace Deposits**

Unconsolidated deposits overlying Unit 1 Shale are identified as terrace deposits. Quaternary-age terrace deposits consist mostly of clay and silts, with lesser amounts of sandy silts, silty clays, gravelly silty clays, gravelly sandy clays, gravelly clays, and silty sandy clays. Terrace deposits are remnants of alluvial deposition during Pleistocene high water stages of the Illinois and Arkansas Rivers. Subsequent downcutting of these river systems has left these deposits high above present day river valleys. Terrace deposits range from 0 to 16.5 feet thick, averaging about 8 feet thick throughout the Process Area. Terrace deposits are relatively thicker just to the southwest of the MPB, but thin rapidly to less than 2 feet north of the MPB. Terrace deposits exceed 10 feet in thickness in the north-central part of the Process Area, including the Sanitary Lagoon, Emergency Basin, North Ditch, the Interim Storage Cell, and the DUF<sub>4</sub> Building. Terrace deposits also exceed 10 feet in thickness in the area of the Sub-Station and extending eastward from the Process Area.

### **6.2.4 Alluvium**

Fluvial deposits associated with recent (Holocene) activity of the Illinois and Arkansas Rivers are identified as alluvium. Alluvium is found primarily in the southwest portions of the site, adjacent to the Illinois/Arkansas River. Alluvium consists mostly of silt, silty clay, and sandy gravel, with lesser amounts of silty sand and gravel. Alluvium thickness ranges from 0 feet to greater than 35 feet thick, with the greatest thickness found near the westernmost extent of the site boundaries. The alluvium ranges from about 15 to about 25 feet thick in the Agland area west and southwest of the Fertilizer Pond Area.

### **6.2.5 Colluvium**

Colluvium deposits include all unconsolidated sediment in the site not identified as either terrace or alluvium deposits. These deposits include, but are not limited to, fluvial deposits along

smaller streams and outflows, subaerial sediment gravity flows and mass waste deposits, found mostly on the slopes surrounding the Process Area and in outfall drainages, and in-situ deposits formed by breakdown of older rocks by weathering and erosion. Colluvium typically consists of silts, clays, and/or sands with varying amounts of gravel. Colluvium thickness ranges from 0 to over 20 feet; most colluvium deposits are less than 6 feet thick. The colluvium deposits with the maximum thickness are found in stream drainages south of the Fertilizer Pond Area. Colluvium deposits found on the slopes adjacent to the Industrial Area tend to be fairly thin, and are generally less than 3 feet thick.

#### **6.2.6 Akota Formation**

The geologic units that directly underlie the Facility are a series of alternating shale and sandstone units of the Atoka Formation. Locally, the near surface members of the Atoka Formation have been named, in order of descending stratigraphic position, Unit 1 Shale, Unit 1 Sandstone, Unit 2 Shale, Unit 2 Sandstone, Unit 3 Shale, Unit 3 Sandstone, Unit 4 Shale, Unit 4 Sandstone, and Unit 5 Shale. Data from injection monitor well, 2331, located just east of Clarifier A, indicates a series of alternating shales, sandstones, and siltstones to approximately 390 feet bgs. The Spiro Sandstone is the basal member of the Atoka Formation (Sutherland, 1988), and locally occurs from about 300 to 390 feet bgs and is a salt-water bearing unit (SFC, 1997). The base of the Atoka Formation lies unconformably on the Wapanucka limestone (Figure 6-3). The nearest surface exposure of the Wapanucka limestone occurs approximately 10 miles northeast of the facility (SFC, 1997).

The Unit 1 Shale is grayish black to dark grayish brown, soft, fissile, typically silty and sandy near contact with underlying sandstone. Typically Unit 1 Shale is highly weathered, weathering to a brownish or reddish yellow clay or silty clay with remnants of laminated, gray shale. XRD analysis shows Unit 1 Shale consists of quartz, chlorite, interstratified chlorite-smectite, and illite. Unit 1 Shale is laterally continuous under much of the central and eastern portion of the Industrial Area, and extends eastward from the Industrial Area. Unit 1 Shale attains a maximum thickness of approximately 14 feet in the northeast corner of the Yellowcake Storage Area. Unit 1 Shale exceeds 10 feet thick in most of the Yellowcake Storage Area, centered on and northeast of the MPB, and in a small area east of the south guardhouse. An outlier, up to 15.5 feet thick, of



Unit 1 Shale is found near the northern end of the Facility. This outlier and two other thin outliers in the Fertilizer Pond Area are clearly isolated from the main body of Unit 1 Shale residing in the Industrial Area.

The Unit 1 Sandstone is a quartz arenite, consisting of greater than 90 percent very fine to medium grained, subrounded to rounded quartz, with occasional minor silt and gravel. Unit 1 Sandstone is typically pale brown to dark gray, hard to very hard, and is highly cemented with calcite, iron oxide, and/or silica cement. Near contact with underlying Unit 2 Shale, Unit 1 Sandstone commonly becomes silty, poorly cemented, and soft. The Unit 1 Sandstone ranges from very slightly to highly fractured, with the most intensely fractured sandstone containing closely spaced (<2 cm spacing) wide (0.5-1mm) fractures. Fractures are unfilled or calcite filled. Unit 1 Sandstone underlies most of the Industrial Area, extends eastward from the Industrial Area, and is found as an isolated outlier under the Fertilizer Pond Area. Unit 1 Sandstone is thickest in the SX Building area. Unit 1 Sandstone exceeds four feet in thickness in an area centered on the SX Building and extending southeastward to the south guardhouse, and in another small area centered on the northeast corner of Pond 2. Typically Unit 1 Sandstone is between 2 and 3 feet thick, and thins rapidly at its outer edges.

Unit 2 Shale is dark gray to grayish black, soft, fissile, and commonly silty or sandy, with occasional, thin sandstone lenses. Unit 2 Shale is highly weathered, weathering to a yellow brown or brownish gray clay or silty clay with remnants of laminated, gray shale. The clay tends to be very soft, plastic, and moist. XRD analysis shows that Unit 2 Shale consists of quartz, chlorite, and illite. Unit 2 Shale is laterally continuous under most of the Industrial Area, extending westward to the Facility boundary, south to the Fertilizer Pond Area, and east and southeast of Highway 10. Unit 2 Shale is partially bisected by the 001, 005, and 007 streams. Unit 2 Shale is commonly between 4 and 6 feet thick, with a maximum thickness east of the Industrial Area. Unit 2 Shale exceeds 8 feet in thickness in an area along the northernmost part of the site, and in a small area in the northeast portion of the Fertilizer Pond Area. Unit 2 Shale is generally thinner than 3 feet in the easternmost portions of the Industrial Area.

Unit 2 Sandstone is a quartz arenite, consisting of greater than 90 percent very fine to fine grained, subrounded to rounded quartz, with little to no silt or gravel. Unit 2 Sandstone is

typically brownish gray to very dark gray, moderately hard to very hard, and is highly cemented, mostly with silica cement. Unit 2 Sandstone becomes shaley near the contact with the underlying Unit 3 Shale. Unit 2 Sandstone ranges from slightly to highly fractured, with the most intensely fractured sandstone containing closely spaced (<2 cm spacing) wide (0.5-1mm) fractures. Fractures are unfilled or filled with clay or calcite. Like Unit 2 Shale, Unit 2 Sandstone is laterally continuous under most of the Industrial Area, extending westward to the Facility boundary, south to the Fertilizer Pond Area, and east and southeast of Highway 10. Unit 2 Sandstone is partially bisected by the 001, 005, and 007 streams and is generally thickest along the eastern boundary of the Facility. The thickness exceeds 10 feet near Fertilizer Pond 4 (maximum thickness of 14 feet), south of the Decorative Pond, south of the DUF<sub>4</sub> building, and just north of the northeast corner of the Industrial Area. Unit 2 Sandstone is over 6 feet thick in large areas near the Fertilizer Pond Area, south and southeast of the Decorative Pond, and in the northern portions of the Industrial Area. Unit 2 Sandstone is generally less than 4 feet thick west and southwest of the SX Building, and on site east of the Facility boundary.

Unit 3 Shale is dark gray to grayish black, soft, fissile, and commonly silty or sandy, with occasional, thin sandstone lenses. Unit 3 Shale weathers to a yellow brown or olive brown clay or silty clay with remnants of laminated, gray shale. The clay tends to be very soft, plastic, and wet. XRD analysis shows that Unit 3 Shale consists of quartz, chlorite, and illite. Unit 3 Shale is laterally discontinuous within its areal limits, commonly grading laterally to a shaley sandstone before pinching out entirely in some locations. Unit 3 Shale extends westward to the Facility boundary, south to the Fertilizer Pond Area, and east and southeast of Highway 10. Unit 3 Shale is partially bisected by the 001, 005, and 007 streams, is commonly between 2 and 4 feet thick, and is thickest south of the DUF<sub>4</sub> building (maximum 18.5 feet thick). Unit 3 Shale exceeds 6 feet thick in only two other locations, an area west and southwest of Pond 2, and in the Yellowcake Storage Area. Unit 3 Shale pinches out and is completely missing in a large area extending southward from the southeast corner of the Industrial Area, and in smaller areas centered on the Fluoride Clarifier, the Emergency Basin, the northwest corner of Pond 2, and Pond 6.

Unit 3 Sandstone is a quartz arenite, consisting of greater than 90 percent very fine subrounded to rounded quartz, with little to no silt or gravel. Unit 3 Sandstone is typically gray to very dark gray, moderately hard to very hard, and is highly cemented, mostly with silica cement. Unit 3 Sandstone is generally massive with occasional, very tight fractures, commonly calcite cemented. Unit 3 Sandstone commonly becomes shaley near the contact with the underlying Unit 4 Shale. Unit 3 Sandstone is laterally continuous under most of site, except for the southwest and southernmost portions of the property, where it is not found. Unit 3 Sandstone is slightly bisected by the 005 and 007 streams, and is bisected by the 001 Stream under the storm water reservoir (Figure 4-1). Unit 3 Sandstone is commonly between about 4 and 8 feet thick, and is thickest in the central and eastern portions of the Industrial Area, where it exceeds 10 feet. Maximum thickness (15.6 feet) of Unit 3 Sandstone is found near the northeast corner of the Administration Building. Unit 3 Sandstone also exceeds 10 feet thick southwest of the Pond 2 and in the easternmost portions of the SFC.

Unit 4 Shale is dark gray to black, soft to very soft, and very thinly laminated to fissile. Unit 4 Shale weathers to a yellow brown to light brown silty clay with remnants of laminated, gray shale. Unit 4 Shale commonly becomes hard, brittle, and sandy near its base. Thin intervals of very hard, pyritized Unit 4 Shale are found at widely scattered locations, mostly east of the Industrial Area and south of the Fertilizer Pond Area. XRD analysis shows Unit 4 Shale consists of quartz, chlorite, and illite. Unit 4 Shale is laterally continuous throughout most of the site, and ranges from 0 feet thick at the southwest corner of the property, to almost 40 feet thick under the hill at the southernmost Facility boundary. Under most of the Industrial Area Unit 4 Shale is between 16 and 18 feet thick, and is between 13 and 19 feet thick under most of the Fertilizer Pond Area. Unit 4 Shale exceeds 20 feet thick in the following areas, in the southernmost Pond 2, the Agland area, the northwest corner of the property, and in the southernmost portions of the property.

Unit 4 Sandstone is a quartz arenite, consisting of greater than 90 percent very fine, subrounded to rounded quartz, with little to no silt or gravel. Unit 4 Sandstone is typically light gray to dark gray, hard to very hard and dense. Unit 4 Sandstone is slightly to moderately fractured, and most commonly contains widely to very widely spaced, thin, calcite filled fractures. Unit 4 Sandstone

is laterally continuous under most of site, and is commonly between about 8 and 14 feet thick. Unit 4 Sandstone is thickest (about 18 feet thick) along the Illinois River just south of the 005 Stream, and is less than 8 feet thick north of the Fluoride Holding Basin No. 2, and at the southwestern portion of the property.

Unit 5 Shale is dark gray to grayish black, soft, and fissile. Unit 5 Shale is laterally continuous under the site. Ten boreholes have penetrated Unit 5 Shale, and based on this limited lithological data, the thickness of Unit 5 Shale exceeds 22 feet under the entire Facility.

### **6.3 Regional Hydrogeology**

Regional groundwater flow in the area of the Facility is generally westward towards the Illinois or Arkansas Rivers. Groundwater in the region occurs principally in alluvium along the Arkansas and Illinois rivers and some terrace deposits along the Arkansas River. Water quality in alluvium and terrace deposits is generally good to excellent, but most of the water samples are hard to very hard (median hardness 255 parts per million [ppm]), making the water suitable for irrigation (Marcher, 1969). The only major bedrock hydrological unit near the Facility occurs approximately 10 miles northeast of the Facility in the Mississippian-age Keokuk and Reed Springs formations (Figure 6-6 and 6-6a). This hydrological unit is considered to be moderately favorable for groundwater supplies, yielding as much as 20 gpm, locally more (Marcher, 1969). The Akota Formation produces limited quantities of groundwater. Most wells in the Akota Formation yield only a fraction of a gallon per minute to a few gallons per minute (Marcher, 1969). Water quality is generally considered poor to fair, with 57 percent of the wells tested containing more than 250 ppm sulfate, 10 percent contained more than 250 ppm chloride, and 53 percent contained more than 500 ppm total dissolved solids (Marcher, 1969).

## **7.0 SITE HYDROGEOLOGIC CONCEPTUAL MODEL**

Data and interpretations generated during the course of this investigation, as well as data and conclusions presented in previous investigations at the Facility, have allowed for a development of a comprehensive site hydrogeologic conceptual model. Facility lithologic and topographic data were used to develop an extensive site hydrostratigraphic model that incorporates detailed

interpretations of the lateral extent and layer thickness of surface cover and bedrock units across the Facility. Groundwater flow and COC transport through the hydrologic units have been defined based on the review of potentiometric, hydraulic, and geochemical data. The combination of these data presents a detailed depiction of the migration of the site-derived COCs and the potential point of exposure pathways. These interpretations provide the conceptual framework on which the numerical modeling results are based.

## 7.1 Hydrostratigraphic Model

A three-dimensional hydrostratigraphic model of the shallow geology at the Facility and surrounding watershed has been developed with Environmental Visualization System (EVS) software developed by the Ctech Development Corporation. EVS incorporates a three-dimensional spatial interpolation scheme (kriging) that assigns calculated layer elevations of multiple geologic surfaces to points across a model domain grid. The model has been generated with site data and includes 10 geologic layers from surface Quaternary deposits stratigraphically down to Unit 5 Shale. The site data used to generate the model include lithologic data from boreholes, survey data from outcrop exposures, and topographic data of the ground surface. A detailed discussion of the lithologic data and the development of the hydrostratigraphic model is presented in Appendix H. EVS input and output files are presented on the CD included with this report. The lateral extent of the model is bounded on the west by Illinois and Arkansas Rivers, on the northwest by the Salt Branch drainage, and on the southeast by the drainage paralleling the Carlile School Fault.

It was observed during model development that the kriging algorithm produced significant inaccuracies near topographic surfaces. The program's tendency is to warp the subsurface geologic boundaries to mimic the topographic features of the Facility. A Fortran program, *evstrim.exe*, was created to allow independent kriging of the geologic surfaces and the alluvial/topographic surfaces. The program was used to trim the subsurface geologic model to the bottom of the alluvial layer (model layer 1) and then combines the file into one geologic model. The resulting geologic framework more accurately depicted the conceptual geologic model interpreted from site data and field observations. The *evstrim.exe* code is presented in Appendix I.

The hydrostratigraphic model is presented in Figures 7-1 to 7-8. Figure 7-1 presents a bedrock geology map of the hydrostratigraphic units that subcrop below the Quaternary surface deposits. The presence of the bedrock units is strongly dependent upon surface topography. The stratigraphically higher units (Unit 1 Shale through Unit 3 Sandstone) are only found in areas of relatively high elevation, such as in the vicinity of the Process Area. In the lower lying portions of the Facility, such as the Agland and the bottoms of drainages adjacent to the Robert S. Kerr Reservoir, the stratigraphically higher units have been eroded away, leaving stratigraphically lower units (Unit 4 Shale through Unit 5 Shale) as the uppermost bedrock units. Along the Robert S. Kerr Reservoir, Unit 5 Shale is the uppermost bedrock unit adjacent to the northern Facility, and Unit 4 Sandstone is the uppermost bedrock to the south, in the Agland area.

The terrace, colluvium, and alluvium deposits are treated as a single unit in the hydrostratigraphic model and are named Quaternary surface deposits (Figures 7-3 to 7-8). For the purpose of the hydrostratigraphic model these units are treated as a single unit because they form a relatively continuous layer of similar age that overlies older bedrock formations. It should be noted, however, that these deposits are considered to be distinct hydrologic units due to their differing depositional mechanisms and hydraulic properties.

Figures 7-3 through 7-8 present selected cross-sections of the model. The cross-section locations are presented in Figure 7-2. Sections A-A', B-B', and C-C' trend north-south, and are generally perpendicular to groundwater flow. Sections D-D' and E-E' trend east-west, and are generally parallel to groundwater flow. Section F-F' trends northeast-southwest. The general westward dip of the bedrock, towards the Robert S. Kerr Reservoir, is clearly displayed in these cross-sections.

In general, the stratigraphically higher units, Unit 1 Shale, Unit 1 Sandstone, Unit 2 Shale, Unit 2 Sandstone, Unit 3 Shale, and Unit 3 Sandstone, are relatively thin and are not laterally extensive across the model domain. Unit 1 Shale, where present, is typically about six feet thick, however near the Emergency Pond and the Yellowcake Storage Pad Unit 1 Shale is greater than 10 feet thick. The stratigraphic units from Unit 1 Sandstone downward through Unit 3 Sandstone are each generally less than three feet thick. The Unit 3 Shale frequently pinches out entirely, and

the other stratigraphically upper units commonly thin to less than one foot thick. In contrast, the deeper units, Unit 4 Shale, Unit 4 Sandstone, and Unit 5 Shale, are laterally extensive across the model domain, and typically have thicknesses greater than 10 feet.

## 7.2 Groundwater Occurrence

Groundwater originates from precipitation, irrigation and the fire water suppression system that infiltrates through the Quaternary surface cover. The fire water suppression system had numerous leaks and is estimated to supply approximately 7,500 ft<sup>3</sup>/day to the surface deposits in the Process Area. Once precipitation has entered the subsurface it migrates downward through the bedrock units and flows radially away from the potentiometric high that corresponds to the topographic high in the pastureland east of Highway 10. Subsurface flow discharges to the surface waters that surround the watershed including Robert S. Kerr Reservoir to the west, Salt Branch to the north, and the Salt Branch tributary that parallels the Carlile School Fault to the east. June 2001 potentiometric surface maps for the hydrologic units are presented in Figures 7-9 through 7-13. A conceptualized schematic of the site hydrogeology is displayed in Figure 7-14.

The stratigraphic units from the surface down to, and including, Unit 5 Shale are not connected to regional groundwater flow upgradient of the watershed defined above. Based on the hydrostratigraphic model, bedrock units above and including Unit 4 Sandstone are not laterally extensive across the Salt Branch drainage, and are therefore disconnected from upgradient groundwater flow in this area. Unit 5 Shale is partially continuous across Salt Branch, but it is likely that upgradient groundwater flow in Unit 5 Shale discharges to the Salt Branch creating a hydrologic divide. Along the Salt Branch tributary, east of the Facility, all units except Unit 4 Shale through Unit 5 Shale have been disconnected by erosion. Similar to Salt Branch, this drainage also acts as a hydrologic divide, as indicated by the Unit 4 Shale potentiometric surface map (Figure 7-12). Therefore, upgradient flow will discharge to this drainage and not impact the hydrogeology underlying the Facility.

The Carlile School Fault, where it trends through Salt Branch tributary drainage (Figure 6-4), is not significant to the Facility hydrogeology because it is located in a discharge zone of the

Facility watershed. Therefore, any groundwater being diverted or transmitted by the fault in this area would flow down drainage, away from the Facility. In the extreme southeast corner of the Facility, where the fault leaves the Salt Branch tributary, a hydrologic divide is not present. However, any flow across the fault in this area is likely to be greatly restricted by the lateral discontinuity and near vertical dip of geologic layers resulting from vertical displacement along the fault and also by the near vertical dip of the geologic layers adjacent to the fault (SFC, 1997).

Underlying the Facility, flow is generally to the west, and primarily occurs through the fissile shale units. The transmissivity of the shale units is highly heterogeneous due to large variations in unit thickness and hydraulic conductivity. The slug testing results indicate that the hydraulic conductivity varies from two to three orders of magnitude in individual shale units (Appendix J and Table 4-9). Overall the measured conductivity of the shale units ranges from 1.88 ft/day to 0.00416 ft/day. The shale conductivity is strongly dependent on the degree of fissility within the in the individual units, and the extent of the fissility in the shales appear to be spatially random. The distribution of conductivity does not appear to represent a spatial pattern, nor does it appear to be related to any geologic features at the Facility. The most poignant evidence indicating the randomness of shale conductivity is the slug test results from wells MW111A and MW114A. These wells were both completed in Unit 4 Shale, with a lateral separation of approximately 20 feet (Figure 4-1). The calculated conductivity of MW111A is more than an order of magnitude greater than the results at MW114A (Table 4-8).

Groundwater in the shale units discharge laterally to streams that flow to the Robert S. Kerr Reservoir, hillside colluvium, and/or to Arkansas/Illinois River alluvium; additionally the hydrostratigraphic model indicates that Unit 5 Shale discharges directly to the Robert S. Kerr Reservoir adjacent to the northern portion of the Facility. The horizontal hydraulic gradient in the terrace/Unit 1 Shale in the MPB area is approximately 0.008 ft/ft. In the deeper shale units, the horizontal gradient ranges from 0.01 to 0.04 ft/ft across the Facility. Groundwater in the colluvium and alluvium also discharges to the Robert S. Kerr Reservoir and its tributaries. The horizontal hydraulic gradient in the alluvium ranges from 0.0059 to 0.0081 ft/ft (Figure 7-13). Minor flow also occurs in the terrace deposits in areas where it is partially saturated.



The sandstone units are highly cemented and transmit insignificant volumes of groundwater relative to the shale units. Estimates of vertical hydraulic conductivity of Unit 4 Sandstone range from  $2.25 \times 10^{-5}$  ft/d to  $4.75 \times 10^{-5}$  ft/day (SFC, 1998a) are several orders of magnitude smaller than observed in the shale units. However, localized zones of dense, unfilled fractures have been observed in lithologic core samples, suggesting that preferential pathways through the sandstone units may exist. Because the fracture zones do not appear to be laterally extensive, it is likely that groundwater transmission through fractures in the sandstones is primarily vertical, with no significant lateral transmission of groundwater occurring.

A downward vertical gradient persists between all of the bedrock units over the majority of the Facility. The observed downward gradient ranges between 0.08 and 0.35 ft/ft. The vertical flow component is significantly smaller than the horizontal component due to the extremely low vertical conductivity of the sandstone units. Vertical groundwater flow also occurs through the hundreds of wells and boreholes that are completed in multiple shale units across the Facility. These features act as vertical conduits that hydraulically connect shale units that would be naturally buffered by the sandstone units. They are distributed over the entire Facility, excluding the Agland, but have the greatest density in the vicinity of the Process Area, Solid Waste Burial Areas, the Fertilizer Pond Area, and Pond 2.

### 7.3 COC Transport

Solute transport pathways primarily follow groundwater flow paths through the subsurface. COCs are laterally transported through the upper fractured shale units where they discharge to the hillside colluvium or directly to surface water. COC mass in the upper shale units is also discharged downward to lower shale units in localized areas where sandstone is fractured and also through the wells and boreholes that were completed in multiple shale units. Lateral COC transport through the sandstone units is negligible due to their extremely low hydraulic conductivity and effective porosity.

The movement of uranium and arsenic through the subsurface is retarded by chemical adsorption/desorption reactions that limit the respective solute velocities. The velocity of any

solute in groundwater is given by the groundwater velocity divided by the solute specific retardation factor.

Nitrate is an anion and has a negligible affinity to shales and sandstones that consist primarily of silica (no charge) and clay minerals (negative charge). As such, a conservative retardation factor for nitrate is 1, and the average solute velocity for nitrate is the same as the groundwater velocity. Nitrate, therefore, is significantly more mobile than uranium and arsenic.

## **8.0 HYDROGEOLOGIC NUMERICAL MODEL**

Groundwater flow and solute transport modeling of the site was conducted in order to predict the future migration of site-derived COCs. The design of the flow and transport models is based on the hydrogeologic conceptual model discussed in Section 7.0. The models simulate 1,000-year predictive scenarios based on steady-state flow conditions and current distributions of COCs dissolved in groundwater. The predictive scenarios incorporate post-decommissioning modifications to topography, flow field, and COC source materials to more accurately represent future conditions. Modeling results were evaluated to estimate potential future concentrations at exposure points, and surface water and groundwater source loading to Robert S. Kerr Reservoir.

### **8.1 Groundwater Vistas**

Groundwater Vistas Version 3.09 (Rumbaugh and Rumbaugh, 2001) is a pre- and post-processing modeling environment for Microsoft Windows that couples a model design system with comprehensive graphical analysis tools. This program provides visualization of model development and results, and allows for enhanced model quality and accuracy. Although Groundwater Vistas supports a wide variety of flow and transport models, it was used in this project for the development of MODFLOW and MT3DMS modeling files and for processing modeling results.

### **8.2 Groundwater Flow Model**

The USGS three-dimensional finite difference model, MODFLOW 96, (McDonald and Harbaugh, 1988) was used as the flow model for simulating flow at the Facility. The McDonald-Harbaugh model is a finite difference groundwater flow model developed by the USGS. It is widely used and well documented. It is a true three-dimensional flow model, except for the assumption that the vertical component of flow is aligned with gravity. It has the capability of simulating a heterogeneous aquifer with evapotranspiration, variable well pumpage, drains, rivers, variable recharge, and different boundary conditions under either artesian or water table conditions.

### 8.3 Solute Transport Model

MT3DMS (Zheng and Wang, 1999) is a three-dimensional multi-species transport code originally written under contract to the EPA and later modified for the COE. The code has been extensively tested is widely used and accepted. MT3DMS has comprehensive capabilities for simulating advection, dispersion and chemical reactions of contaminants in groundwater flow systems.

MT3DMS is developed for use with any block-centered finite-difference flow model such as MODFLOW. The results from the MODFLOW flow model can be directly imported into the transport simulation. After the flow field is developed by MODFLOW, the information needed for the transport model can be saved and then subsequently used by the transport model.

MT3DMS is based on a modular structure to permit simulation of transport components independently or jointly. MT3DMS interfaces directly with the USGS finite-difference groundwater flow model, MODFLOW, for the head solution, and supports all the hydrologic and discretization features of MODFLOW. MT3DMS has been widely accepted by practitioners and researchers alike and applied in numerous field-scale modeling studies in the United States and throughout the world. The MT3DMS code has a comprehensive set of solution options, including the method of characteristics (MOC), the modified method of characteristics (MMOC), a hybrid of these two methods (HMOC), the standard finite-difference method (FDM), and the third order total variation diminishing (TVD) method.

One limitation with MT3DMS is the inability to use the river and stream package simultaneously. Simulating rivers and ponds, boundaries typically simulated using the river package, with constant head nodes circumvented this difficulty.

### 8.4 Groundwater Flow Model Design

The groundwater flow regime at the Facility was simulated based on the conceptual model described in Section 7.0. The model was initially designed and calibrated to represent current (pre-decommissioning) steady-state conditions. The model was then modified to incorporate post-decommissioning modifications to accurately represent the future hydraulic flow field.

#### 8.4.1 Model Grid

The grid framework was imported directly to MODFLOW from the hydrostratigraphic model discussed in Section 7.1. The model domain, shown in Figure 8-1, consists of 122 columns, 123 rows, and 6 layers. A cross-section of the model grid displaying this design is presented in Figure 8-2. Grid spacing for the central portion of the flow model is 50 feet. A telescoping grid was implemented on the fringes of the model domain to reduce model computations in areas where less resolution of hydraulic head is required. In these areas, the grid spacing was expanded to 100 and 200 feet.

Figures 7-1 through 7-8, which display the hydrostratigraphic model, are also accurate representations of the model layer geometry. As with the hydrostratigraphic model, Layer 1 represents the Quaternary surface deposits that consist of the terrace deposits in the processing area, the colluvial material on the steeper slopes of the Facility, and the alluvium located in the river bottomlands. Layers 2 through 6 are representative of Unit 1, 2, 3, 4, and 5 Shale, respectively. The model domain is designed as a quasi-three dimensional system where the low-permeability sandstone units are implicitly modeled. In this approach, the sandstone units are only represented by vertical conductance between shale units. Vertical water fluxes between shale units are calculated based upon sandstone vertical hydraulic conductivity and thickness (i.e. distance between shale units). No lateral water flux or lateral solute transport is calculated in the sandstone units. The bottom of model Layer 6 (Unit 5 Shale) is modeled as a no-flow boundary. Model layers and the corresponding geologic units are related in Figures 8-3 through 8-8 and in Table 8-1.

In low-lying areas where upper bedrock units have been eroded away, colluvium or alluvium directly overlies lower bedrock units. Because finite difference models do not allow complete pinching out of a model layer, there are active cells in layers where the respective bedrock unit does not exist. Cells in these areas of the domain could not be modeled as inactive because it would disconnect the hydraulic communication between the underlying bedrock unit and the overlying surface deposits. Therefore, in order to retain vertical hydraulic connection, cells in layers where the bedrock unit has been eroded away have been assigned the properties of the overlying surface deposit unit. The layer thickness of these cells is 0.2 feet.

#### 8.4.2 Boundary Conditions

Hydrogeologic boundary conditions that are incorporated in the model domain include recharge, evapotranspiration, streams, rivers, ponds, drains, and no-flow boundaries. Figures 8-9 through 8-16 present the boundary conditions incorporated into the model layers.

The shallow groundwater system at the Facility is bounded by no-flow boundaries that hydraulically separate the area of concern near the site from the surrounding groundwater system. These boundaries include groundwater divides and the Carlile School Fault. Areas of the model domain that are separated from the site by no-flow boundaries are not significant to the hydrogeology of the site, and therefore, are simulated with no-flow cells. Of the 90,036 total model cells, 65,451 (73 percent) are active. Groundwater divides areas of discharge or recharge that control the flow of an aquifer. Divides are typically formed by the discharge of groundwater to creeks and rivers, and recharge from precipitation and infiltration. Areas representing discharge divides include the Arkansas and Illinois Rivers, and the Salt Branch.

The southeastern portion of the model, including the tributary of the Salt Branch, lie within the area faulted by the Carlile School Fault. The fault has been interpreted as a no-flow zone. The local hydrogeology in the vicinity of the faulted area appears to be controlled by the tributary of the Salt Branch, which is a local discharge zone. If groundwater were being discharged across the fault, it would discharge into the Salt Branch or its tributary.

##### 8.4.2.1 Recharge

Arial recharge resulting from the infiltration of precipitation is modeled based on a percentage of average annual rainfall measured in the nearby town of Sallisaw, Oklahoma. The average annual rainfall was calculated to be 42 inches per year. Rainfall occurring at the Facility percolates as recharge, flows overland to streams and ponds as runoff, or evaporates. The percentage of rainfall contributing to recharge is estimated to be approximately 5 percent, or 2.2 inches per year ( $5.0 \times 10^{-4}$  feet per day). The recharge rate is increased in the valley bottoms and Oak woodland areas. During precipitation events, valley bottoms collect large amounts of runoff from higher elevations, which result in localized areas of higher infiltration. The dense

vegetation in the woodland areas restricts runoff, which creates a greater percentage of precipitation available for recharge. Recharge rates in the valley bottoms and Oak woodland were estimated during model calibration to be 7.9 inches per year ( $1.8 \times 10^{-3}$  feet per day).

Recharge to the shallow groundwater system is increased by some operational practices at the Facility. Irrigation water plus the natural recharge in the Agland area is equal to an average annual rate of 7.9 inches per year ( $1.8 \times 10^{-3}$  feet per day). The leaky fire water system in the Process Area also increases the recharge to the subsurface. Accurate leakage rates to the groundwater system are not available, but the total recharge rate in the Process Area was estimated to be 3.8 inches per year ( $8.7 \times 10^{-4}$  feet per day) during model calibration. This equates to 7,500 ft<sup>3</sup>/day of recharge attributable to the fire water suppression system. The distribution of modeled recharge rates is presented in Figure 8-9.

#### 8.4.2.3 Evapotranspiration

Three vegetation types were identified relating to evapotranspiration (ET) at the Facility. These included the Oak woodland, Bluestem prairie grasslands and Bermuda grass pasturelands. A detailed discussion of the derivation of ET rates and extinction depths are presented in Appendix K. These values were used as initial estimates of ET rate and extinction depth in the Evapotranspiration Package. The final model values of ET rate and extinction depth were estimated during model calibration. The calibrated values of ET rate for the Oak woodland, Bluestem prairie grasslands and Bermuda grass pasturelands, are  $5.0 \times 10^{-3}$ ,  $3.0 \times 10^{-3}$ ,  $2.4 \times 10^{-2}$  feet per day, respectively. Calibrated values of extinction depth are 5.0, 3.0, and 6.5 feet, respectively. The extinction depth, as used in the MODFLOW Evapotranspiration Package, is the depth at which evapotranspiration no longer occurs.

The distribution of the vegetation types was determined based on site inspection and evaluation of aerial photographs. The distribution of the three different vegetation types used in the model is presented in Figure 8-10.

#### 8.4.2.3 Streams

The several streams that exist on the Facility have been simulated using either the Prudic Stream Package for MODFLOW or Constant Head Cells. Stream characteristics were based on field observations. Stream locations were obtained from drawings provided by the Facility, and are presented in Figure 2-5. The stream locations as simulated by the model are presented in Figure 8-11.

The Prudic package for MODFLOW was used to simulate 001, 004, 005, and 007 streams, as well as Creek A, located south of the Fertilizer Pond Area, and the unnamed streams north of the Storm Water Reservoir. The Prudic package calculates stream flow and stage using the Manning Equation and stream dimensions. The Manning Equation requires a roughness coefficient, stream cross-sectional area, stream slope, and stream hydraulic radius to calculate stream flow in each reach of a modeled stream segment. Flows from upstream tributaries are summed and used as initial flow in the first reach of the downstream segment.

The hydraulic radius and the cross-sectional area of the stream are calculated based on the stream width and the groundwater elevation. Initial surface water elevations and the streambed elevations were calculated using a FORTRAN 77 program. The program is designed to read the elevation of the land surface in the stream cell from a binary file containing Layer 1 elevation saved by Groundwater Vistas and to calculate the stream elevation based on an initial stage estimate of one foot.

The slope of each stream reach was calculated using site topographic survey information provided by SFC. These data were used instead of available USGS topographic maps because additional work completed by the Facility has resulted in more accurate topographic data. The average stream width was estimated to be five feet based on field observation. Mannings coefficient was estimated to be 0.025 for a natural stream (Daugherty and others, 1985). Calibrated roughness coefficients ranged from 0.04 in the grassy areas to 0.001 where flow was over smooth bedrock.



Stream stage is calculated based on the Manning calculated stream flow and stream cross-sectional area. Surface water-groundwater exchange is then calculated in a similar manner as the river package with stream head, stream width, stream length, streambed thickness, and streambed hydraulic conductivity.

The value of stream cell conductance was estimated during calibration to 100 ft<sup>2</sup>/day. Calculated stream flow was used as a calibration target for 001/Creek A, 004, 005, and 007 streams. The estimated flows for these streams is discussed and presented in Section 2.3.2. Stream parameters were adjusted during model calibration until calculated stream flow approached these estimates.

The Salt Branch and its tributary (Figure 2-2) were simulated using constant head nodes because an estimation of flow in these streams is not necessary. Observed stream flow data are not available for comparison with calculated values. Also, the evaluation of predicted surface water COC concentration is not necessary because the COCs are not transported toward these streams. The constant head elevation representing each stream segment is equal to the top of model Layer 1 (ground surface) for each node.

#### 8.4.2.4 Rivers

MT3DMS does not allow for the simultaneous execution of the Prudic Package (streams) and River Package in the same simulation. It was determined that simulating stream-aquifer interaction with the Prudic Package is of greater importance than simulating the Illinois and Arkansas River-aquifer interaction with the River Package. Therefore, the Illinois and Arkansas Rivers are simulated using Constant Head Cells (Figures 8-11 through 8-16). A constant elevation of 460 feet amsl was applied to all Robert S. Kerr Reservoir nodes based on review of USGS topographic maps of the area and the mean pool elevation reported by the COE (RSA, 1991). The simulation results using the constant head package were compared to the simulation using the river package. The results were nearly indistinguishable.

#### 8.4.2.5 Ponds

Three site surface water impoundments, the Storm Water Reservoir, Decorative Pond, and Emergency Basin/North Ditch, are simulated with Constant Head Cells (Figures 8-11 through 8-

15). The ponds are simulated in the appropriate model layers based on review of the hydrostratigraphic model (Section 7.0). The Storm Water Reservoir is simulated in model layers 1 through 5 (colluvium, Unit 3 Shale, and Unit 4 Shale) at an elevation of 510 feet amsl. The Decorative Pond is simulated in model Layers 1 and 2 (terrace and Unit 1 Shale) at an elevation of 540 feet amsl. The Emergency Basin/North Ditch is simulated in model Layer 1 (terrace) at an elevation of 550 feet amsl.

#### **8.4.2.5 Drains**

There are four groundwater drains simulated within the model domain with the Drain Package (Figures 8-11 and 8-12). The CSD is described in detail in Section 2.1.22. The pipe bedding serves as a preferential groundwater pathway from the Process Area to 001 Outfall. The pipe bedding was installed on the surface of Unit 1 Sandstone and the drain was therefore simulated in Unit 1 Shale (model Layer 2). The second arm of the CSD, which runs east west from south of the MPB to the emergency catch basin, is also simulated in Unit 1 Shale (model Layer 2).

Two groundwater drains in the terrace deposits are located near the northwest corner of Pond 2 and along the southern edge of Pond 2. An additional drain is located on top of Unit 1 Sandstone, the along the 005 stream, between the Emergency Basin and the 005 Outfall. French drain systems located adjacent to pond 2 and in the 005 stream were simulated in Layer 1. An additional French drain in the 005 stream was simulated in Layer 2. The Drain Package parameters for all of the simulated groundwater drains were estimated during model calibration.

#### **8.4.3 Flow Model Parameters**

Equivalent porous media (EPM) modeling methods have been applied to simulate groundwater flow through the fractured shale and sandstone units. The EPM approach replaces the primary and secondary hydraulic properties associated with a fractured porous medium with effective hydraulic properties that are representative of a single porous medium with comparable water fluxes and velocities. The validity of EPM use increases proportionally with the degree of fracture interconnectivity and decreases in fracture spacing. Therefore, the EPM approach is

considered to be valid for the shale units that consist of dense, fissile-like fractures that have a high degree of interconnectivity.

The modeled hydraulic conductivity for each shale unit is based on the analyses of the slug tests described in Section 4.2. Slug test results are summarized in Table 4-8. For each shale unit, the average measured value was used as an initial value in model calibration. The average values were adjusted within the observed range of variation in order to achieve an acceptable model calibration. Vertical hydraulic conductivity for each shale unit was estimated to be 10 percent of the calibrated horizontal hydraulic conductivity value. The calibrated hydraulic conductivity value for each hydrologic unit is presented in Table 8-2. As discussed in Section 7.2, the slug test results indicate large heterogeneities in the shale units that appear to be random in nature. An extraordinarily large number of closely spaced conductivity estimates would be necessary to accurately depict the variation in the shale units. Therefore, each unit was assigned a single value that is considered to be representative of the average hydraulic conductivity of each respective shale unit.

The hydraulic conductivity of the Arkansas/Illinois River floodplain alluvium was estimated from a single slug test conducted at well MW120. The results of the slug test indicate that the hydraulic conductivity is approximately 5 ft/day. During flow model calibration, it was observed that 5 ft/day resulted in a steeper gradient in the alluvium than is observed. The alluvium hydraulic conductivity value was increased to 50 ft/day, and resulted in a more representative gradient in the alluvium. A conductivity value of 50 ft/day is within the typical range of alluvial sediments (Freeze and Cherry, 1979).

Measurements of sandstone hydraulic conductivity have only been conducted in Unit 4 Sandstone. Estimates of vertical conductivity of Unit 4 Sandstone range from  $2.50 \times 10^{-5}$  to  $4.75 \times 10^{-5}$  ft/day. The mean value of  $3.63 \times 10^{-5}$  was used as an initial estimate for all of the sandstone units, and was independently varied during calibration.

The hydraulic effects of the wells and borings completed in multiple shale units were simulated by distributing cells with high vertical conductivities across the Facility. The cells form vertical columns of high conductivity media in Layers 1 through 5 (Quaternary surface cover to Unit 4

Shale). The vertical conductivity of the cells is 0.05 ft/day. The horizontal conductivity of the cells is 0.5 ft/day. Vertical leakance was adjusted to 0.05 ft/day in the high conductivity locations. Each high conductivity cell is 50 feet by 50 feet, and therefore represents multiple vertical conduits. Highly conductive cells were located based on the spatial distribution and density of the wells and borings completed in multiple shale units based on data provided by SFC. Figure 8-17 presents locations of the modeled high conductivity cells in relation to the distribution of the wells and borings completed in multiple shale units. The majority of the high conductivity cells are located in the vicinity of the Process Area. They are also located near the Solid Waste Burial Areas, the Fertilizer Pond Area, and Pond 2.

#### **8.4.4 Flow Model Calibration**

The objective of the calibration process is to refine the numerical model by adjusting model input parameters so that model output more accurately represents observed data. The model was calibrated to the average annual groundwater elevations measured in 69 wells. These wells were selected because they are screened in one shale layer and the sand pack did not extend to an adjacent shale layer. Wells that are screened in multiple wells or in hydraulic communication with adjacent shale units via the sand pack were considered to provide unreliable head estimates. The model was also compared to stream flow values as estimated by Oklahoma Department of Environmental Quality (OKDEQ) mean annual flow per unit drainage area model and site inspection (Section 2.3.2)

Figures 8-18 through 8-23 display calibrated head maps of each model layer. Model calibration targets and residuals (observed head minus calculated head) are presented in Table 8-3. Calibration statistics including mean residual (MR), mean absolute residual (MAR), and standard deviation (SD) are also presented in Table 8-3. The MR and MAR are -1.51 feet and 3.48 feet, respectively. The value of SD is 5.00 feet. The mass balance error of the calibrated model is 0.49 percent.

A plot of observed heads versus calculated heads is presented in Figure 8-24. Generally, the points on Figure 8-24 trend on a 1:1 slope indicating that residuals are consistent over the total range of calculated heads. No other trends are evident that suggest a pattern in the residuals.

Calibration quality can be quantified by evaluating the calibration residuals in relation to the overall model response. (Anderson and Woessner, 1992). Values of residual error (RE) have been calculated by dividing absolute residuals by the range in calculated head in the model domain, 123.74 feet (Table 8-3). Prior to calibration, criteria were established to assess the quality of the calibration. Calculated heads with RE less than 0.050 (i.e. 5 percent error) are considered to be good. Values of RE between 0.050 and 0.100 are considered to be satisfactory. The values of RE calculated from MAR and SD are 0.028 and 0.040, respectively, and indicate a good quality of calibration.

Values of RE have also been analyzed on an individual basis. Of the 69 calibration targets, 57 (83 percent of targets) have a value of RE less than 0.050, and are categorized as good. Nine targets are categorized as satisfactory. The remaining three targets have RE values greater than 0.100. Of these, MW012B has the greatest RE value of 0.168. However, the observed head at MW012B is anomalous when compared to the observed heads at nearby wells MW007B and MW072B. MW007B and MW072B both exhibit heads 30 foot higher than at MW012B. The other 2 targets with RE values greater than 0.100 are equal to or less than 0.121, and only slightly exceed the satisfactory classification.

Flow rates in four site streams have also been evaluated during the calibration process. Stream flow rates for 001/Creek A, 004, 005, 007 streams are presented and discussed in Section 2.3.2. It should be noted that the OKDEQ stream flow function is a generalized, empirical equation, and practically only represents an order of magnitude estimate. Therefore, residuals less than an order of magnitude are considered to be reasonable. Stream flow in 001/Creek A and 005 streams are consistent with the OKDEQ estimates. The flow estimate for 004 and 007 streams is less than the respective OKDEQ estimates.

The flow model calibration is considered to be very good. Both head and stream flow target criteria have met the pre-defined calibration goals. The favorable calibration results indicate the model produces a reasonable representation of observed groundwater flow conditions at the Facility. The calibration results also provide high levels of confidence in the flow model's ability to predict future hydrologic conditions under the post-decommissioning setting.

#### 8.4.5 Predictive Scenario

After flow model calibration was achieved, the model was modified to incorporate changes to the surface topography and groundwater flow system that will result from decommissioning activities (Section 3.0). The modified groundwater flow model was used for the long-term solute transport prediction simulations. The modifications were based on the reclamation activities described in Final Decommissioning Alternatives Study Report, June 8, 1998 (SFC, 1998b). The surface elevation was altered to reflect regrading in the Process Area and the geometry of the proposed disposal cell. The modified topography and disposal cell footprint, as incorporated into the model, are presented in Figure 8-25. Recharge was modified to be 0 ft/day over the disposal cell footprint, and 0.0022 ft/day in a band on the north, west, and south sides of the footprint to simulate additional infiltration resulting from precipitation running off of the cell cover. Recharge is not increased on the east side of the cell in response to surface drain system that is proposed for this area. The drain boundary conditions simulating the CSD and French drains near Pond 2 and 005 stream were removed from the model. The Constant Head Cells simulating the Decorative Pond, Storm Water Reservoir, and Emergency Basin/North Ditch have been removed as well. Cells within the Process Area that are used to simulate open borings or wells screened in multiple shales remained in place.

The calculated long-term steady state potentiometric surfaces for the post reclamation modeling are presented in Figures 8-26 through 8-31. The impacts of these changes are significant only in the vicinity of the Process Area where the heads have decreased slightly primarily due to the removal of the leaky fire water system. Despite the change in heads, groundwater flow under the Process Area is still to the west, toward the Robert S. Kerr Reservoir. Heads in other areas of the model domain are practically unchanged. One consequence of the lower heads west of the Process Area is that 004 drainage becomes dry. River loading from the 004 drainage is, therefore, negligible.

#### 8.5 Solute Transport Model

Groundwater solute transport modeling of the Facility COCs has been conducted in order to estimate their future migration in the groundwater system underlying the Facility. The identified

COCs included in the transport simulations are nitrate, uranium, and arsenic. A discussion of the selection of the COCs is presented in Section 5.7. Transport modeling parameters were determined based on Facility geochemical testing (Section 5.5) and calibration simulations. Predictive 1,000-year simulations were then executed based on post-decommissioning modifications to the site topography and subsurface flow field, as described in Section 8.4.5. The modeling results provide calculated concentrations of the COCs throughout the alluvial and bedrock hydrologic units as well as in potential surface water exposure points surrounding the Facility.

### 8.5.1 Mathematical Approach

The transport solution has been obtained by formulating the three-dimensional Advection-Dispersion Equation with the Third-Order Total Variation Diminishing Method (TVD). The TVD formulation is presented and discussed in detail by Zheng (1990). The TVD method is characterized by stable solutions that are inherently mass conservative. TVD solutions typically produce much less numerical dispersion than finite difference solutions and smaller mass balance errors than Hybrid Method of Characteristic solutions.

### 8.5.2 Transport Model Parameters

The input parameters for the transport simulations include linear distribution coefficient ( $K_d$ ), lithologic bulk density ( $\rho_b$ ), effective porosity ( $\phi_e$ ), and longitudinal, transverse, and vertical dispersivity ( $\alpha_L$ ,  $\alpha_T$ ,  $\alpha_V$ ). Horizontal and vertical groundwater flux terms and heads were imported from groundwater flow modeling results described in Section 8.4.

Bulk density of each hydrologic unit is required (along with  $K_d$ ) to calculate the retarded velocity of the solutes. A value of  $2.69 \text{ g/cm}^3$  is used for the shale units, and a value of  $1.76 \text{ g/cm}^3$  is used for the alluvial units.

The longitudinal dispersivity in all layers has been initially estimated based on an empirical, scale dependent equation from Xu and Eckstien (1995). The transverse dispersivity and vertical dispersivity were estimated to 10 percent and 1 percent of the longitudinal dispersivity,

respectively (Fetter, 1999). Estimated values of longitudinal, transverse, and vertical dispersivity using Xu and Eckstien are 50 feet, 5 feet, and 0.5 feet, respectively. Effective porosity was estimated to be 25 percent for the alluvial units and 10 percent for the shale units based on visual inspection of lithologic samples and model calibration. Effective porosity and longitudinal dispersivity were further refined using the Ogata-Banks advection dispersion equation (ADE) solution (Section 8.5.3).

Linear distribution coefficients for uranium and arsenic in Units 1 through 4 Shale were developed from the column desorption and batch testing described in Section 5.5. In Unit 1, 2, and 4 Shale, two estimates of  $K_d$  were made from separate borehole locations. Ultimately,  $K_d$  derived from laboratory geochemical testing could not reproduce observed conditions in site wells. Bulk  $K_d$  values were estimated during model calibration.

Nitrate is an anion and will likely have little affinity to shales and sandstones that consist primarily of silica (no charge) and clay minerals (negative charge). Therefore, the  $K_d$  for nitrate has been assumed to be zero, allowing it to be transported as a conservative solute with no retardation in all layers. Table 8-4 presents the modeled  $K_d$  values for the COCs in all of the model layers.

Nitrate is known to degrade to nitrite and elemental nitrogen under certain natural conditions. MT3DMS allows for the biochemical degradation of compounds using a first order irreversible rate expression. However, because the extensive data requirements, and because biochemical reactions are generally more complex than is modeled by a first order rate relationship, a conservative approach of no biodegradation was assumed.

### 8.5.3 One-Dimensional Transport Analysis

One-dimensional solute transport analyses were conducted in order to estimate physical transport parameters, including groundwater velocity and longitudinal dispersivity, based on measured COC concentrations. Measured nitrate concentrations at selected wells were analyzed with the Ogata-Banks solution to the advection-dispersion equation (Ogata and Banks, 1961). The Ogata-Banks solution models one-dimensional solute transport in a uniform flow field, with initial



conditions of  $C(x,0) = 0$ , and boundary conditions of  $C(0,t) = C_0$ , and  $C(\infty,t) = 0$ . These conditions represent the migration of a solute from a constant source through a system with zero concentration. The Ogata-Banks solution is expressed as:

$$\frac{C}{C_0} = \frac{1}{2} \left[ \operatorname{erfc} \left( \frac{x - v_x t}{2\sqrt{\alpha_L v_x t}} \right) + \exp \left( \frac{x}{\alpha_L} \right) \operatorname{erfc} \left( \frac{x + v_x t}{2\sqrt{\alpha_L v_x t}} \right) \right]$$

Where:

$C/C_0$	=	relative solute concentration (dimensionless)
$v_x$	=	groundwater velocity (L t <sup>-1</sup> )
$\alpha_L$	=	longitudinal dispersivity (L)
$t$	=	time since start of constant source (t)
$x$	=	distance from constant source (L)

The analysis consisted of comparing the calculated value of  $C/C_0$  to the measured value. Velocity was varied so that the measured and calculated breakthrough ( $C/C_0=0.5$ ) matched. Longitudinal dispersivity was then varied until the distribution or "spreading" of the calculated curve fit the measured data. The analyses were only conducted where the location, magnitude, and timing of the constituent release are reasonably constrained.

Nitrate was chosen, in part, because it is considered to be conservative in the subsurface. Its migration is not chemically depleted or retarded in the subsurface, and therefore, is transported at the same rate as groundwater. As a result, the velocities determined from the analysis are representative of groundwater velocities. Five wells have been identified that exhibit the conditions consistent with the Ogata-Banks solution, and also are located near sources that are reasonably constrained. These wells include 2322A, 2341, 2354, 2356, and MW095A.

The results of the one-dimensional analyses are presented in Figures 8-32 through 8-36. Near the Fertilizer Pond Area (monitoring wells 2322A, 2341, 2354, and 2356), estimates of groundwater velocity range from 0.072 ft/day to 0.145 ft/day. Values of dispersivity range from 1 ft to 15 ft. The analysis at MW095A indicates that down gradient of Pond 2, the average groundwater velocity is 0.115 ft/day, and the longitudinal dispersivity is 20 feet.

#### 8.5.4 Transport Model Calibration

The transport model was calibrated with a procedure that consisted of comparison of historical geochemical conditions to those predicted by historical transport simulations. The calibration simulations incorporated existing hydrologic conditions (as modeled in Section 7.6) to represent the historical migration of the COCs during the time period from January 1, 1990 to January 1, 2001. Initial chemical concentrations observed in January 1, 1990 are incorporated into the calibration simulation for each COC. The 1990 starting time was selected because it is the earliest time when sufficient groundwater concentration data are available for initial model concentrations. This is primarily because many of the monitoring wells were installed in 1990. A significant amount of the COC mass had already entered the groundwater system by 1990. This eliminates the need to simulate many of the complex site sources. Modeling the site COC sources is a significant challenge due to the unknown and most likely variable nature of the location, geometry, timing, and magnitude of the COC sources. It is evident by the data that some sources continued to contribute COC mass to the groundwater after 1990 and even after 1993, when the Facility ceased operations. Where appropriate, these sources were incorporated into the calibration simulations.

Nitrate, a compound assumed to be a conservatively transported constituent, was used to calibrate the effective porosity and dispersion of the transport model. The solute velocity of nitrate, therefore, is equal to groundwater velocity. Nitrate distribution at the site was estimated using available monitoring well data from 1990. Contours of nitrate concentrations were developed for each layer of the model and imported as initial conditions. In cases where a monitoring well was completed in multiple layers, nitrate concentrations were assumed to be the same in all penetrated layers. The initial nitrate concentrations for each model layer are presented in Figures 8-37 through 8-41. Measured nitrate concentrations were compared to modeled nitrate concentrations in key wells. Effective porosity and dispersion were adjusted until the values were approximately the same, mimicking arrival times and concentration. Chemographs containing observed and calculated COC concentrations for the target well are presented in Appendix F. Using this method, the effects of retardation in uranium and arsenic transport can be calibrated independently of effective porosity and dispersion. Calibrated effective porosity was 25 percent for alluvial units, and 10 percent for shale units. Longitudinal

dispersion was calibrated at 20 feet. These values are consistent with observations of lithologic samples, the site conceptual hydrogeologic model, and with the values estimated using the Ogata-Banks analysis. Further estimates of the longitudinal dispersion and effective porosity were obtained using the inverse modeling program PEST (Doherty, 1994, 1995, 2000 and 2001). Both parameters for each model layer were allowed to vary over two orders of magnitude. The PEST estimates of both effective porosity and longitudinal dispersion exhibited less than five percent difference than those estimated from the Ogata-Banks equation and manual calibration.

The values used in calibration provide good correlation with most of the monitoring well data (Appendix F). There are instances where the model does not predict monitoring well data well. These wells are generally located close to a suspected nitrate source. Since the exact location, geometry or strength of the source is unknown, no attempt to correct the calibration simulation for active continuing sources. It is assumed that these sources will be removed during decommissioning and will have not significant effect on future predictions.

Once effective porosity and dispersion were calibrated, uranium and arsenic calibration simulations were completed to estimate  $K_d$ . The distribution of uranium and arsenic concentrations were estimated using data from groundwater monitoring wells for each layer. As in the nitrate calibration, wells completed in multiple layers were assumed to be representative of the in-situ concentration of all the penetrated layers.

The  $K_d$  value was then adjusted until modeled concentrations matched measured concentrations. It should be noted that the calibrated  $K_d$  value used in the model actually represents a bulk parameter used as an effective  $K_d$  value that incorporates numerous factors affecting the transport of each constituent. Among these factors are pH, ionic strength of the solute, the presence of organic compounds, number of competing cations, and permeation of the ion exchange sites of the aquifer material. The  $K_d$  values used in the model are not representative of those obtained through batch laboratory tests.  $K_d$  values obtained from laboratory tests meet the strict definition of  $K_d$ , whereas  $K_d$  values used in the model are values that make the arrival times and contaminant magnitude in the model behave as observed.

Additionally, the modeling results in some locations were sensitive to initial concentrations used. Although a better fit to late time data could be improved by altering the initial conditions, these alterations would be more reflective of source calibration than  $K_d$  calibrations. Although some changes in the magnitude of the initial conditions were warranted by the data, these changes were kept to a minimum.

Initial uranium concentrations for each model layer in the uranium transport calibration are presented in Figures 8-42 through 8-46. Historically, the primary sources of site-derived uranium to groundwater are the MPB, SX Building, and Solid Waste Burial Areas (Section 5.8). Data from the majority of wells near these areas (i.e. MW010, MW012, MW012A, and MW087A) display decreasing uranium concentrations over time, and indicate that source loading is no longer occurring (Appendix F). As a result, no source term was included in the uranium transport calibration. Two wells MW025 and MW067A exhibit increasing concentrations over time, however data from these wells represent the initial breakthrough of the solute front. It is anticipated that the concentrations in these wells will decrease in the future. Uranium sources were also not included to simulate desorption and/or dissolution of uranium from soils. Although significant soil concentrations have been measured at the Facility, there is no apparent correlation between soil concentrations and groundwater concentrations.

Values of  $K_d$  in the calibrated uranium transport model were estimated from comparison of observed and calculated concentrations at 54 well locations. As with the arsenic simulation, values of effective porosity and dispersivity were obtained from the nitrate calibration results. The observed and calculated chemographs for all of the wells included in the uranium calibration are presented in Appendix F. A value of  $K_d$  has been estimated for the Quaternary surface deposits and each shale unit. A unique  $K_d$  value could not be developed for the individual lithologies that make up the surface deposits (terrace deposits, colluvium, alluvium, and fill material) due to lack of observed data in these units. Therefore, all of the surface deposit lithologies are assigned the same  $K_d$  value. The calibrated  $K_d$  values range from 0.16 L/kg to 0.92 L/kg, and are presented in Table 8-4.

Initial arsenic concentrations for each model layer in the arsenic transport calibration are presented in Figures 8-47 through 8-51. Historically, the primary sources of site-derived arsenic

to groundwater are the MPB, SX Building, the Pond 2 Area, the Emergency Basin (Section 5.8). Additional arsenic sources to groundwater include the fluoride clarifier, setting basins and holding basin. In general, data from wells near these areas display decreasing arsenic concentrations over time, indicating the source has diminished or ceased. (Appendix F). A few wells, notably MW095A, exhibit steady or increasing arsenic concentrations over the time interval of interest. To maintain arsenic concentrations, an arsenic source was required in Pond 2, Fluoride Clarifier, the Fluoride Settling Basins, Fluoride Burial Area and the Fluoride Holding Basin #1. The source concentration was applied to recharge in all of these areas, with two exceptions. Pond 2 required 11.51  $\mu\text{g/L}$  recharge source and the eastern-most Burial Site required 2  $\mu\text{g/L}$  recharge source. It is anticipated that the concentrations in these wells will decrease in the future. Arsenic sources were also not included to simulate desorption and/or dissolution of arsenic from soils or aquifer material. It is possible that some portion of the arsenic present at the facility is not the result of an arsenic release, but rather, a dissolution of mineral phase arsenic of the aquifer material due to changing redox conditions.

Values of  $K_d$  in the calibrated arsenic transport model were estimated from comparison of observed and calculated concentrations at 34 well locations. Values of effective porosity and dispersivity were obtained from the nitrate calibration results. The observed and calculated chemographs for all of the wells included in the arsenic calibration are presented in Appendix F.

$K_d$  values in the calibrated arsenic transport model were determined to be 0.1 L/kg for hydrostratigraphic units. The resulting calibrated arsenic  $K_d$  were the result of manual calibration to match existing data. The inverse model, PEST, was also used to guide the selection of  $K_d$ . In Unit 3 Shale,  $K_d$  was estimated by PEST at 8 L/kg. All other layer were estimated within 15 percent higher  $K_d$  than calibrated value of 0.1 L/kg. As a conservative measure, the lower value was implemented in all layers.

The calibrated  $K_d$  value does not compare well with the values determined in the laboratory. The average  $K_d$  determined by laboratory tests ranged from four to hundreds of L/kg. The discrepancy may be due to sample preparation that included grinding of the sample that would increase the available surface area for adsorption.

### 8.5.5 Prediction Simulations

Following the calibration of transport parameters, predictive simulations were conducted to estimate the future concentration distributions in the subsurface and at potential surface water exposure points. Potential surface water exposure points include Robert S. Kerr Reservoir, Salt Branch, and 001, 004, 005, and 007 outfalls. Heads and groundwater flux terms used in the predictive transport simulations are from the post-decommissioning groundwater flow simulation described in Section 7.0. This flow simulation incorporates topographical modifications, as well as removal of the Combination Stream Drain, the various french drain systems, and the stormwater pond. The post decommissioning flow model also assumes that all of the poorly constructed/abandoned wells and boreholes will remain in place, and will continue to act as vertical transport pathways between hydrologic units. This is a conservative assumption because most, if not all, of these wells and borings will be properly abandoned during site decommissioning. Finally, the predictive simulations assume that any existing COC source material above the water table will be remediated during decommissioning activities and that the only COC mass remaining in the system is either dissolved in groundwater, or sorbed to geologic materials below the water table.

Although the decommissioning activities have been assumed to be completed at the start of the predictive simulation, they are presently under review, and it is uncertain when they will be implemented (Section 3.0). The effects of this assumption are not believed to have significant effects on the long-term COC transport through the subsurface. Initial concentrations in the alluvium and bedrock units are from the geochemical sampling results from 2001 presented in Section 5.0. Maps displaying the initial concentrations for nitrate, uranium, and arsenic are presented in with the modeling results in Section 8.5.6.

### 8.5.6 Transport Model Predictions

Model results are displayed as maximum calculated concentrations and the maximum concentration represents the greatest value in all of the model layers at any point. Plots of maximum concentration are indicative of the extent and magnitude of the COCs in the entire

groundwater system, and are not necessarily representative of the distribution of a COC in any one layer.

The maximum initial concentrations for nitrate in the prediction simulation are presented in Figure 8-52. This map indicates that at the beginning of the simulation nitrate is widely distributed across the Facility, but is most highly concentrated near source areas such as Pond 2, the Fertilizer Pond Area, and the SX Building. Nitrate has reached the Arkansas/Illinois River between the 008 and 005 streams. The maximum calculated nitrate concentrations at the 5, 25, 50, and 100-year time steps are presented in Figures 8-53 through 8-56. Generally, nitrate in both the Process Area and the Fertilizer Pond Area is transported toward the Arkansas/Illinois River between streams 008 and 005. Some nitrate originating in the Fertilizer Pond Area is transported toward the river through the Agland Area. At the 50-year time step, all calculated concentrations are below 500 mg/L, and concentrations of 100 mg/L are only exceeded in a few areas near the Fertilizer Ponds and 008 stream. At the 125-year time step, no calculated concentrations exceed 10 mg/L, and nitrate is effectively removed from the system.

Figures 8-57 through 8-62 are chemograph plots of calculated COC concentrations at selected observation point locations. Observation points 2, 3, 4, and 6 are located along or within the Facility boundary (observation points 1 and 5 are discussed in Section 8.5.6.4). Calculated nitrate concentrations are in excess of the 10 mg/L MCL at the observation points 2 and 4. Concentrations at these locations exceed 250 mg/L and 300 mg/L, respectively, at early times, but decrease to less than 10 mg/L by 50 years.

Maximum initial arsenic concentration in the uranium transport calibration are presented in Figure 8-63. This figure represents the arsenic distribution at the end of the calibrated transport simulation (January 1, 2001).

Arsenic transport is generally westward from the above-mentioned source areas to the Illinois/Arkansas River to the west. Figures 8-64 through 8-67 illustrate the maximum modeled arsenic concentration in any model layer as single plume maps for selected transport times. Arsenic is discharged to the river system between the 008 Stream and the 007 Stream. The highest arsenic concentrations are transported down the 008 Stream. Eight MT3D observation

points were placed to observe the calculated arsenic concentrations as transport progressed. The location of the observation points are depicted on Figure 8-63. Figures 8-68 through 8-75 contain chemograph plots of calculated concentration at the observation point locations.

In general, significant arsenic concentration reduction is accomplished through dispersion of the plume. Significant discharge to the river system does, however, occur. River loading is discussed further in Section 8.5.6.4. Calculated arsenic concentrations in the 5-year simulation exceed 1,000  $\mu\text{g/L}$  near the southwest corner of Pond 2. Although westward migration of this area of high arsenic concentration is evident, it remains persistent until about year 175.

Of the eight observation points simulated, the highest arsenic concentration occurs in Observation Point 4, located near well MW095A. Calculated concentrations in observation point 4 peak at 240  $\mu\text{g/L}$  and exceed 10  $\mu\text{g/L}$  for 75 years. The plume maximum passes through Observation Point 4, the 008 Stream seep, and Observation Point 5 and then to the river system. The lowest modeled arsenic concentrations were simulated in Observation Point 3, located northwest of Fluoride Holding Pond No. 2, which did not exceed 10  $\mu\text{g/L}$ .

Model results displaying the maximum calculated uranium concentrations at the initial concentration and 50, 100, 250, 500, and 1,000-year time steps are presented in Figures 8-76 through 8-80. Uranium originating in the MPB and SX Building areas is transported northwest to the 005 Stream, and south to the 001 Stream. Uranium originating in the Solid Waste Burial Areas is transported down the 007 Stream. Generally, the transport rate of uranium is less than that of nitrate and arsenic due to its larger calibrated values of  $K_d$ . Calculated concentrations exceeding the 30  $\mu\text{g/L}$  MCL are present after the 500-year time step in 005 Stream and between the present locations of Pond 2 and the Stormwater Reservoir. There are no calculated concentrations greater than 30  $\mu\text{g/L}$  after the 750-year time step.

Calculated uranium concentrations are in excess of 30  $\mu\text{g/L}$  at the Facility boundary along 005 and 007 streams. Figure 8-81 displays calculated groundwater concentrations in Unit Shale 4 and 5 at the Facility boundary in each stream. These plots represent points where concentrations are the highest in both areas. Uranium is calculated to arrive at the Facility boundary in the 007



Stream in approximately 80 years. The maximum calculated concentration in Unit 4 Shale is 17.9 µg/L at 250 years. In Unit 5 Shale calculated concentrations exceed the uranium MCL from approximately 125 years to 350 years. The maximum concentration in Unit 5 Shale is 70.9 µg/L. In 005 Stream, uranium is calculated to arrive at the Facility boundary at approximately 300 years. The maximum concentration in Unit 4 Shale is 18.9 µg/L and below the uranium MCL. The maximum concentration in Unit 5 Shale in the 005 Stream is 139.9 µg/L at 500 years. The uranium concentration is calculated to exceed the MCL from 400 years to 750 years.

#### **8.5.6.1 Stream Concentration Calculations**

The objective of the transport modeling effort was to estimate source loading to the river and surface water concentrations in flowing streams. Although source loading to the river derived from the aquifers was readily available using Groundwater Vistas, no estimate was available for the loading from the streams that drain from the Facility and flow into the river system. As mentioned previously, MODFLOW calculates the flow in streams using the Prudic Stream Package. The MODFLOW output file contains the model-calculated inflow, outflow of the stream reach, and the stream flux to or from the aquifer. A FORTRAN 77 program, STRMCALC.FOR, was written to calculate the concentration of each constituent in each stream reach using a simple mixing approach.

Since the flow of each stream reach and the flux from the aquifer node was calculated by MODFLOW, the concentration of the aquifer node could be multiplied by the flux to obtain the loading to the stream from the aquifer. Concentrations for each stream node were obtained from the binary concentration file saved by MT3D. The concentration for the first node on all streams was set to zero, assuming that there was no initial stream flow. The only contaminant entering the first stream cell would be contributed by the aquifer. The resulting concentration of the stream could be calculated.

The downstream stream node would then mix the flow and concentration from the previous stream node, along with the flux and concentration from the aquifer, in a sequential manner using the equation:

$$C = (C_{UP} * F_{UP} + C_A * Q_A) / (Q_A + F_{UP}) \quad (\text{Equation 1})$$

Where:

$C_{UP}$  = Upstream Concentration

$F_{UP}$  = Upstream Flow

$Q_A$  = Aquifer Flux

$C_A$  = Aquifer Concentration

Concentrations were calculated in all reaches of a stream segment. When calculating the contributions of tributaries to the first reach of a stream segment, the equation was expanded to:

$$C = (C_{UP1} * F_{UP1} + C_{UP2} * F_{UP2} + C_A * Q_A) / (Q_A + F_{UP1} + F_{UP2}) \quad (\text{Equation 2})$$

Where:

$C_{UP1}$  = Upstream Concentration from Tributary 1

$F_{UP1}$  = Upstream Flow from Tributary 1

$C_{UP2}$  = Upstream Concentration from Tributary 2

$F_{UP2}$  = Upstream Flow from Tributary 2

$Q_A$  = Aquifer Flux

$C_A$  = Aquifer Concentration

Subsequent reach concentrations are calculated as before using Equation 1. When the reach was losing (the aquifer flux was negative), the concentration was held constant and only the flow was diminished according to the MODFLOW calculated value. The results of these calculations are presented in Table 8-5. No source loading to the aquifer from the resultant stream discharge to the aquifer was considered. This function is not available to MT3D and would have resulted in numerous recursive model simulations. Since the transport model required substantial computation time requirements, the recursive simulations would be prohibitive. The benefits of conducting the simulations are negligible, since all streams tend to lose flow to the aquifer in the near river reaches. Additionally, no attempt was made to account for biochemical decay of nitrate in the stream, which could be substantial. This approach is considered to be conservative in that all mass was transported to the river. The only instance where mass was removed from the stream was when surface water re-entered the groundwater system. Mass was then removed in accordance with the volume of surface water reduction.

### 8.5.6.2 Stream Modeling Results

Calculated arsenic concentrations in site streams are shown in Figure 8-82. The calculated arsenic concentration in the all streams remains below the 10 µg/L standard for the entire simulation. The 005 Stream exhibits the greatest calculated stream concentration at the beginning of the predictive simulation. Arsenic concentration is initially 1.4 µg/L and diminishes less than 0.1 µg/L within 75 years.

Calculated nitrate concentration in site streams is depicted in Figure 8-83. Nitrate concentrations are estimated to be less than the MCL of 10 mg/L for the entirety of the 1,000-year simulation. The calculated nitrate concentration in the 005 stream decreases from 8.6 mg/L at the beginning of the simulation to less than 2.0 mg/L at 18 years. The calculated nitrate concentration at the 007 stream is effectively zero mg/L for the entire simulation.

Calculated uranium concentrations in site streams are illustrated in Figure 8-84. Although calculated uranium concentrations in all streams remain below the protective standard of 30 µg/L, concentrations in the 007 Stream are 28 µg/L. The concentration remains high for only a brief period and diminishes rapidly to essentially 0 µg/L after 100 years. The difference between calculated uranium concentration and MCL may be within the error of the method of calculation implemented and the MCL may be exceeded for a few years.

### 8.5.6.3 Seeps and Pools

A facility inspection was conducted to locate seeps and pools in the drainage areas of the Facility. Craig Harlin and Scott Munson of SFC conducted the inspection on August 27, 2001. During the inspection, three seeps and associated pools were encountered. The location and description of the seeps and pools are included in Table 2-3 and are included in Figure 2-5.

Since seeps and pools would provide a pathway to potential receptors, the seeps were simulated using observation points to establish the estimated nitrate and uranium concentration of the surface water. The discharge rate of these seeps was not estimated. The concentration of the

seeps was obtained by placing an observation point in MT3D at the coordinates shown given in Table 2-3.

Nitrate concentration at the three site groundwater seeps is presented in Figure 8-85. The calculated concentration at 008 Seep increases from 171.9 mg/L at the beginning of the simulation to a maximum of 352.0 mg/L at 32 years. The concentration at the 008 Seep is less than the MCL, 10 mg/L, after approximately 65 years. The calculated concentration at the 005 Seep slightly exceeds the MCL from 8 to 15 years. The maximum concentration at 005 Seep is 10.8 mg/L. The calculated nitrate concentration at the 007 Seep is effectively 0 mg/L for the entire simulation.

Arsenic concentration at the three site groundwater seeps is presented in Figure 8-86. The calculated concentration at 008 seep increases from about 17 µg/L at the beginning of the simulation to a maximum of 78 µg/L at 32 years. The concentration at 008 Seep is than the MCL, 10 µg/L, after approximately 100 years. The calculated concentration at the 005 Seep slightly exceeds the MCL from 8 to 15 years. The maximum concentrations at the 005 and 007 seeps never exceed 10 µg/L for the entire simulation.

Modeled uranium concentrations in the 007 Seep are summarized on Figure 8-87 and indicate slight exceedance of the 30 µg/L MCL. The calculated concentrations are greater than 30 µg/L from approximately 100 years to 200 years, and a maximum concentration of 35 µg/L is reached. The maximum calculated concentrations at 005 Seep and 008 Seep are slightly less than the 30 µg/L MCL, 21.3 µg/L and 10 µg/L, respectively.

#### **8.5.6.4 River Loading**

River loading of the three COCs was calculated by multiplying the flux into the constant head nodes representing the Illinois and Arkansas Rivers by the concentration of the aquifer material. This calculation was performed using the Groundwater Vistas program. The resulting nitrate mass loading rate, reported in units of mg/L \* ft<sup>3</sup>/day was converted to mg/day by multiplying by 28.32 L/ft<sup>3</sup>. Arsenic and uranium concentrations were reported as µg/L \* ft<sup>3</sup>/day and were converted similarly.

The nitrate in groundwater discharges to the Arkansas and Illinois Rivers in the between the 001 and 005 streams. Figures 8-57 and 8-61 present calculated groundwater concentration discharging to the river at observation points 1 and 5, near the 004 and 001 streams, respectively. The nitrate concentration at Observation Point 1 in layers 5 and 6 decreases from greater than 80 mg/L at the start of the simulation to less than 10 mg/L at approximately 40 years. The highest concentration at Observation Point 5 occurs in Layer 1 at 6.3 years. The groundwater concentration entering the river at this location is less than 10 mg/L at approximately 60 years.

Calculated nitrate mass loading to the river over time is presented in Figure 8-88. The loading occurs as a sharp-fronted pulse that has a maximum loading rate of 10.4 kg/day at 15.8 years. The loading rate then quickly decreases to less than 2.0 kg/day at 50 years. At 100 years, the calculated loading rate is less than 0.4kg/day.

The arsenic in groundwater discharges to the Arkansas and Illinois Rivers in the between the 001 and 005 streams. Figures 8-68, 8-72 and 8-76 present calculated groundwater concentration discharging to the river at observation points 1, 5 and 8. The arsenic concentration at Observation Point 1, 27 µg/L, in layer 6 is greatest at 15 years and diminishes to less than 5 µg/L at approximately 30 years. The highest concentration at Observation Point 5, 69 µg/L, occurs in Layer 1 at 15 years. The groundwater concentration entering the river at this location is less than 5 µg/L at approximately 90 years. Observation Point 8 exhibits the greatest concentration, 28 µg/L, at 15 years and falls below the 5 µg/L protective standard at 25 years.

Calculated arsenic mass loading to the river over time is presented in Figure 8-89. The loading occurs as a sharp fronted pulse that has a maximum loading rate of 0.0028 kg/day at 15 years. The loading rate then quickly decreases to less than 0.0005 kg/day at 50 years. At 100 years, the calculated loading rate is less than 0.00015 kg/day.

The model results indicate that uranium in groundwater discharges to the Arkansas and Illinois Rivers in the areas near the 001, 005, and 007 streams. Figure 8-90 presents calculated groundwater concentration discharging to the river versus time in Unit 5 Shale (Layer 6) near the 001, 005, and 007 streams. Groundwater discharge to the river near streams 005 and 007 both have maximum concentrations slightly higher than the MCL of 30 µg/L, 36.3 µg/L and 41.7

µg/L, respectively. The calculated concentration discharging to the river near the 001 Stream appears to reach a maximum of 3.6 µg/L at 1,000 years. Calculated uranium mass loading to the river over time is presented in Figure 8-91. The calculated groundwater loading occurs in two distinct pulses. The initial pulse enters the river at approximately 250 years in response to the discharging of mass from the 007 stream. Peak loading during the initial pulse is calculated to be 0.355 g/day. The second pulse results from mass in the 005 Stream entering the river. This pulse peaks at 0.514 g/day at 550 years. At 1,000 years, the calculated uranium mass loading to the river is 0.103 g/day.

### 8.5.7 Sensitivity Analysis

A sensitivity analysis was conducted in order to determine the model-calculated response to changes in selected model parameters. Sensitivity analyses for the flow and transport models were conducted using UCODE (Poeter and Hill, U.S.G.S., 1998). Transport sensitivity analysis was conducted on the calibrated uranium transport model. To calculate dimensionless sensitivities of the simulated parameters, the application models, in this case MODFLOW and MT3DMS, are executed for each parameter. For the flow model these parameters include hydraulic conductivity, recharge, and evapotranspiration. Transport model parameters implemented in the sensitivity analyses include  $K_d$ , dispersion and porosity. UCODE then calculated the difference between the perturbed (slightly different) simulated responses to the unperturbed simulated response. These differences are used to calculate forward difference sensitivities. The changes in parameter values are then compared against change in the sum of the weighted residuals.

The results of the flow model sensitivity analyses for each parameter are presented in Figures 8-92 and 8-93. Figure 8-92 depicts the composite dimensionless sensitivity by parameter. Parameters that were selected for sensitivity analysis are identified in Table 8-6. Sensitivity was divided into two subjective categories: high and low. Parameters Kx12, Kx14, Kx16, R6, R5, ET2 and ET3 are classified as highly sensitive. The remaining parameters, Kx15, Kx13, Kx18, Kx11, R3, R4, and ET5 are classified as low sensitive parameters. In general, parameters with low sensitivity may have inaccuracies that slightly influence the model results. Conversely,

highly sensitive parameters that contain relatively small inaccuracies in parameter estimates may have large implications in the model results.

Figure 8-93 displays the UCODE determined dimensionless sensitivities for each parameter for each target well. Most wells have low sensitivity to variation in the sensitivity parameters examined. The five wells that display the greatest sensitivity are MW96A, MW99A, MW50B, MW112, and MW113. While the magnitude of sensitivity in these five wells is greater than most other wells, the proportional sensitivity to each parameter is about the same. MW112 and MW113 are located south of the Fertilizer Ponds. MW96A, MW99A, and MW50B are all located north and west of the Fluoride Holding Basin.

As stated previously, transport sensitivity analysis was conducted on the calibrated uranium model. The uranium model was selected because of its increased significance in model prediction errors. Parameters that were selected for sensitivity analysis are identified in Table 8-7.

Figure 8-94 summarizes the composite scaled parameter sensitivities. The parameters were subjectively divided into high sensitive and low sensitive parameters. Unlike the flow analysis, no parameters fell into the moderately sensitive category. Only A11, Kd33, and KD37 were classified as low sensitivity parameter. The transport model results appear to be sensitive to most of the  $K_d$  values used in the model. Bedrock porosity also appears to be a high sensitive parameter. The calculated sensitivity results are unsurprising. The  $K_d$  parameter and porosity both have significant contribution in the calculation of solute velocity and should affect the transport modeling results. Little transport occurs in the terrace materials, therefore, parameter Kd37 variations should have little impact on the transport modeling results.

## 9.0 ANALYSIS AND CONCLUSIONS

The overall reclamation objective for the SFC Facility is to provide post-closure site conditions that provide long-term protection of public health, safety and the environment. The site investigation and predictive flow and transport modeling in this report have focused on understanding the site post-closure groundwater conditions. Specifically, the transport modeling effort was designed to determine if groundwater COCs present a potential future hazard to the public or the environment. To make this determination, the predicted future groundwater COC concentrations at the exposure points, developed in Section 8.0 of this report, must be compared to appropriate protective human and ecological values. The following sections develop these appropriate protective values and discuss the relationship between the values and the modeling results.

### 9.1 Appropriate Protective Values

Determination of appropriate protective values for the specific Site groundwater COCs depends on the type of future receptors and the potential exposure routes to which those receptors may be subjected. Potential receptors at the site include human and other terrestrial organisms as well as aquatic receptors in the rivers and drainages in and adjacent to the Facility. The potential exposure routes for the human and other terrestrial organisms are primarily from consumption of surface water at seeps, stream drainages or rivers. Direct groundwater consumption has not been specifically addressed, as it is believed that the saturated shale units below the site do not constitute a viable drinking water supply for domestic consumption because of insufficient yield and/or poor water quality such that there is a reasonable assurance that there will be no potential future exposure through this exposure route. The reader is referred to Appendix K, which contains a technical memorandum that addresses this issue in greater detail. Aquatic receptors may be exposed via both water ingestion and direct exposure. Since aquatic receptors may be resident in potentially affected water bodies and may have continual exposure, these receptors are believed to have a greater likelihood of exposure and potential risk than terrestrial species.

For humans, potential exposure concentrations are compared to drinking water standards promulgated in 40 CFR 141 (Safe Drinking Water Act). These values are also utilized for



screening-level comparisons for other possible terrestrial receptors. Use of these MCLs for this purpose is overly-conservative since these values are based on very conservative exposure and effect assumptions associated with a human residential exposure scenario, an exposure scenario that is highly unlikely at this site.

In addition to the standard species expected to occur near the Facility, due to the greater likelihood of completed exposure pathways and higher exposure levels for aquatic species, the possible occurrence of sensitive aquatic species was evaluated. The Natural Heritage Program of the Oklahoma Biological Survey does not list any Federally listed threatened or endangered aquatic species for Sequoyah County. There are, however, two aquatic species of potential concern listed by Oklahoma State that may occur in the County. The longnose darter (*Percina nasuta*) is listed as endangered by the State, and the alligator snapping turtle (*Macrolemys temminckii*) is listed as having a closed hunting season and as a species of special concern (SS2 ranking). The longnose darter has only been found in a few small streams along the far-eastern edge of Oklahoma, and is unlikely to occur near the SFC Site (Wagner and others, 1985). The alligator snapping turtle's habitat includes deepwater rivers, oxbows, sloughs, and lakes (Behler and King 1997). Therefore, there is potentially-suitable habitat for this turtle near the Site in either the Illinois or the Arkansas River, but not in the smaller feeder drainages to the rivers themselves.

Both Federal and Oklahoma State water standards relevant to human and aquatic biota surface water exposure were reviewed (Table 9-3). Applicable Federal standards are the MCL values promulgated under the Safe Drinking Water Act and the National Recommended Water Quality Criteria (NRWQC), promulgated under Section 304(a) of the Clean Water Act (40 CFR 131), for protection of aquatic biota. Oklahoma water regulations are outlined in Title 785 Chapter 45 of the Oklahoma Administrative Code. Waters designated as Public or Private Water Supply must meet Raw Water Numerical Criteria (785:45-5-10) and water column criteria to protect for the consumption of fish flesh and water. All waters with a designated use as fish and wildlife propagation must achieve protective values for toxic substances (785:45-5-12). These criteria are to be met at all times outside of the regulatory mixing zone as defined in 785:45-5-26. As listed in the Oklahoma State Regulations, the Arkansas River near the site has designated uses of: 1)

Emergency Water supply, 2) Warm Water Aquatic Community water, and 3) Primary Body Contact recreational water. The Illinois River has designations of: 1) Public and Private Water Supply, 2) Trout Fishery, 3) a Class I irrigation water, 4) Primary Body Contact recreational water, and 5) a High Quality Water.

Three COCs have been identified by SFC: arsenic, uranium, and nitrate. The protective values for these COCs are discussed in the following section, relative to applicable regulatory limits and exposure to terrestrial and aquatic receptors in the Arkansas and Illinois Rivers, and tributaries that originate on or near the site.

The recently revised (October 2001) Federal arsenic MCL is 10 parts per billion (ppb). The existing Oklahoma arsenic Raw Water Criteria is 40 ppb. The Illinois River would need to meet this criteria outside of the mixing zone (long-term average concentration) due to its designation as a Public and Private Water Supply. The NRWQC values are general arsenic values and are highly dependent on chemical speciation of the arsenic and the specific species at potential risk. Derivation of site-specific criteria may be applicable to the SFC Site. The general values listed are conservative values that assume the presence of the more toxic arsenic (III) form and sensitive species.

The MCL listed by the EPA for uranium is 30 ppb. The Canadian Maximum Acceptable Concentration or MAC (~MCL) is 100 ppb for drinking water. There are no NRWQC values or Oklahoma State numerical criteria values for uranium. Other potentially applicable and relevant values are the Colorado water criteria for protection of aquatic life of 2.4 ppm for acute exposure and 1.5 ppm for chronic (CDPHE, 2001). The Colorado values are hardness dependent and are listed for a hardness value of 100 ppm (expressed as  $\text{CaCO}_3$ ). At a hardness of 400 ppm, the acute value is 11.1 ppm and the chronic value is 6.9 ppm. The Oak Ridge National Laboratory Guidance (ORNL, 1998) lists a radiological screening level for U-238+daughter products that is protective of fish of  $4.55\text{E}3$  pCi/L. Assuming an activity factor of  $0.68$  pCi/ $\mu\text{g}$ , this ORNL value results in a "safe" uranium concentration of 6.7 ppm for fish. Additional uranium safe and toxic values from the literature are listed in Table 9-1. A reasonable safe level for fish from this data is 1 ppm.

The Federal and State regulatory limits for nitrate in drinking water is 10 ppm. There are no NRWQC or State numerical criteria for protection of aquatic life. Values from the literature on safe and toxic water concentrations of nitrate to fish and aquatic invertebrates are shown in Table 9-2. Amphibians appear to be more sensitive to nitrate than purely aquatic species. The lowest reported toxic concentration to aquatic invertebrates is 65.5 ppm. Fish are not affected by nitrate concentrations up to at least 3,000 ppm. Based on the available literature values, a protective value of 10 ppm is set for aquatic biota.

Table 9-3 summarizes available ARARs and selected appropriate protective standards, as developed above, for humans and for aquatic life.

## **9.2 Status of Future Protection from Groundwater**

The degree of protection of humans as well as terrestrial and aquatic ecological receptors from potential impacts due to exposure to future groundwater concentrations are evaluated by comparing the transport modeling results presented in Section 8.0 and the appropriate protective standards developed in Section 9.1. The critical model output includes the peak constituent concentrations in the Site streams and the total loading from streams and groundwater discharge to the River.

The following section addresses the status of protection from groundwater conditions in two steps. The first addresses the concentrations and potential exposures in the streams as well as the constituent loads these streams carry. The second addresses the concentrations and potential exposures in the river from stream loading and the groundwater discharging directly to the rivers.

### **9.2.1 Stream Concentrations and Conditions**

The predicted concentrations of arsenic, uranium, and nitrate in the streams and seeps are discussed in Sections 8.5.6.2 and 8.5.6.3. The estimated loading of these constituents to the river, as a result of the Site discharge is discussed in Section 8.5.6.4. These stream outfall concentrations are also illustrated in Figures 8-82 through 8-84. The predicted results show that there is insufficient loading of arsenic, uranium, or nitrate in any stream to present a potential future hazard to humans from concentrations of nitrate, arsenic or uranium in the streams. While

there are some transient exceedances of the MCL values in the seeps (Figures 8.85-8.87), especially for nitrate, the likely point of exposure to humans is the streams, which have predicted concentrations below the protective levels (MCLs) over all of the compliance period. Additionally, all predicted concentrations of arsenic and uranium in the seeps are below protective standards developed in Section 9.1 (Table 9-3) for aquatic life. As shown in Table 9-2, fish are unlikely to be effected by nitrate concentrations as high as 3,000 mg/L. Aquatic invertebrates and amphibians, however, may be at risk at lower nitrate levels more than fish. The maximum nitrate concentration of 9 ppm (005 Stream) is below levels reported as toxic to these organisms (Table 9-2), but is at the high end of concentrations that are reported as no observed adverse effects levels (NOAEL). With the exception of threatened and endangered species, the overall ecological concern is protecting the population of each species, rather than individual organisms. Given, that only the 005 Stream on the site is predicted to contain elevated nitrate levels, and that these concentrations will exist for a reasonably short time period (less than 20 years), the overall population of invertebrates and amphibians within the overall watershed, or even within the Facility boundary, will not be significantly impacted due to the limited spatial and temporal nature of the elevated nitrate levels.

In terms of terrestrial receptors, ruminants (i.e. deer, cattle, sheep) are the most sensitive receptor. Acute toxicity to cattle has been reported at nitrate concentrations of 500 mg/L (Francis, 1994). Dogs and rats are not affected by dietary nitrate concentrations as high as 10,000 mg/kg (equivalent to mg/L; Francis, 1994). The EPA summarizes extensive work conducted by the Food and Drug Administration on nitrate toxicity to animals. Based on these results, no observed adverse effect levels (NOAEL) of 66 NO<sub>3</sub> mg/kg body weight per day were reported for mice and 41 mg NO<sub>3</sub>/kg body weight per day for rabbits (IRIS, 2001). These values can be converted to water concentrations by accounting for the weight of these species and their daily water consumption. This conversion results in safe drinking water concentrations of 330 mg/L for mice (based on deer mice) and 422 mg/L for rabbits (based on eastern cottontail values). From this discussion, the highest stream nitrate concentration of 9 ppm is not expected to negatively impact terrestrial receptors.

### 9.2.2 River Loading and Calculated Concentrations

The potential future concentrations in the river, due to loading of site-derived constituents from the groundwater and stream drainages, are evaluated using the methods and criteria presented in the Oklahoma Water Resources Board (OWRB) Rules Chapters 45 (Oklahoma's Water Quality Standards) and Chapter 46 (Implementation of Oklahoma's Water Quality Standards). This approach looks at the total waste loads to the river from both groundwater and stream drainage discharges.

The transport modeling has demonstrated that nitrate is the sole critical COC and is being loaded to the River both by direct groundwater discharge and through discharge of the 001 Drainage, which receives load from site groundwater up gradient from the river. The Arkansas River from the Arkansas State line to the mouth of the Canadian River, including Robert S. Kerr Reservoir, has a designated beneficial use of Public and Private Water Supply (PPWS) and has a Fish and Wildlife Service subcategory designation of Warm Water Aquatic Community (WWAC; 785:45 Appendix A). Section 785:46-7-1(e) of the OWRB Rules states that human health criteria apply to the receiving waters designated PPWS. Therefore, because OWRB Chapter 45 does not have aquatic protection standards for nitrate, the human health standard of 10 mg/L is the controlling standard. Further, Section 785:46-7-2(a) states that long-term average receiving stream flows shall be used to implement water column numerical criteria to protect human health. This means that the mean annual flow of the River at the reach where loading is occurring is the appropriate flow to consider when calculating the allowable Waste Load Allocation (WLA, 785:45-5-4).

For this site, the only WLA of concern is the total mass of nitrate being loaded to the river per unit time. The allowable WLA can be established through a mass balance calculation using the following equation:

$$C_u Q_u + C_e Q_e = C(Q_u + Q_e) \quad (\text{Equation 1})$$

Where:

$C_u$  = upstream concentration (assumed to be very small or zero)

$Q_u$  = upstream receiving water flow (mean annual flow)

$C_e$  = concentration of the effluent being discharged into the River

$Q_e$  = flow rate of this effluent discharge  
 $C$  = regulatory protective standard (10 mg/L)

This equation may be simplified in the following manner. First, the assumption is made that the quantity  $C_u$  is very small or essentially zero, eliminating background mass term ( $C_u Q_u$ ). This leaves the term  $C_e Q_e$ , which is the allowable WLA. Second, it can reasonably be assumed that the quantity  $Q_e$  (the combined flows of the ground water and the streams) is much smaller than the quantity  $Q_u$  (the flow rate of the river). This assumption reduces the right side of the equation to  $C Q_u$ . Given  $C$  is the 10 mg/L protective standard and  $Q_u$  is the annual average flow of the river (1,610 cfs or 3,938,284,627 liters per day), the allowable WLA is, therefore,  $3.9 \times 110$  mg/day (39,383 Kg/day). This allowable WLA is three orders of magnitude greater than the estimated 10.4 Kg/day maximum peak loading to the river from all sources predicted by the transport model (see Section 8.5.6.4). Therefore, it is clear that the contribution of nitrate to the river adjacent to the site has no potential to pose a present or potential future hazard to public health safety or the environment. Similarly, arsenic and uranium pose no present or potential future hazard to any receptor in the river.

### 9.3 Conclusions

The transport modeling, based on detailed understanding of site-specific hydrologic, geologic and geochemical conditions, indicates that there are no significant hazards to humans in the site surface waters or adjacent river resulting from arsenic, nitrate, or uranium in the site groundwater. The arsenic and uranium concentrations in the streams are also below protective levels for ecological receptors. Further, there are no present or potential future hazards from nitrate in the river or any of the surface drainage streams, with the possible exception of the 005 Stream. Though transient (less than 5 years) concentrations in this stream are less than concentrations reported as effecting aquatic invertebrates and amphibians, the maximum concentrations are at the upper end, or exceed, reported NOAEL values for these organisms. Any potential impacts to these biotic groups, however, will be limited due to the rapid decrease in stream concentrations, and the limited spatial scale (i.e. one stream on the site) of elevated concentrations.

## 10.0 REFERENCES

- American Public Health Association (APHA), 1992. *Standard Methods for the Examination of Water and Wastewater*. In A.E. Greenberg and others (eds.) 18<sup>th</sup> Edition. American Public Health Association, Washington, D.C.
- Anderson, M.P. and W.W. Woessner, 1992. *Applied Groundwater Modeling: Simulation of Flow and Advective Transport*. New York, New York, Academic Press Inc.
- Behler, J.L. and F.W. King, 1997. *National Audobon Society Field Guide to North American Reptiles and Amphibians*. Alfred A. Knopf, New York, NY.
- Bohn, H.L., B.L. McNeal, and G.A. O'Connor, 1985. *Soil Chemistry*. 2nd Edition. John Wiley & Sons, New York.
- Brookins, D.G., 1988. *Eh-pH Diagrams for Geochemistry*. Springer-Verlag, Berlin. pp. 176.
- Colorado Department of Public Health and Environment (CDPHE), 2001. Regulation No. 31-The Basic Standards and Methodologies for Surface Water (5 CCR 1002-31).
- Camargo, J.A. and J.V. Ward, 1992. "Short-term Toxicity of Sodium Nitrate to Non-target Freshwater Invertebrates." *Chemosphere* 24: 23-28
- Camargo, J.A. and J.V. Ward, 1995. "Nitrate Toxicity to Aquatic Life: A Proposal of Safe Concentrations for Two Species of Neararctic Freshwater Invertebrates." *Chemosphere* 31:3211-3216.
- Daugherty, R., J. Franzini, and E. Finnemore, 1985. *Fluid Mechanics with Engineering Applications*. McGraw-Hill, New York.
- Davis, J.A. and D.B. Kent, 1990. "Surface Complexation Modeling in Aqueous Geochemistry." In M.F. Hochella and A.F. White (Editors), Mineral-Water Interface Geochemistry. Reviews in Mineralogy. Mineralogical Society of America, Washington D.C., pp. 177-260.
- Doherty, J., 1994. PEST: Model-Independent Parameter Estimation. Watermark Computing.
- Doherty, J., 1995. PEST Utilities for MODFLOW and MT3D Parameter Estimation. Watermark Computing.
- Doherty, J., 2000. PEST-ASP. Model-Independent Parameter Estimation. Watermark Computing.

- Doherty, J., 2001. Manual for Groundwater Data Utilities. Watermark Numerical Computing.
- Domenico, P.A. and F.W. Schwartz, 1998. Physical and Chemical Hydrogeology. Wiley, New York.
- Duff, M.C. and C. Amrhein, 1996. "Uranium(VI) Adsorption on Goethite and Soil in Carbonate Solutions." *Soil Science Society of America Journal*. 60:1393-1400.
- Dzombak, D.A. and F.M.M. Morel, 1990. *Surface Complexation Modeling-Hydrous Ferric Oxide*. John Wiley & Sons, New York. pp. 393.
- Earth Science Consultants, 1998. Treatability Study Report, Sequoyah Fuels Corporation, Gore Oklahoma. Consultant Report. December.
- Fetter, C.W. 1999. *Contaminant Hydrology*. 2<sup>nd</sup> Ed., Upper Saddle River, New Jersey: Prentice Hall, Inc.
- Francis, A. 1994. Toxicity Summary for Nitrates. Prepared for U.S. Army Environmental Center, Aberdeen Proving Ground, MD. Contract DE-AC05-84OR21400.
- Freeze, R.A. and J.A. Cherry 1979. *Groundwater*. Englewood Cliffs, New Jersey: Prentice Hall, Inc.
- Hamilton, S. J., 1995. "Hazard Assessment of Inorganics to Three Endangered Fish in the Green River, Utah." *Ecotoxicology and Environmental Safety* 30: 134-142.
- Harlin, C., 2001. Site Manager at Sequoyah Fuels Company, Gore, Oklahoma. Personal communication to M. Gard, Shepherd Miller, Inc., Fort Collins, Colorado. August 24.
- Hecnar, S.J., 1991. "Acute and Chronic Toxicity of Ammonium Nitrate Fertilizer to Amphibians from S. Ontario." *Environ. Toxicol. Chem.* 14: 2131-2137.
- Holdway, D. A., 1992. "Uranium Toxicity to Two Species of Australian Tropical Fish." *Sci. Total Environ.* 125: 137-158.
- Integrated Risk Information System (IRIS), 2001. Nitrate (CASRN 14797-55-8). United States Environmental Protection Agency.
- International Centre for Diffraction Data. 1993. Mineral Powder Diffraction File. ICDD, Swarthmore, PA.



- Jenne, E.A., 1968. "Controls on Mn, Fe, Co, Ni, Cu, and Zn Concentrations in Soils and Water: The Significant Role of Hydrous Mn and Fe Oxides." *American Chemical Society Advances in Chemistry Series*. 7337-387.
- Jove Colon, C.F., Brady, P.V., Siegel, E.R. and Lindgren, E.R., 2001. Historical Case Analysis of Uranium Plume Attenuation. NUREG/CR-6705, U.S. Nuclear Regulatory Commission, Washington, D.C.
- Langmuir, D.L. and A.C. Riese, 1985. "The Thermodynamic Properties of Radium." *Geochimica et Cosmochimica Acta*. 49:1593-1601.
- Langmuir, D.L., 1997. *Aqueous Environmental Geochemistry*. Prentice Hall, New Jersey.
- Lovley, D., E. Phillips, Y. Gorby, and E. Landa, 1991. "Microbial Reduction of Uranium." *Nature*, Vol. 350, pp. 413-416.
- Marcher, M.V., 1969. "Hydrologic Atlas 1, Reconnaissance of the Water Resources of the Fort Smith Quadrangle, East-central Oklahoma." Oklahoma Geological Survey, scale 1:250,000, 4 sheets.
- McDonald, M.G. and A.W. Harbaugh, 1988. *A Modular Three-dimensional Finite-difference Groundwater Flow Model*. U.S. Geological Survey Professional Paper.
- Meade, T.L., 1974. *The Technology of the Closed System Culture of Salmonids*. University of Rhode Island, Narragansett, RI.
- Miller, M.A., Eames, L. E., and Prezbindowski, D.R., 1989. "Upper Mississippian and lower Pennsylvanian lithofacies and palynology from northeastern Oklahoma: a field excursion." In *American Association of Stratigraphic Palynologists*, Field trip guidebook, pp. 64.
- Mitchum, D. L. and T. D. Moore, 1966. "Study of Water Pollution Problems which Affect Fish and Other Aquatic Forms." Laramie, University of Wyoming, Game and Fish Laboratory Report FW-3-R-13.
- Ogata, A., and R. Banks, 1961. "A Solution of the Differential Equation of Longitudinal Dispersion in Porous Media." U.S. Geological Survey Professional Paper 411-A.
- Oak Ridge National Laboratory (ORNL), 1998. Radiological Benchmarks for Screening Contaminants of Potential Concern for Effects on Aquatic Biota at Oak Ridge National Laboratory, Oak Ridge, Tennessee. BJC/OR-80.

Parkhurst, B. R., R. G. Elder, J. S. Meyer, D. A. Sanchez, R. W. Pennak, and W. T. Waller, 1984. "An Environmental Hazard Evaluation of Uranium in a Rocky Mountain Stream." *Environ. Toxicol. Chem.* 3: 113-124.

Parkhurst, D.L. and C.A.J Appelo, 1999. "User's Guide to PHREEQC (Version 2) - A Computer Program for Speciation, Batch-Reaction, One-Dimensional Transport, and Inverse Geochemical Calculations." USGS Water-Resources Investigations Report 99-4259. United States Geological Survey, Denver, Colorado.

Pierce, M.L. and Moore, C.B., 1980. Adsorption of arsenite on amorphous iron hydroxide from dilute aqueous solution. *Environ. Sci. Technol.*, 14: 214.

Pierce, M.L. and C.B. Moore, 1982. "Adsorption of Arsenite and Arsenate on Amorphous Iron Hydroxide." *Water Resources*. 16:1247-1253.

Pierce, R.H., J.M. Weeks, and J.M. Prappas, 1993. "Nitrate Toxicity to Five Species of Marine Fish." *J. World. Aquaculture Soc.* 24:105-107.

Poeter, E., and M. Hill, 1998. "Documentation of UCODE, A Computer Code for Universal Inverse Modeling." USGS Water-Resource Investigations Report 98-4080. United States Geological Survey, Denver, Colorado.

Raven, K.P., Jain, A. and Loeppert, R.H., 1998. Arsenite and arsenate adsorption on ferrihydrite: Kinetics, equilibrium, and envelopes. *Environ. Sci. Technol.*, 32(3): 344-349.

Reardon, E.J., 1981. " $K_d$ 's - Can they be used to describe reversible ion sorption reactions in contaminant migration?" *Ground Water*, 19(3): 279-286.

Roberts/Schornick & Associates, Inc. (RSA), 1991. "Sequoyah Fuels Corporation Facility Environmental Investigation Findings Report." Consultant Report. Volumes I – V. July 31.

Rumbaugh, J., and D. Rumbaugh, 2001. Groundwater Vistas, Version 3.09, developed by Environmental Simulations, Inc. Herndon, Virginia.

Sawhney, B.L. 1989. "Interstratification in Layer Silicates." In J.B. Dixon and S.B. Weed (eds.) *Minerals in Soil Environments*. Soil Science Society of America, Madison, Wisconsin. pp. 789-824.

Sequoyah Fuels Corporation (SFC), 1997. "Final RCRA Facility Investigation of the Sequoyah Fuels Uranium Conversion Industrial Facility."

Sequoyah Fuels Corporation (SFC), 1998a. "Site Characterization Report." December 15.

- Sequoyah Fuels Corporation (SFC), 1998b. "Final Decommissioning Alternatives Study Report [FDASR]." June 8.
- Sequoyah Fuels Corporation (SFC), 1999. "Decommissioning Plan." March 26.
- Shepherd Miller, Inc. (SMI), 2001. "Hydrogeochemical Characterization Work Plan." Consultants Report. April.
- Stephens, D. W., B. Waddell, and J. B. Miller, 1988. "Reconnaissance Investigation of Water Quality, Bottom Sediment, Biota Associated with Irrigation Drainage in the Middle Green River Basin, Utah, 1986-1987." USGS Water-Resources Investigations Report 88-4011, U. S. Geological Survey, Salt Lake City, Utah.
- Stumm, W. and J.J. Morgan, 1996. Aquatic Chemistry. Wiley, New York.
- Sutherland, P.K., 1988. "Late Mississippian and Pennsylvanian Depositional History in the Arkoma Basin Area." Oklahoma and Arkansas: Geological Society of America Bulletin, v. 100, pp. 1787-1802.
- Tarzwel, C. M. and C. Henderson, 1960. "Toxicity of Less Common Metals to Fishes." *Ind. Wastes* 5: 12.
- U.S. Army Corps of Engineers (COE), 1982. "Engineering and Design Stability for Earth and Rockfill Dams." EM1120-2-1902.
- U.S. Environmental Protection Agency (EPA), 1999. "Understanding Variation in Partition Coefficient,  $K_d$ , Values. Volume II: Review of Geochemistry and Available  $K_d$  Values for Cadmium, Cesium, Chromium, Lead, Plutonium, Radon, Strontium, Thorium, Tritium ( $^3\text{H}$ ), and Uranium." Office of Air and Radiation. EPA402-R-99-004B. August.
- U.S. Nuclear Regulatory Commission (NRC), 1998. "Sequoyah Fuels Corporation (SFC) Site evaluation of faults and faulting: Input to safety evaluation report." Note to James Shepherd, Sequoyah Fuels Corporation, from Philip Justus, NRC, December 3.
- Wagner, B.A., A.A. Aschelle, O.E. Maughan, 1985. "Status and Distribution of the Longnose Darter, *Percina nasuta*, and the Neosho Madtom, *Noturus placidus*." In Oklahoma. Proceed. Okla. Acad. Sci. 65: 59-60.
- Welch, A.H., D.B. Westjohn, D.R. Helsel, and R.B. Wanty. 2000. "Arsenic in Groundwater of the United States: Occurrence and Geochemistry." *Groundwater*. Vol. 38, pp. 589-604.

- Xu, M., and Y. Eckstein. 1995. "Use of Weighted Least Squares Method in Evaluation of the Relationship Between Dispersivity and Field Scale." *Groundwater*, Vol. 33, No. 6:905-908.
- Zachara, J.M. and S.C. Smith, 1994. "Edge Complexation Reactions of Cadmium on Speciman and Soil-derived Smectite." *Soil Science Society of America Journal*, 58(3): 762-769.
- Zheng, C., and P. Wang, 1999. *MT3DMS: A Modular Three-Dimensional Multispecies Transport Model for Simulation of Advection Dispersion and Chemical Reactions of Contaminants in Groundwater Systems; Documentation and User's Guide*. Washington D.C.
- Zheng, C. 1990. *A Modular Three-dimensional Transport Model for Simulation of Advection, Dispersion and Chemical Reactions of Contaminants in Groundwater Systems*. U.S. Ada, Oklahoma, Environmental Protection Agency.

## TABLES

**Table 2-1      Annual Average Flow**

Year	Annual Average Flow (cfs)	Year	Annual Average Flow (cfs)
1939	543.3	1970	2164.6
1940	623.4	1971	1150.0
1941	2006.7	1972	1153.8
1942	2293.9	1973	3999.0
1943	1821.7	1974	2717.0
1944	1532.1	1975	2266.3
1945	3811.9	1976	1402.9
1946	2250.9	1977	434.5
1947	1210.1	1978	1524.3
1948	1815.8	1979	955.1
1949	2226.1	1980	445.5
1950	2513.5	1981	593.4
1951	1595.6	1982	1213.5
1952	918.1	1983	1011.6
1953	185.6	1984	1585.9
1954	695.0	1985	2542.9
1955	778.9	1986	2639.0
1956	337.9	1987	1746.5
1957	2816.8	1988	1548.8
1958	1695.3	1989	1493.4
1959	1363.7	1990	2977.2
1960	1546.4	1991	1957.0
1961	2258.7	1992	1909.4
1962	1205.9	1993	3203.4
1963	351.3	1994	1738.5
1964	365.0	1995	1964.5
1965	872.3	1996	1590.7
1966	937.0	1997	1385.0
1967	359.6	1998	1822.5
1968	1939.2	1999	1921.1
1969	1829.8	2000	2066.2
<b>Total annual average flow</b>			<b>1610.0</b>

Flow data from Tenkiller Dam Gauging Station

**Table 2-2 Stream Flow Calculations**

Stream	Drainage Area (mi <sup>2</sup> )	Calculated Mean Annual Flow (cfs)
001	0.063	0.056
004	0.019	0.017
005	0.031	0.027
007	0.069	0.061

**Table 2-3 Location and Description of Seeps and Pools**

Seep and Pool	Northing	Easting	Description	Comments
007 Outfall Pool	197483.5	2835845.3	about 4½' Long X 4' Wide X 2" Deep	Located on top of sandstone No significant algae or bug life present
005 Outfall Seep and Pool	Located about 40 feet southwest of MW-100B		about 12' Long X 7' Wide X 5" Deep	Significant algae and bug life present in pool Located on top of sandstone
008 Outfall Seep and Pool	195156.8	2834289	1' X 3' X 2" Deep	Some flow observed but very slight Located on top of sandstone

**Table 4-1      Location Summary**

<b>Location</b>	<b>Borehole</b>	<b>Monitoring Well</b>
1	NA	MW-118
2	BH-328	MW-111A, MW-114A, MW-120
3	BH-330	
4	BH-327	MW-110A
5	BH-331	MW-113A
6	BH-329	MW-112A
7	BH-333 BH-334	
8	BH-339 BH-340	
9	SAME AS LOCATION 3	
10	BH-332	
11	BH-335	MW-115A
12	BH-338	MW-117
13	BH-337	MW-119A
14	BH-336	MW-116A



**Table 4-2 Monitoring Well Survey Information**

Monitoring Well	Northing <sup>1</sup>	Easting <sup>1</sup>	Top of PVC Elevation <sup>2</sup>	Stickup (ft) <sup>3</sup> (PVC height above ground surface)	Ground Surface Elevation <sup>4</sup>
MW-110A	194734.729	2838412.800	554.934	2.34	552.594
MW-111A	193655.492	2833803.491	483.095	2.90	480.195
MW-112A	192595.278	2833775.339	485.713	2.83	482.883
MW-113A	192791.609	2836049.545	504.498	2.90	501.598
MW-114A	193665.618	2833804.796	483.019	2.93	480.089
MW-115A	194834.682	2835592.937	528.052	2.34	525.712
MW-116A	194444.654	2837511.146	542.637	2.82	539.817
MW-117	194357.346	2834786.146	491.248	3.14	488.108
MW-118	196921.188	2836603.199	551.359	2.7	548.659
MW-119A	194780.707	2836858.314	541.327	2.91	538.417
MW-120	193645.224	2833802.577	482.763	2.59	480.173

1 State plane coordinates of PVC well casing.

2 Surveyed top of PVC well casing, feet above mean sea level

3 Stickup measured during well construction.

4 Ground surface elevation (feet above mean sea level) calculated using surveyed top of PVC well casing and stickup measured during completion

**Table 4-3 Borehole Survey Information**

Borehole	Northing <sup>1</sup>	Easting <sup>1</sup>	Ground Surface Elevation <sup>2</sup>	Total Depth Elevation <sup>3</sup> (Depth) <sup>4</sup>
BH-327	194737.544	2838429.968	549.519	499.519
BH-328	193658.419	2833793.889	479.860	432.860
BH-329	192596.303	2833765.847	482.458	441.458
BH-330	195232.190	2835267.952	538.550	485.050
BH-331	192778.644	2836051.066	500.959	458.959
BH-332	196421.514	2836778.759	559.406	543.406
BH-333	195906.448	2836846.613	564.919	536.919
BH-334	195890.142	2836847.933	565.355	541.855
BH-335	194835.138	2835602.774	525.631	507.631
BH-336	194456.380	2837511.637	539.378	519.178
BH-337	194784.183	2836948.621	543.191	529.191
BH-338	193949.250	2834874.424	484.708	478.708
BH-339	195204.274	2836453.104	549.652	500.652
BH-340	195204.274	2836450.104	549.652	534.152

1 State plane coordinates

2 Surveyed ground surface elevation, feet above mean sea level

3 Elevation (feet above mean sea level)

**Table 4-4 Borehole Summary**

Borehole	Total Depth <sup>1</sup>	Alluvium or terrace <sup>1</sup>	Unit 1 Shale	Unit 1 Sandstone <sup>1</sup>	Unit 2 Shale <sup>1</sup>	Unit 2 Sandstone <sup>1</sup>	Unit 3 Shale <sup>1</sup>	Unit 3 Sandstone <sup>1</sup>	Unit 4 Shale <sup>1</sup>	Unit 4 Sandstone <sup>1</sup>	Unit 5 Shale <sup>1</sup>
BH-327	50	0-10		10-14.8	14.8-15.7	15.7-16.7	16.7-18.9	18.9-24.2	24.2-40.6	40.6-TD	
BH-328	47	0-24.0							24.0-39.3	39.3-TD	
BH-329	41	0-15.2							15.2-33.0	33.0-39.3	39.3-TD
BH-330	53.5	0-13.0				13.0-20.4	20.4-23.0	23.0-29.7	29.7-46.1	46.1-TD	
BH-331	42	0-11.0						11.0-19.0	19.0-TD		
BH-332	16	0-10	10-16								
BH-333	28	0-4.4	4.4-19	19-25.8	25.8-27.1	27.1-TD					
BH-334	23.5			21-23.5							
BH-335	18	0-1.0				1.0-12.9	12.9-13.0	13.0-16.5	16.5-TD		
BH-336	20.2	0-6		6.0-7.5	7.5-11.0	11.0-18.3	18.3-TD				
BH-337	14	0-5.0		5.0-7.0	7.0-10.0	10.0-TD					
BH-338	6	0-TD									
BH-339	49	0-11		11-12.3	12.3-21	21-26.9	26.9-30	30-36.5	36.5-TD		
BH-340	15.5			12-14							

<sup>1</sup> Depth in feet below ground surface

**Table 4-5 Monitor Well Completion Data**

Monitor Well	Open Borehole Elevation <sup>1</sup> (Depth <sup>2</sup> )	Bottom of Screen Elevation <sup>1</sup> (Depth <sup>2</sup> )	Top of Screen Elevation <sup>1</sup> (Depth <sup>2</sup> )	Bottom of Sand Filter Pack Elevation <sup>1</sup> (Depth <sup>2</sup> )	Top of Sand Filter Pack Elevation <sup>1</sup> (Depth <sup>2</sup> )	Top of Bentonite Pellets Elevation <sup>1</sup> (Depth <sup>2</sup> )	Top of Bentonite Chip Elevation <sup>1</sup> (Depth <sup>2</sup> )	PVC Stickup <sup>3</sup>	Nominal Borehole Diameter
MW-110A	507.594 (45.0)	507.934 (44.66)	518.574 (34.02)	507.594 (45.0)	520.594 (32.0)	NA	524.194 (28.4)	2.34	8.5
MW-111A	441.695 (38.5)	442.745 (37.45)	448.095 (32.1)	441.695 (38.5)	451.295 (28.9)	454.395 (25.8)	457.695 (22.5)	2.90	8.625
MW-112A	450.483 (32.4)	451.313 (31.57)	461.663 (21.22)	450.483 (32.4)	463.983 (18.9)	NA	467.983 (14.9)	2.83	8.5
MW-113A	460.398 (41.2)	460.348 (41.25)	475.698 (25.9)	460.398 (41.2)	479.198 (22.4)	482.598 (19.0)	NA	2.90	8.5
MW-114A	441.139 (38.95)	443.089 (37.0)	448.099 (31.99)	441.139 (38.95)	451.089 (29.0)	453.089 (27.0)	455.089 (25.0)	2.93	9
MW-115A	510.812 (14.9)	512.712 (13.0)	518.042 (7.67)	512.712 (13.0)	519.712 (6.0)	521.712 (4.0)	521.112 (4.6)	2.34	8.5
MW-116A	525.617 (14.2)	525.477 (14.34)	530.817 (9.00)	525.477 (14.34)	532.817 (7.0)	533.817 (6.0)	535.117 (4.7)	2.82	8.5
MW-117	472.578 (15.53)	473.508 (14.6)	478.858 (9.25)	473.508 (14.6)	480.518 (7.59)	482.518 (5.59)	NA	3.14	8
MW-118	541.359 (7.3)	541.319 (7.34)	546.659 (2.0)	541.319 (7.34)	547.159 (1.5)	548.159 (0.5)	NA	2.70	8
MW-119A	523.917 (14.5)	524.417 (14.0)	529.757 (8.66)	524.417 (14.0)	531.417 (7.0)	533.817 (4.6)	NA	2.91	8.5
MW-120	456.173 (24.0)	455.723 (24.45)	471.073 (9.1)	455.723 (24.45)	473.673 (6.5)	475.073 (5.1)	476.673 (3.5)	2.59	8.25

1 Feet Above Mean Sea Level

2 Feet Below Ground Surface

3 Above Ground Surface

**Table 4-6 Monitor Well Development Data**

Monitor Well/Piezometer	Development Volume (gal)	Development Date	Comments
MW-110A	80	6/5/01	Bailed then purged with RediFlo2
MW-111A	24.75	6/5/01	Bailed dry three times
MW-112A	41	6/5/01	Bailed three times, can't bail dry
MW-113A	32.5	6/4/01	Bailed twice, can't bail dry
MW-114A	15.5	6/5/01	Bailed dry three times
MW-115A	0.6	NA	Monitor well dry, bailed water added during well construction
MW-116A	4.5		
MW-117	6	6/5/01	Bailed dry twice
MW-118	0	NA	Monitor well dry
MW-119A	4.0	6/5/01	
MW-120	270	6/6/01	Bailed then purged with RediFlo2

**Table 4-7 Monitor Well Static Water Levels**

Monitoring Well	Date	Depth to Water Below top of PVC (feet)	Static Water Elevation (feet above mean sea level)
MW-110A	6/13/01	19.40	533.194
MW-111A	6/15/01	15.17	465.025
MW-112A	6/12/01	17.11	465.773
MW-113A	6/12/01	2.80	498.798
MW-114A	6/15/01	15.34	464.749
MW-115A	6/16/01	Dry	Dry
MW-116A	6/13/01	Dry	Dry
MW-117	6/12/01	12.14	475.968
MW-118	6/13/01	Dry	Dry
MW-119A	6/16/01	Dry	Dry
MW-120	6/15/01	14.99	465.183

**Table 4-8 Slug Test Results**

Well	Date	Hydro-stratigraphic Unit	Horizontal Hydraulic Conductivity (ft/day)	Analytical Method
MW010	02/12/02	Gravel Backfill	23.79	Bouwer-Rice, 1976 (Unconfined)
MW117	06/12/01	Alluvium	0.0223	Bouwer-Rice, 1976 (Unconfined)
MW120	06/16/01	Alluvium	5.01	Bouwer-Rice, 1976 (Unconfined)
MW097	02/12/02	Colluvium	19.86	Bouwer-Rice, 1976 (Unconfined)
MW008	12/04/90	Terrace/Shale 1	0.0156	Bouwer-Rice, 1976 (Unconfined)
	06/15/01	Terrace/Shale 1	0.0134	Bouwer-Rice, 1976 (Unconfined)
MW012	12/06/90	Terrace/Shale 1	0.00556	Bouwer-Rice, 1976 (Unconfined)
MW013	12/06/90	Terrace/Shale 1	0.0110	Bouwer-Rice, 1976 (Unconfined)
MW016	12/06/90	Terrace/Shale 1	0.0382	Bouwer-Rice, 1976 (Unconfined)
	12/09/90	Terrace/Shale 1	0.0480	Bouwer-Rice, 1976 (Unconfined)
	06/15/01	Terrace/Shale 1	0.0129	Bouwer-Rice, 1976 (Unconfined)
MW017	12/06/90	Terrace/Shale 1	0.0311	Bouwer-Rice, 1976 (Unconfined)
	12/06/90	Terrace/Shale 1	0.126	Bouwer-Rice, 1976 (Unconfined)
MW026	06/15/01	Terrace/Shale 1	0.0310	Bouwer-Rice, 1976 (Unconfined)
MW073	06/13/01	Terrace/Shale 1	0.261	Bouwer-Rice, 1976 (Unconfined)
MW076	06/15/01	Terrace/Shale 1	0.00416	Bouwer-Rice, 1976 (Unconfined)
MW102	06/14/01	Terrace/Shale 1	0.0297	CBP, 1967 (Confined)
MW035A	06/13/01	Shale 2	1.35	CBP, 1967 (Confined)
MW040A	06/13/01	Shale 2	0.327	CBP, 1967 (Confined)
MW042A	06/13/01	Shale 2	0.0318	CBP, 1967 (Confined)
MW085A	06/15/01	Shale 2	0.0700	CBP, 1967 (Confined)
2346	06/12/01	Shale 3	0.489	CBP, 1967 (Confined)
MW037A	06/13/01	Shale 3	0.0103	Bouwer-Rice, 1976 (Unconfined)

**Table 4-8 Slug Test Results (continued)**

Well	Date	Hydro-stratigraphic Unit	Horizontal Hydraulic Conductivity (ft/day)	Analytical Method
MW084A	06/14/01	Shale 3	0.0217	CBP, 1967 (Confined)
MW093A	02/12/02	Shale 4	0.94	Bouwer-Rice, 1976 (Unconfined)
MW095A	02/12/02	Shale 4	1.88	Bouwer-Rice, 1976 (Unconfined)
MW097A	02/12/02	Shale 4	0.35	Bouwer-Rice, 1976 (Unconfined)
MW110A	06/13/01	Shale 4	0.0343	CBP, 1967 (Confined)
MW111A	06/15/01	Shale 4	0.0482	Bouwer-Rice, 1976 (Unconfined)
MW112A	06/12/01	Shale 4	1.30	Bouwer-Rice, 1976 (Unconfined)
MW113A	06/12/01	Shale 4	0.00730	CBP, 1967 (Confined)
MW114A	06/16/01	Shale 4	0.00466	Bouwer-Rice, 1976 (Unconfined)

Note CBP = Cooper, Bredehoeft & Papadopoulos

**Table 4-9 Average, Maximum, and Minimum Values of Hydraulic Conductivity**

Hydrologic Unit	Average Hydraulic Conductivity (ft/day)	Maximum Hydraulic Conductivity (ft/day)	Minimum Hydraulic Conductivity (ft/day)
Alluvium/Colluvium	8.30	19.9	0.0223
Shale 1/Terrace	0.0521	0.261	0.00416
Shale 2	0.445	1.35	0.0318
Shale 3	0.174	0.489	0.0103
Shale 4	0.571	1.88	0.00466

**Table 5-1 Core Samples Used in the Mineralogical and Geochemical Testing**

Plan Location (Figure 4-1)	Shale Unit	Borehole Designation	Sample Depth (ft)
7	1	BH-333	4.0 to 20.0
10	1	BH-332	10.7 to 16.0
8	2	BH-339	12.0 to 13.0
8	3	BH-339	26.9 to 29.1
9	3	BH-330	20.4 to 23.0
8	4	BH-339	36.5 to 39.0
9	4	BH-330	29.7 to 46.1

**Table 5-2 Calculated  $K_d$  Values for U and As for all Shale Samples**

Location	Unit	Uranium (L/Kg)	Arsenic (L/Kg)
7	1	17.1	NA <sup>1</sup>
10	1	286	>12,000 <sup>2</sup>
8	2	220	>5,650
8	3	40.6	3,968
9	3	67.4	>9,750
8	4	110	7,350
9	4	80.2	18,000

<sup>1</sup> NA indicates that arsenic in all test solutions was below detection (<0.001 mg/L)

<sup>2</sup> "Greater than" symbol indicates that arsenic fell below detection (0.001 mg/L) prior to the end of test. The  $K_d$  value shown was calculated based on the last test that contained detectable arsenic in solution.



**Table 5-3 Saturation Index Values Calculated Using PIREEQC for Important U, As, and F Solid Phases in Selected Wells**

Well I.D.	Uraninite	Coffinite	Ningyoite	Carnotite	Schoepite	Rutherfordine	Tyuyamunite	Autunite
	$\text{UO}_2(\text{c})$	$\text{USiO}_4$	$\text{CaU}(\text{PO}_4)_2 \cdot 2\text{H}_2\text{O}$	$\text{K}_2(\text{UO}_2)_2(\text{VO}_4)_2$	$\text{UO}_2(\text{OH})_2 \cdot \text{H}_2\text{O}$	$\text{UO}_2\text{CO}_3$	$\text{Ca}(\text{UO}_2)_2(\text{VO}_4)_2$	$\text{Ca}(\text{UO}_2)_2(\text{PO}_4)_2$
MW-012A	-9.28	-9.70	-15.57	0.63	-1.72	-0.43	1.28	-4.29
MW-012B	-17.64	-20.03	-21.34	-6.50	-7.53	-7.41	-6.05	-13.31
MW-025	-8.63	-8.89	-14.84	-0.68	-2.07	-0.79	0.47	-4.97
MW-025A	-7.79	-8.19	-12.87	-0.79	-3.04	-1.78	-0.01	-5.75
MW-042A	-14.18	-14.58	-18.58	-4.53	-6.10	-5.45	-3.33	-11.18
MW-059A	-12.75	-13.25	-16.74	-3.22	-5.33	-3.73	-2.22	-9.24
MW-064A	-13.40	-13.89	-17.97	-4.13	-5.78	-4.61	-3.07	-10.71
MW-067A	-11.67	-12.17	-17.00	-1.57	-3.47	-2.53	-0.77	-6.88
MW-075	-10.03	-11.63	-15.70	-2.42	-3.50	-1.67	-1.18	-7.26

Well I.D.	Uranophane	K-Autunite	Radium Sulfate	Aluminum Arsenate	Calcium Arsenate	Iron Arsenate	Fluorite
	$\text{Ca}(\text{UO}_2)_2(\text{SiO}_3\text{OH})_2$	$\text{K}_2(\text{UO}_2)_2(\text{PO}_4)_2$	$\text{RaSO}_4$	$\text{AlAsO}_4 \cdot 2\text{H}_2\text{O}$	$\text{Ca}_3(\text{AsO}_4)_2 \cdot 6\text{H}_2\text{O}$	$\text{FeAsO}_4 \cdot 2\text{H}_2\text{O}$	$\text{CaF}_2$
MW-012A	-7.68	-4.86	-8.91	-3.61	-14.89	-5.75	-4.50
MW-012B	-21.30	-13.49	-9.95	-8.65	-17.20	-7.85	-1.80
MW-025	-10.71	-6.56	-9.66	-6.57	-20.73	-6.79	-3.11
MW-025A	-10.01	-6.59	-9.08	-3.55	-14.88	-6.85	-4.61
MW-042A	-15.76	-12.86	-11.40	-4.41	-12.22	-3.96	-1.18
MW-059A	-14.46	-10.52	-8.13	-2.40	-10.87	-4.43	-2.12
MW-064A	-15.00	-12.12	-99.0	-6.18	-10.19	-2.80	+0.84
MW-067A	-10.38	-7.75	-6.87	-4.31	-14.62	-5.64	-2.37
MW-075	-14.70	-9.04	-8.59	-6.06	-15.12	-4.55	-0.70

**Table 5-4 Important Uranium-Controlling Minerals in Oxidized and Reduced Environments (USEPA, 1999)**

Reduced Environments [U(IV) Minerals]	
Uraninite	$\text{UO}_2(\text{c})$
Coffinite	$\text{USiO}_4(\text{c})$
Ningyoite	$\text{CaU}(\text{PO}_4)_2 \cdot 2\text{H}_2\text{O}$
Oxidized Environments [U(VI) Minerals]	
Carnotite	$\text{K}_2(\text{UO}_2)_2(\text{VO}_4)_2$
Schoepite	$\text{UO}_3 \cdot 2\text{H}_2\text{O}$
Rutherfordine	$\text{UO}_2\text{CO}_3$
Tyuyamunite	$\text{Ca}(\text{UO}_2)_2(\text{VO}_4)_2$
Autunite	$\text{Ca}(\text{UO}_2)_2(\text{PO}_4)_2$
K-Autunite	$\text{K}_2(\text{UO}_2)_2(\text{PO}_4)_2$
Uranophane	$\text{Ca}(\text{UO}_2)_2(\text{SiO}_3\text{OH})_2$

**Figure 5-5 Partition Coefficient ( $K_d$ ) Values Determined for Arsenic and Uranium in Laboratory Batch Tests**

Sample	Matrix type	Adsorption $K_d$		Arsenic $K_{d-srbd}^a$ (ml/g)	$K_{df}^b$ (ml/g)	Uranium $K_{d-srbd}$ (ml/g)	$K_{df}$ (ml/g)
		As	U				
005-S-01-01	Soil			46	726	1327	530
005-S-01-02	Shale			84	857	598	535
005-S-02-01	Soil	331					
005-S-02-02	Shale	348					
005-03N-1	Soil		762				
005-03N-2	Shale		1028				
005-04M-1	Soil	817	738				
005-04S-1	Soil	540	611	40	3733	258	182
005-04S-2	Shale			24	1333	308	108
005-05M-1	Soil			43	835	4212	2176
MW010-4-1	Soil		793				
MW010-4-2	Gravel		2340				
E1-1	Terrace material		572				
E2-1	Terrace material		798				

<sup>a</sup> Values determined using the hydroxylamine hydrochloride extraction procedure.

<sup>b</sup> Values determined using the EPA 3050 digestion procedure at the end of the rinse protocol.

**Table 5-6 Analytical Results for the Special Groundwater Sampling of Nine Selected Wells (June 2001) <sup>1</sup>**

Parameter	MW-012A		MW-012B		MW-025		MW-025A		MW-042A	
	Filtered	Unfiltered	Filtered	Unfiltered	Filtered	Unfiltered	Filtered	Unfiltered	Filtered	Unfiltered
Orthophosphate	<0.1		3.3		<0.1		<0.1		<0.1	
Radium-226 (pCi/L)	0.347±0.273		0.045±0.142		0.561±0.151		0.420±0.21		0.046±0.081	
Uranium	5.31	4.96	0.0126	0.0154	11.0	111	376	469	1.32	<1
Alkalinity (as CaCO <sub>3</sub> )	127		975		2		131		95	
Ammonia as N	<0.2		0.6		0.3		<0.2		<0.2	
Chloride	4,640		28.5		23.8		3,890		311	
Fluorine	0.4		2.1		1.1		0.4		1	
Nitrate	210		<1		704		482		21.1	
Nitrite	0.012		0.021		0.041		<0.01		<0.01	
Sulfate	113		12.5		6.7		67.7		<1	
Sulfide	<1		<1		<1		<1		<1	
Total Organic Carbon	<1		2.9		4.8		9.3		<1	
Total Suspended Solids		40.4		464		2340		94		552
Aluminum	2.04	1.66	0.051	13.7	1.27	90.3	2.87	0.37	0.257	26.5
Arsenic	0.051	0.05	<0.01	0.007	0.04	0.073	0.034	0.036	0.516	0.526
Calcium	887	687	2.82	5.6	386	240	915	1110	121	110
Total Iron	0.02	0.563	<0.02	9.19	0.044	98.5	0.027	5.7	0.054	26.3
Ferrous Iron	<0.01		<0.01		0.02		0.05		<0.01	
Magnesium	287	238	0.986	<2	170	117	332	390	22.3	29.6
Manganese	0.074	0.073	<0.01	0.054	4.35	4.05	0.046	0.142	<0.005	0.474
Potassium	12.2	10	1.17	4.72	2.2	24.5	8.15	10.4	1.36	9.98
Silicon	10.5	10.5	0.123	22	14.8	73.5	10.7	33.6	11.6	37.5
Sodium	1,060	886	472	399	90.5	121	435	456	60.5	56.2
Vanadium	<0.05		<0.035		<0.05		<0.05		<0.05	
Eh (mV)	484		429		534		400		461	
pH	5.48		7.64		4.23		5.56		6.12	
Temp (°C)	18.9		20.0		16.2		17.0		18.9	
Conductivity (µS/cm)	16,247		1,908		5,733		15,132		1,580	

**Table 5-6 Analytical Results for the Special Groundwater Sampling of Nine Selected Wells (June 2001)**  
(continued)

Parameter	MW-059A		MW-064A		MW-067A		MW-075	
	Filtered	Unfiltered	Filtered	Unfiltered	Filtered	Unfiltered	Filtered	Unfiltered
Orthophosphate	< 0.1		< 0.1		< 0.1		< 0.1	
Radium-226 (pCi/L)	0.978±0.168		0±0.070		2.22±0.456		0.081±0.130	
Uranium	0.0109	0.0185	0.045	0.0136	0.272	0.271	< 1	< 1
Alkalinity (as CaCO <sub>3</sub> )	346		446		< 2		< 1	
Ammonia as N	< 0.2		< 0.2		< 0.2		< 0.2	
Chloride	63.7		45.6		155		268	
Fluorine	2.7		7.6		0.5		2.8	
Nitrate	2,560		2		1.3		< 1	
Nitrite	0.114		< 0.01		< 0.01		< 0.01	
Sulfate	359		185		1,990		278	
Sulfide	< 1		< 1		< 1		< 1	
Total Organic Carbon	2.5		1.8		2.4		8.3	
Total Suspended Solids		5.6		45.6		49.6		278
Aluminum	3.67	3.37	0.201	3.47	1.12	5.41	0.394	10.1
Arsenic	1.42	1.4	4.29	3.86	0.026	0.032	1.96	2.28
Calcium	1490	1380	102	77.3	229	164	38.8	26.6
Total Iron	0.015	0.438	0.109	4.52	0.032	4.27	< 0.02	7.06
Ferrous Iron	< 0.01		< 0.01		< 0.01		< 0.01	
Magnesium	476	444	26.8	16.3	153	123	14.9	1.76
Manganese	0.248	0.097	0.047	0.153	0.018	0.151	< 0.01	0.549
Potassium	6.22	6	1.5	2.57	3.33	4.1	0.57	3.22
Silicon	8.41	9.59	9.27	13.2	8.63	14.6	0.69	24.6
Sodium	343	302	96.6	77.3	349	225	230	178
Vanadium	< 0.05		< 0.05		< 0.05		< 0.035	
Eh (mV)	475		440		460		455	
pH	5.64		6.3		6.27		5.51	
Temp (°C)	16.9		17.7		17.0		17.2	
Conductivity (µS/cm)	16,750		1,330		4,255		1,501	

1 Results expressed as mg/L unless otherwise indicated. Shaded cells indicate "not measured".

**Table 5-7 Concentrations of Key Analytes Measured from 1991 to 1995**

LOC_ID	DATE	AS (mg/L)	FE (mg/L)	MN (mg/L)	U (mg/L)	LOC_ID	DATE	AS (mg/L)	FE (mg/L)	MN (mg/L)	U (mg/L)
2301A	26-Apr-95	0.042	0.856	0.039	5.5	MW050A	14-Oct-94	<0.053	1.65	0.067	554
2301B	05-May-95	0.007	2.53	0.226	40.7	MW050B	25-Apr-95	<0.005	0.028	0.005	<5
2302A	14-Apr-95	<0.005	0.664	1.83	<5	MW050B	11-Oct-95	<0.005	0.054	0.007	<5
2302B	26-Apr-95	<0.005	0.057	0.013	<5	MW051A	26-Apr-94	<0.552	0.114	0.045	8.2
2341	05-May-95	0.023	0.405	0.108	<5	MW053	14-Apr-95	<0.005	1.99	0.105	32.9
2351	06-May-94	0.357	0.404	0.646	40.7	MW053A	26-Apr-95	<0.005	0.071	0.012	<5
MW003A	18-Apr-96	0.01	0.25		0.67	MW057A	26-Apr-94	2.27	0.549	0.853	5.8
MW005	19-Apr-94	<0.05	0.102	0.074	<5	MW059A	26-Apr-94	1.58	0.115	0.128	<5
MW005	11-Apr-95	<0.005	0.09	0.075	<5	MW059A	18-Apr-96	1.6	0.08		4.9
MW005A	27-Apr-94	<0.05	0.116	<0.001	<5	MW059B	20-Apr-95	0.035	25	1.06	29.2
MW007	19-Apr-94	<0.05	0.2	<0.001	<5	MW059B	11-Oct-95	0.019	6.96	0.088	8.1
MW007	13-Oct-94	<0.053	0.623	0.021	<5	MW061A	19-Apr-95	1.277	9.16	0.188	<5
MW007	11-Apr-95	<0.005	1.04	0.003	<5	MW062B	21-Apr-95	<0.005	0.648	0.012	<5
MW007A	27-Apr-94	<0.05	0.037	<0.001	<5	MW062B	10-Oct-95	<0.005	0.246	0.012	<5
MW007A	13-Oct-94	<0.053	0.165	0.008	<5	MW063A	20-Apr-95	<0.005	0.652	0.045	<5
MW007B	05-May-95	<0.005	5.08	0.108	<5	MW064A	19-Apr-95	3.45	3.27	0.095	<5
MW007B	10-Oct-95	0.01	3.78	0.122	10	MW067	05-May-95	0.005	0.281	0.635	<5
MW010	13-Apr-95	0.068	24.4	3.84	9030	MW067A	21-Apr-95	0.006	14.6	0.343	15.3
MW010A	20-Apr-95	0.019	0.749	0.006	<5	MW072	12-Apr-95	0.006	2.52	0.25	<5
MW012B	15-Jun-95	0.014	10.8	<0.102	20.3	MW072A	26-Apr-94	<0.05	0.272	0.007	<5
MW012B	13-Oct-95	0.011	2.701	0.028	15.5	MW072B	18-Apr-95	<0.005	0.404	<0.001	<5
MW022A	18-Apr-96	0.029	<0.03		<0.57	MW072B	10-Oct-95	<0.005	0.217	0.025	<5
MW025	14-Apr-95	<0.005	3.61	1.33	53700	MW084	14-Apr-95	<0.005	3.4	0.153	16.9
MW025A	26-Apr-95	0.008	0.312	0.054	930	MW084A	26-Apr-95	<0.005	0.396	0.073	<5
MW038A	26-Apr-94	<0.05	<0.01	0.006	<5	MW086	21-Apr-95	0.007	0.028	0.45	<5
MW042	12-Apr-95	3.218	46.1	13.7	<5	MW086A	26-Apr-95	0.006	0.066	0.013	271
MW042A	26-Apr-94	0.075	0.121	0.012	<5	MW087	25-Apr-95	0.051	2.69	0.161	<5
MW045A	26-Apr-94	<0.053	0.654	0.089	22.4	MW087A	25-Apr-95	0.058	2.07	0.175	53
MW050A	28-Apr-94	<0.05	0.105	0.001	579	MW092A	16-Apr-96	<0.005	<0.006		<0.57

**Table 5-7 Concentrations of Key Analytes Measured from 1991 to 1995 (continued)**

LOC_ID	DATE	AS (mg/L)	FE (mg/L)	MN (mg/L)	U (mg/L)	LOC_ID	DATE	AS (mg/L)	FE (mg/L)	MN (mg/L)	U (mg/L)
MW095A	11-Oct-94	0.056	0.053	0.038	<5	STA09	22-Aug-95	0.006	1.07	0.031	<5
MW095A	20-Jan-95	0.048	0.053	0.016	<5	STA10	19-Jul-95	0.029	53.8	4.49	<5
MW095A	19-Jul-95	0.035	4.17	0.088	<5	STA10	22-Aug-95	0.006	0.196	0.012	<5
MW095A	22-Aug-95	0.05	<0.017	0.011	<5	STA11	19-Jul-95	<0.005	0.554	0.27	<5
MW102A	21-Apr-95	0.141	11.9	1.1	<5	STA11	22-Aug-95	<0.005	0.18	0.251	<5
MW103A	21-Apr-95	0.083	1.85	0.138	<5						
MW104B	21-Apr-95	0.023	25.7	0.228	6.8						
MW104B	10-Oct-95	<0.005	0.244	0.026	<5						
MW105B	21-Apr-95	<0.005	0.295	0.006	<5						
MW105B	10-Oct-95	<0.005	0.394	0.006	<5						
Q-MW042	12-Apr-95	3.392	36.4	13.2	<5						
Q-MW064A	19-Apr-95	3.32	0.035	0.144							
Q-STA03	19-Jul-95	0.012	10.4	0.205	<5						
STA01	20-Oct-95	<0.005	0.301	0.141	<5						
STA02	19-Jul-95	0.006	23.3	0.61	<5						
STA02	22-Aug-95	<0.005	0.407	4.92	<5						
STA03	19-Jul-95	0.011	10.2	0.217	<5						
STA03	22-Aug-95	0.031	0.07	0.225	<5						
STA04	19-Jul-95	<0.005	14.5	0.1	<5						
STA04	22-Aug-95	<0.005	0.084	0.094	<5						
STA05	19-Jul-95	<0.005	0.406	0.024	<5						
STA05	22-Aug-95	<0.005	0.111	0.015	<5						
STA06	19-Jul-95	0.008	42.6	1.51	<5						
STA06	22-Aug-95	<0.005	0.637	0.011	<5						
STA07	19-Jul-95	0.008	9.76	0.344	<5						
STA07	22-Aug-95	0.006	3.74	0.096	6.2						
STA08	19-Jul-95	0.045	85.6	1.56	<5						
STA08	22-Aug-95	<0.005	0.563	0.012	<5						
STA09	19-Jul-95	0.016	41.6	0.9	<5						

**Table 5-8 Percentage Distribution of As(V), F, and U(VI) in the form of Aqueous Species for Selected Wells Calculated Using PHREEQC**

Sample	%H <sub>2</sub> AsO <sub>4</sub> <sup>-</sup>	%HAsO <sub>4</sub> <sup>-2</sup>	%AlF <sup>+2</sup>	%AlF <sub>2</sub> <sup>+</sup>	%F <sup>-</sup>	%UO <sub>2</sub> CO <sub>3</sub>	%UO <sub>2</sub> (CO <sub>3</sub> ) <sub>2</sub> <sup>-2</sup>	%UO <sub>2</sub> (HPO <sub>4</sub> ) <sub>2</sub> <sup>-2</sup>	%UO <sub>2</sub> <sup>+2</sup>
MW-012A	89.4	10.6	91.4	3.1	1.9	68.9	25.0	3.3	1.11
MW-012B	8.2	91.8	0.00	0.003	99.6	0.003	1.0	94.7	0.000
MW-025	98.8	0.53	61.4	12.0	3.9	14.9	0.010	1.27	69.0
MW-025A	87.8	12.2	93.6	2.16	1.54	43.8	17.9	36.4	0.586
MW-042A	75.6	24.4	1.58	8.1783	58.4	2.78	2.34	94.7	0.005
MW-059A	85.0	15.0	55.5	17.1	3.46	16.6	23.1	57.9	0.078
MW-064A	67.1	32.9	0.003	0.13	90.3	5.66	32.5	58.6	0.002
MW-067A	63.2	36.8	18.6	16.0	33.7	11.1	43.7	39.5	0.009
MW-075	92.4	7.6	0.16	2.19	70.6	43.9	30.0	24.1	0.109



**Table 5-9 Wells Used for Estimation of Distribution of COCs**

Loc ID	Easting	Northing	Completion	Date sampled	Fluoride (mg/L)	Nitrate (mg/L)	Uranium (mg/L)	Arsenic (mg/L)
<b>Primary Wells</b>								
MW-003	2837278.8	195542.8	1SH	4/12/01	0.700	<1.0	4.60	0.008
MW-005	2837527.7	195617.6	1SH	4/12/01	<0.200	<1.0	2.81	<0.005
MW-007	2837540.3	195837.9	1SH	4/12/01	0.800	<1.0	12.40	<0.005
MW-008	2837366.3	195738.3	1SH	4/12/01		54.6		
MW-010	2837015.8	195507.9	1SH	4/12/01	1.000	10.4	6000.00	0.026
MW-012	2836955.1	195847.1	1SH	4/18/01	0.700	302.0	73.90	
MW-014	2836940.6	195984.9	1SH	4/19/01	6.900	23.5	23400.00	
MW-015	2837034.8	195996.8	1SH	4/18/01		676.0		
MW-017	2837239.9	195997.1	1SH	4/19/01				0.059
MW-018	2836995.8	195607.5	1SH	4/18/01	0.900	2.5	1170.00	<0.005
MW-019	2836905.8	195509.9	1SH	4/18/01		<1.0	<1.00	<0.005
MW-023	2837135.4	195863.1	1SH	4/18/01	2.300			
MW-024	2836709.5	195824.2	1SH	4/19/01	0.500	532.0	3.16	
MW-025	2836783.1	195915	1SH	6/14/01	1.1	704.0	11000.00	0.04
MW-030	2837024.2	195398.5	1SH	4/11/01		<1.0	<1.00	0.039
MW-031	2836894.8	195336.6	1SH	4/11/01		<1.0	12.40	
MW-032	2837137	195396.9	1SH	4/12/01				0.108
MW-035	2836270	196331.1	1SH	4/10/01	0.300	1.8	4.04	2.100
MW-036	2836343	195954.4	1SH	4/10/01	0.200	31.6	<1.00	<0.005
MW-038	2836071.4	196243.7	1SH	4/4/01				<0.005
MW-039	2835935.7	196186.9	1SH	4/5/01		3.7	<1.00	<0.005
MW-040	2836100.6	195947.9	1SH	4/10/01	6.800	786.0	<1.00	0.092
MW-042	2836438.6	195246.6	1SH	4/11/01	1.100	1.0	<1.00	0.616
MW-049	2836196.3	196571.2	1SH	4/19/01		<1.0	<1.00	<0.005
MW-050	2836151.9	196894.1	1SH	4/4/01		<1.0	<1.00	<0.005
MW-053	2836589.5	196074.9	1SH	4/18/01		2.1	15.80	
MW-054	2836236.7	196075.3	1SH	4/10/01	3.000	511.0	<1.00	0.080
MW-055	2835912.1	195961.2	1SH	4/11/01	0.300	1.8	26.40	0.010
MW-075	2836778.4	196386.8	1SH	6/14/01	2.8	<1.0	<1.00	2.280

**Table 5-9 Wells Used for Estimation of Distribution of COCs (continued)**

Loc ID	Easting	Northing	Completion	Date sampled	Fluoride (mg/L)	Nitrate (mg/L)	Uranium (mg/L)	Arsenic (mg/L)
<b>Primary Wells</b>								
MW-076	2836444	195639.4	1SH	4/18/01		<1.0	<1.00	
MW-078	2836707.6	196661.7	1SH	4/17/01		<1.0	1220.00	
MW-079	2836987.7	196172.6	1SH	4/17/01		<1.0	5.92	
MW-084	2836670.2	195644.1	1SH	4/18/01		<1.0	1.86	<0.005
MW-102	2836127.3	195437.5	1SH	4/18/01		<1.0	4.39	0.006
MW-103	2835681.9	195589.1	1SH	4/18/01		119.0	<1.00	
MW-026	2836802.4	195792.2	1SH	4/19/01		<1.0	<1.00	
MW-072	2837530.7	196436.6	1SH	4/12/01	0.500	1.2	<1.00	<0.005
MW-077	2837004.3	196657.7	1SH	4/17/01			1.70	
2301B	2836451.6	196494.4	2SH	4/17/01	0.700	18.8	27.60	<0.005
MW-013A	2836959.4	195717.3	2SH	4/18/01		35.0	27.00	0.023
MW-035A	2836263.5	196328.7	2SH	4/10/01	0.400	70.9	53.60	0.017
MW-043	2836516.9	194991	2SH	4/6/01	0.600	1.9	<1.00	0.086
MW-048	2835230.2	195739.6	2SH	4/11/01	0.500	17.7	1.43	
MW-066	2836687.9	195338.1	2SH	4/11/01		11.3	<1.00	0.025
MW-116A	2837511.146	194444.654	2SH	8/23/01	0.8	<1.0	22.70	0.010
MW-119A	2836858.314	194780.707	2SH	8/23/01	1.7	<1.0	8.97	0.075
MW-036A	2836348.6	195953.9	2SH	4/10/01		17.3	<1.00	
MW-040A	2836110.3	195956.1	2SH	4/10/01		245.0	<1.00	
MW-042A	2836442.9	195238.7	2SH	6/14/01	1.0	21.0	1.30	0.516
MW-050A	2836155.9	196900.3	2SH	4/4/01	0.400	17.3	420.00	<0.005
2342	2835321	193351.8	3SH	4/6/01	0.200	126.0	<1.00	
2343	2836459.9	193402.9	3SH	4/5/01	0.600	2540.0	3.65	
2344	2836495.6	193084.9	3SH	4/6/01		26.1	1.10	
2346	2836241.6	193138.5	3SH	4/6/01		1050.0	5.70	
MW-038A	2836076.6	196241.5	3SH	4/4/01				<0.005
MW-039A	2835929.2	196182.9	3SH	4/5/01		92.8	<1.00	
MW-049A	2836203.3	196570	3SH	4/19/01		39.8	1.23	
MW-084A	2836676.8	195644.2	3SH	4/18/01		<1.0	<1.00	<0.005

**Table 5-9 Wells Used for Estimation of Distribution of COCs (continued)**

Loc ID	Easting	Northing	Completion	Date sampled	Fluoride (mg/L)	Nitrate (mg/L)	Uranium (mg/L)	Arsenic (mg/L)
<b>Primary Wells</b>								
MW-115A	194834.682	2835592.937	3SH	8/23/01	2.1	<1.0	13.90	0.068
MW-007A	2837540.9	195844.8	3SH	4/12/01	1.000	3.5	<1.00	<0.005
MW-063	2836698.2	194836.9	3SH	4/6/01	3.300		<1.00	<0.005
FTP-2B	2835787.4	193408.5	4SH	4/6/01	0.600	<1.0	<1.00	
MW-037A	2836057.6	196408.1	4SH	4/4/01		26.0	<1.00	
MW-062A	2836153.4	194763.9	4SH	4/10/01	0.500	<0.2	<1.00	0.090
MW-063A	2836704.5	194838.4	4SH	4/6/01	0.500	1.1	<1.00	<0.005
MW-087A	2836454.5	196656.1	4SH	4/17/01		2.0	46.00	0.069
MW-089A	2835979.4	196919.5	4SH	4/4/01		1.4	<1.00	
MW-093A	2834987.2	194910.6	4SH	4/5/01		97.2	<1.00	0.026
MW-099A	2836019.7	197252.9	4SH	4/4/01		1.2	3.37	
MW-109A	2837070	196970	4SH	4/10/01			<1.00	
MW-110A	2838412.8	194734.729	4SH	8/23/01	0.6	<1.0	3.11	<0.030
MW-111A	2833803.491	193655.492	4SH	8/23/01	0.7	<1.0	16.30	0.014
MW-112A	2833775.339	192595.278	4SH	8/23/01	0.3	<1.0	0.71	<0.030
MW-113A	2836049.545	192791.609	4SH	8/23/01	0.9	<1.0	12.40	<0.030
MW-114A	2833804.796	193665.618	4SH	8/23/01	0.7	<1.0	7.98	0.010
MW-096A	2835669.9	197285.1	4SH	4/4/01		2.3	<1.00	
MW-097A	2834493.1	195387.3	4SH	4/4/01		<1.0	<1.00	0.008
MW-007B	2837532.2	195843	5SH	4/3/01	2.400	<1.0	<1.00	<0.005
MW-012B	2836955.9	195852.6	5SH	6/14/01	2.1	1.0	15.40	<0.010
MW-050B	2836118.1	196919.4	5SH	4/3/01		<1.0	<1.00	<0.005
MW-059B	2835328.5	195023.2	5SH	4/3/01		1.5	<1.00	<0.005
MW-062B	2836165.8	194765.1	5SH	4/3/01	1.300	<0.2	<1.00	<0.005
MW-072B	2837549.8	196419.8	5SH	4/3/01		0.5	3.08	<0.005
MW-090B	2834952	194176	5SH	4/3/01		<1.0	<1.00	
MW-098B	2834797.4	195698.4	5SII	4/4/01		<1.0	<1.00	<0.005
MW-100B	2835524.1	196661.9	5SH	4/4/01		<1.0	<1.00	<0.005
MW-104B	2836317.8	193501.4	5SH	4/3/01		0.8	<1.00	<0.005

**Table 5-9 Wells Used for Estimation of Distribution of COCs (continued)**

Loc ID	Easting	Northing	Completion	Date sampled	Fluoride (mg/L)	Nitrate (mg/L)	Uranium (mg/L)	Arsenic (mg/L)
<b>Primary Wells</b>								
MW-105B	2834972.4	193728.9	5SH	4/3/01		<0.2	<1.00	<0.005
STA06	2833809.9	194861.1	ALUV	4/20/01		5.3	<1.00	<0.005
STA07	2833166.2	194359.2	ALUV	4/20/01		42.5	<1.00	<0.005
STA08	2832536.2	193950.1	ALUV	4/20/01		33.6	<1.00	<0.005
STA09	2832555.5	193191.7	ALUV	4/20/01		36.2	<1.00	<0.005
STA10	2832918.6	192353	ALUV	4/20/01		28.5	<1.00	<0.005
MW-117	2834786.146	194357.346	ALUV	8/23/01	0.6	<1.0	13.70	0.035
MW-120	2833802.577	193645.224	ALUV	8/23/01	0.9	16.6	8.35	0.017
<b>Supplemental Wells</b>								
2303A	2835903	195962.7	3SH	4/11/01	0.6	265	8.35	0.035
2322A	2835576	194098.8	4SH	4/6/01	<0.2	1170	<1.0	
2345	2835152	193260.1	4SH	4/6/01		<1.0	<1.0	
2347	2837058	193303.8	4SH	4/6/01	0.3	9.3	<1.0	
2348	2836046	194115.5	4SH	4/6/01		178	<1.0	
2349	2836525	194137.5	4SH	4/6/01		748	<1.0	
2351	2836467	193933.5	4SH	4/5/01	0.3	1720	1.56	
MW-003A	2837285	195544	3SH	4/12/01		1.1	88.3	0.009
MW-005A	2837528	195612.2	4SH	4/12/01	0.5	<1.0	<1.0	<0.005
MW-008A	2837366	195743.5	3SH	4/12/01		3.5		
MW-024A	2836711	195809.6	2SS	4/19/01		489	15.9	0.04
MW-031	2836895	195336.6	1SH	4/11/01		<1.0	12.4	
MW-032A	2837138	195400.9	3SH	4/12/01		1.9		0.058
MW-041A	2835239	195344.1	4SH	4/11/01		9.9	1.53	
MW-046A	2835455	195981.9	3SS	4/11/01	0.7	1400	<1.0	0.307
MW-051A	2835238	195543.9	2SS	4/11/01	0.7	2850	5.39	0.277
MW-053A	2836598	196071.3	2SS	4/18/01	0.3	60.3	<1.0	0.011
MW-057A	2835254	195211	3SH	4/11/01	5.7	10200	4.68	3.35
MW-058A	2835554	195013.3	3SH	4/11/01	1.5	3200	<1.0	0.784
MW-059A	2835336	195015.7	4SH	6/14/01	2.7	2560	10.9	1.42

**Table 5-9 Wells Used for Estimation of Distribution of COCs (continued)**

Loc ID	Easting	Northing	Completion	Date sampled	Fluoride (mg/L)	Nitrate (mg/L)	Uranium (mg/L)	Arsenic (mg/L)
<b>Supplemental Wells</b>								
MW-060A	2835796	195028.6	4SH	4/11/01	0.9	197	3.51	0.175
MW-061A	2835959	194877.4	4SH	4/10/01	0.8	0.3	<1.0	0.005
MW-062	2836148	194771.2	2SH	4/10/01	0.5		<1.0	0.074
MW-064A	2836315	194875.1	4SH	6/14/01	7.6	2	4.5	4.29
MW-065	2835939	195133.4	2SS	4/11/01	0.9	<1.0	<1.0	0.112
MW-065A	2835958	195136.7	4SH	4/11/01	1.4	20	2.26	0.595
MW-066A	2836685	195345.9	3SH	4/11/01		10.5	112	0.022
MW-067	2836397	196866.1	2SH	4/17/01				
MW-068	2836606	196873.2	2SH	4/17/01		7.5	1.46	
MW-068A	2836616	196873.7	4SH	4/17/01		<1.0	6.35	<0.005
MW-071A	2836965	195056	4SH	4/10/01		<1.0	<1.0	
MW-076A	2836451	195638.9	2SH	4/18/01		76	313	
MW-077A	2837013	196656.3	4SH	4/17/01			1.15	
MW-078A	2836718	196665.2	4SH	4/17/01		<1.0	7.57	
MW-079A	2836988	196166.2	4SH	4/17/01		2.7	1.76	
MW-081A	2837138	196805.6	4SH	4/17/01			30.4	
MW-082A	2835718	195347.7	4SH	4/18/01	0.4	352	6.41	0.063
MW-087	2836444	196655.7	2SH	4/17/01		<1.0	578	<0.005
MW-088A	2836149	197047.4	3SS	4/4/01		<1.0	16.1	
MW-091A	2835850	194672.9	4SH	4/10/01		<1.0	<1.0	0.029
MW-092A	2835378	194783.2	4SH	4/10/01		3	<1.0	<0.005
MW-094A	2835203	196390.3	4SH	4/4/01		6.5	<1.0	<0.005
MW-095A	2834517	195032.4	4SH	4/10/01		99.3	<1.0	0.016
MW-101A	2836433	194547.3	4SH	4/6/01		<1.0	<1.0	<0.005
MW-102A	2836133	195436.8	4SH	4/18/01		14	<1.0	0.024
MW-103A	2835683	195584	4SH	4/18/01		872	<1.0	0.088

**Table 5-10 Range of pH Values Recorded from 1991 to 1994**

LOC_ID	DATE	pH	LOC_ID	DATE	pH	LOC_ID	DATE	pH	LOC_ID	DATE	pH
2343	25-Nov-91	6.6	MW001	23-Oct-91	7.2	MW063A	01-May-91	8.1	MW038	22-Oct-91	7
MW082A	24-Jan-92	7.1	MW002	23-Oct-91	6.5	MW072A	01-May-91	7.6	MW038A	22-Oct-91	7.6
MW102	24-Jan-92	7.4	MW002A	23-Oct-91	7	MW007	01-May-91	7.5	MW039A	22-Oct-91	6.8
MW102A	24-Jan-92	7.2	MW003	23-Oct-91	7.3	MW007A	01-May-91	7.4	MW040	22-Oct-91	4.5
MW103	24-Jan-92	6.2	MW003A	23-Oct-91	6.7	MW040A	22-Oct-91	6.7	MW073	22-Oct-91	7.3
MW103A	24-Jan-92	7	MW004	23-Oct-91	7.3	MW041A	23-Oct-91	7.8	MW073A	22-Oct-91	7.8
MW102	03-Mar-92	7.3	MW004A	23-Oct-91	7.4	MW042	22-Oct-91	6.7	MW074	22-Oct-91	7.4
MW102A	03-Mar-92	7.2	MW005A	23-Oct-91	7	MW042A	22-Oct-91	7.1	MW077A	23-Oct-91	7.2
MW103	03-Mar-92	6.4	MW006	23-Oct-91	7.1	MW043	22-Oct-91	6.7	MW078	23-Oct-91	6.8
MW103A	03-Mar-92	6.9	MW006A	23-Oct-91	7.3	MW045A	22-Oct-91	7.6	MW078A	23-Oct-91	7.7
MW076	19-Oct-94	7.2	MW007	23-Oct-91	6.9	MW046A	22-Oct-91	7.1	MW080	23-Oct-91	7.1
MW076A	19-Oct-94	6.8	MW007A	23-Oct-91	7.3	MW051A	22-Oct-91	7.3	MW080A	23-Oct-91	7.1
MW082	19-Oct-94	6.6	MW010	23-Oct-91	5.2	MW052A	22-Oct-91	7.3	MW081A	23-Oct-91	7.6
MW082A	19-Oct-94	7	MW010A	23-Oct-91	11.2	MW054	22-Oct-91	6.8	MW087	28-Oct-91	7.3
MW084	19-Oct-94	7.1	MW021	23-Oct-91	6.9	MW057	22-Oct-91	7.2	MW088A	22-Oct-91	7.2
MW084A	19-Oct-94	7.4	MW021A	23-Oct-91	7.2	MW057A	22-Oct-91	7	MW089A	22-Oct-91	7.6
MW102	19-Oct-94	7.3	MW024	28-Oct-91	6.6	MW058A	22-Oct-91	6.8	MW090B	28-Oct-91	8.3
MW102A	19-Oct-94	6.8	MW024A	28-Oct-91	6.4	MW059A	22-Oct-91	7.2	MW091A	22-Oct-91	6.4
MW011	21-Oct-94	5.9	MW025	28-Oct-91	6.4	MW060A	23-Oct-91	6.7	MW092A	23-Oct-91	7.1
MW013	21-Oct-94	6.9	MW025A	28-Oct-91	6.6	MW061A	22-Oct-91	6.9	MW093A	22-Oct-91	7.5
MW013A	21-Oct-94	6.6	MW026	28-Oct-91	7.1	MW062	22-Oct-91	7.2	MW094A	22-Oct-91	7
MW014	21-Oct-94	6.8	MW026A	28-Oct-91	6.4	MW062A	22-Oct-91	7.3	MW095A	22-Oct-91	6.8
MW014A	21-Oct-94	6.6	MW027	28-Oct-91	7	MW063	22-Oct-91	6.1	MW096A	22-Oct-91	7.2
MW016	21-Oct-94	7.1	MW027A	28-Oct-91	6.7	MW063A	22-Oct-91	7.3	MW097A	22-Oct-91	7.4
MW016A	21-Oct-94	7.3	MW031	23-Oct-91	6.6	MW064A	22-Oct-91	6	MW099A	22-Oct-91	6.5
MW018	21-Oct-94	6.2	MW031A	23-Oct-91	7.3	MW065A	22-Oct-91	7.4	MW101A	22-Oct-91	7.2
MW018A	21-Oct-94	6.7	MW035	22-Oct-91	6.3	MW066	22-Oct-91	6.7	2303A	22-Oct-91	7.1
MW075A	21-Oct-94	6.6	MW035A	22-Oct-91	7	MW066A	22-Oct-91	6.5	MW059B	15-Jun-95	7.7
MW012A	24-Oct-94	6.7	MW036	22-Oct-91	6.3	MW067	22-Oct-91	6.2	MW104B	15-Jun-95	7.99
MW095A	20-Jan-95	6.43	MW036A	22-Oct-91	6.8	MW067A	22-Oct-91	7	MW012B	15-Jun-95	7.97
MW063	01-May-91	6.5	MW037A	22-Oct-91	7.5	MW068A	22-Oct-91	7.2	MW050	05-Apr-91	7.3

**Table 5-10 Range of pH Values Recorded from 1991 to 1994 (continued)**

LOC_ID	DATE	pH	LOC_ID	DATE	pH	LOC_ID	DATE	pH	LOC_ID	DATE	pH
MW069	13-Jun-91	6.9	MW083	05-Apr-91	7.7	MW013A	25-Oct-91	6.6	MW086	01-May-91	6.9
MW069A	23-Oct-91	7.4	MW083A	05-Apr-91	7.3	MW012	25-Oct-91	7.2	MW086A	01-May-91	6.9
MW070	23-Oct-91	7.4	MW084	05-Apr-91	7.5	MW012A	25-Oct-91	6.2	MW025	01-May-91	6
MW070A	23-Oct-91	7.1	MW084A	05-Apr-91	7.8	MW058A	23-Apr-91	6.5	MW025A	01-May-91	6.6
MW071A	13-Jun-91	8.4	MW085	05-Apr-91	7.5	MW059A	23-Apr-91	6.4	MW067	17-May-91	6.6
MW071A	22-Oct-91	7.6	MW085A	05-Apr-91	7	MW060A	23-Apr-91	6.6	MW065	21-May-91	7.5
MW072	23-Oct-91	7.2	MW086	05-Apr-91	7.7	MW061A	23-Apr-91	6.8	MW024	30-Apr-91	8.1
MW072A	23-Oct-91	7	MW086A	05-Apr-91	7.6	MW062A	23-Apr-91	7.4	MW024A	30-Apr-91	7.1
MW087A	05-Apr-91	7.8	MW078	23-Apr-91	6.9	MW064A	23-Apr-91	7.2	MW026	30-Apr-91	7.5
MW049	25-Oct-91	7.3	MW078A	23-Apr-91	7.3	MW065A	23-Apr-91	7.5	MW026A	30-Apr-91	7
MW049A	25-Oct-91	7	MW051A	23-Apr-91	6.6	MW049A	23-Apr-91	7	MW075A	30-Apr-91	7.5
MW050	25-Oct-91	7	MW046A	23-Apr-91	6.8	MW049	23-Apr-91	7.1	Q-MW075A	30-Apr-91	7.4
MW050A	25-Oct-91	6.9	2303A	23-Apr-91	7	MW077A	23-Apr-91	7.1	MW079	30-Apr-91	8.3
MW079	25-Oct-91	7.3	MW088A	23-Apr-91	7.1	MW077	23-Apr-91	6.5	Q-MW079A	30-Apr-91	7.7
MW079A	25-Oct-91	6.9	MW089A	23-Apr-91	7.4	MW079A	30-Apr-91	7.8	MW083	24-Oct-91	7.1
MW082	25-Oct-91	6.7	MW052A	23-Apr-91	7.4	MW080	30-Apr-91	7.6	MW083A	24-Oct-91	7
MW082A	25-Oct-91	7.1	MW037A	23-Apr-91	7.4	MW080A	30-Apr-91	7.5	MW017	24-Oct-91	7.4
MW103A	25-Oct-91	7.1	MW038	23-Apr-91	6.9	Q-MW080A	30-Apr-91	7.6	MW017A	24-Oct-91	7.3
MW102	25-Oct-91	7.3	MW038A	23-Apr-91	7.4	MW083	30-Apr-91	7.5	MW016	24-Oct-91	7.2
MW102A	25-Oct-91	7.3	MW039A	23-Apr-91	6.8	MW083A	30-Apr-91	7.7	MW016A	24-Oct-91	7.2
MW076	25-Oct-91	7.3	MW035A	23-Apr-91	6.9	MW087	30-Apr-91	8.1	MW015	24-Oct-91	6.6
MW076A	25-Oct-91	7	MW054	23-Apr-91	6.7	MW087A	30-Apr-91	8	MW014	24-Oct-91	6.8
MW084	25-Oct-91	7.2	MW036	23-Apr-91	5.9	Q-MW087A	30-Apr-91	7.7	MW014A	24-Oct-91	7.7
MW084A	25-Oct-91	7.5	MW036A	23-Apr-91	6.8	2301A	30-Apr-91	7.2	MW023	24-Oct-91	7
MW018	25-Oct-91	6	MW040	23-Apr-91	4.7	2301B	30-Apr-91	7.9	2301A	24-Oct-91	6.8
MW018A	25-Oct-91	6.9	MW040A	23-Apr-91	6.7	2302A	30-Apr-91	6.9	2301B	24-Oct-91	7.6
MW011	25-Oct-91	6	MW090B	23-Apr-91	8.6	2302B	30-Apr-91	7.2	2302A	24-Oct-91	5.7
MW011A	25-Oct-91	6.5	MW087	02-May-91	7.7	MW053	30-Apr-91	7.8	2302B	24-Oct-91	6.8
MW019	25-Oct-91	6.2	MW075	02-May-91	7.4	MW053A	30-Apr-91	7.1	MW047A	24-Oct-91	7.9
2348	25-Oct-91	9.6	MW018	01-May-91	6.4	Q-MW053A	30-Apr-91	7.1	MW065	24-Oct-91	7.8
MW085	25-Oct-91	7.1	MW018A	01-May-91	7.3	MW012	30-Apr-91	7.8	MW005	24-Oct-91	6.5
MW085A	25-Oct-91	6.8	MW050	01-May-91	6.9	MW012A	30-Apr-91	6.8	MW039	24-Oct-91	6.8
MW013	25-Oct-91	7	MW050A	01-May-91	6.9	MW022	24-Oct-91	6.6	MW030A	24-Oct-91	7.1

**Table 5-10 Range of pH Values Recorded from 1991 to 1994 (continued)**

LOC_ID	DATE	pH	LOC_ID	DATE	pH	LOC_ID	DATE	pH	LOC_ID	DATE	pH
MW032	24-Oct-91	6.7	MW017A	26-Apr-91	7.2	MW058A	25-Apr-91	6.8	MW073A	25-Apr-91	8.1
MW032A	24-Oct-91	7	Q-MW017A	26-Apr-91	7.5	MW060A	25-Apr-91	6.9	MW006	25-Apr-91	7.2
MW029	24-Oct-91	6.3	MW023	26-Apr-91	7.3	MW065A	25-Apr-91	7.3	MW006A	25-Apr-91	7.9
MW030	24-Oct-91	6.9	MW016	26-Apr-91	7.1	MW042	25-Apr-91	6.8	MW005	25-Apr-91	7.1
MW028	24-Oct-91	6.8	MW016A	26-Apr-91	6.7	MW042A	25-Apr-91	7.3	MW005A	25-Apr-91	8.2
MW028A	24-Oct-91	7.2	MW015	26-Apr-91	6.7	MW062	25-Apr-91	7.2	MW002	25-Apr-91	6.8
MW020	24-Oct-91	6.4	MW027	26-Apr-91	7.1	MW043	25-Apr-91	6.8	MW002A	25-Apr-91	8
MW020A	24-Oct-91	7.1	MW027A	26-Apr-91	6.3	MW004A	25-Apr-91	8.2	MW003	25-Apr-91	7.3
MW008	24-Oct-91	6.9	MW013	26-Apr-91	7.1	MW020	25-Apr-91	8	MW003A	25-Apr-91	7.2
MW008A	24-Oct-91	10.5	MW013A	26-Apr-91	6.5	MW020A	25-Apr-91	8.3	MW001	25-Apr-91	8.1
MW086	24-Oct-91	7.2	MW014	26-Apr-91	6.7	MW008	25-Apr-91	8.5	MW004	25-Apr-91	8
MW086A	24-Oct-91	6.7	MW014A	26-Apr-91	6.7	MW008A	25-Apr-91	11.5	MW057	01-May-91	7.7
MW075	24-Oct-91	7.1	Q-MW014A	26-Apr-91	6.6	MW021	25-Apr-91	8.4	MW057A	01-May-91	7.5
MW075A	24-Oct-91	7.1	MW085	26-Apr-91	7.5	MW021A	25-Apr-91	8.2	MW098B	22-Oct-91	8.2
MW053	24-Oct-91	7.3	MW085A	26-Apr-91	6.9	MW066	25-Apr-91	8.2	MW100B	23-Oct-91	7.6
MW053A	24-Oct-91	7	Q-MW085A	26-Apr-91	6.9	MW066A	25-Apr-91	8.1	2323	23-Apr-91	4.3
MW087A	24-Oct-91	7.1	MW084	26-Apr-91	7.3	Q-MW022A	25-Apr-91	11.5	2328	23-Apr-91	6.3
MW084A	26-Apr-91	78	MW071	25-Apr-91	8.2	Q-MW009A	25-Apr-91	6.9	2330	23-Apr-91	7.5
MW011	26-Apr-91	6.2	MW009	25-Apr-91	7.8	Q-MW032A	25-Apr-91	6.9			
MW011A	26-Apr-91	6.6	MW032	25-Apr-91	8.3	Q-MW031A	25-Apr-91	6.8			
Q-MW011A	26-Apr-91	6.5	MW029	25-Apr-91	7.2	Q-MW066A	25-Apr-91	8.2			
MW019	26-Apr-91	6.2	MW030	25-Apr-91	8.1	MW044	25-Apr-91	8.2			
MW019A	26-Apr-91	11.9	MW030A	25-Apr-91	8.2						
MW076A	26-Apr-91	7.2	MW031	25-Apr-91	7.6						
MW082A	26-Apr-91	7.1	MW010A	25-Apr-91	11.7						
MW028	25-Apr-91	6.9	MW074	25-Apr-91	8.2						
MW028A	25-Apr-91	7.2	MW067A	25-Apr-91	7.5						
MW022	25-Apr-91	6.8	MW068A	25-Apr-91	7.2						
MW022A	25-Apr-91	11.1	MW069A	25-Apr-91	7.7						
MW009A	25-Apr-91	6.9	MW081A	25-Apr-91	7.8						
MW032A	25-Apr-91	6.9	MW070A	25-Apr-91	7.6						
MW031A	25-Apr-91	6.9	MW073	25-Apr-91	8						



**Table 8-1 Model Layer and Corresponding Geologic Layers**

Model Layer	Geologic Layer
Layer 1	Terrace/Colluvium/Alluvium
Layer 2	Unit 1 Shale
Layer 3	Unit 2 Shale
Layer 4	Unit 3 Shale
Layer 5	Unit 4 Shale
Layer 6	Unit 5 Shale

**Table 8-2 Calibrated Conductive Values**

Hydrologic Unit	Kx (ft/day)	Ky (ft/day)	Kz (ft/day)
Alluvium	50	50	50
Colluvium	8.6	8.6	8.6
Terrace	0.20	0.20	0.002
Unit 1 Shale	0.20	0.20	0.002
Unit 2 Shale	0.125	0.125	0.0125
Unit 3 Shale	0.125	0.125	0.0125
Unit 4 Shale	0.45	0.45	0.045
Unit 5 Shale	0.25	0.25	0.025

**Table 8-3 Computed versus Observed Heads**

Name	Easting (feet)	Northing (feet)	Layer	Observed Head (feet amsl)	Computed Head (feet amsl)	Residual (feet)	Absolute Residual Error (feet/feet)
MW-111	2833814	193663	1	465.03	466.57	-1.54	0.012
MW-117	2834811	194372	1	475.97	487.82	-11.85	0.096
MW-120	2833825	193669	1	465.18	466.65	-1.47	0.012
MW003	2837304	195568	2	556.76	555.17	1.58	0.013
MW007	2837565	195863	2	560.27	561.91	-1.64	0.013
MW008	2837391	195763	2	558.54	558.90	-0.36	0.003
MW012	2836975	195867	2	555.89	556.17	-0.28	0.002
MW013	2836982	195739	2	555.43	554.46	0.97	0.008
MW015	2837060	196022	2	556.64	556.31	0.33	0.003
MW016	2837172	196018	2	555.22	557.02	-1.80	0.015
MW017	2837260	196022	2	559.36	558.23	1.13	0.009
MW021	2837412	195894	2	557.99	560.63	-2.64	0.021
MW022	2837199	195623	2	558.05	554.21	3.84	0.031
MW023	2837150	195888	2	557.70	557.16	0.54	0.004
MW025	2836808	195940	2	555.51	553.12	2.39	0.019
MW026	2836827	195817	2	555.60	553.82	1.78	0.014
MW027	2836883	195883	2	555.43	555.22	0.21	0.002
MW052	2835998	196764	2	527.98	532.00	-4.02	0.032
MW070	2837395	196575	2	558.55	559.36	-0.80	0.006
MW073	2837602	196183	2	560.22	562.36	-2.14	0.017
MW076	2836469	195664	2	553.26	549.90	3.36	0.027
MW079	2837013	196198	2	556.05	556.92	-0.87	0.007
MW083	2837296	196305	2	558.35	558.96	-0.61	0.005
MW084	2836695	195669	2	552.71	548.51	4.20	0.034
MW085	2836734	195536	2	551.58	550.56	1.02	0.008
MW102	2836152	195463	2	550.08	547.25	2.82	0.023
MW036A	2836362	195976	3	548.87	548.52	0.34	0.003
MW040A	2836127	195981	3	542.27	544.46	-2.19	0.018
MW042A	2836461	195264	3	542.50	540.98	1.52	0.012
MW045A	2835681	195996	3	528.75	536.27	-7.52	0.061
MW046	2835463	196002	3	526.24	529.14	-2.90	0.023
MW048	2835245	195761	3	523.59	524.50	-0.91	0.007
MW085A	2836727	195526	3	549.91	549.38	0.52	0.004
2344	2836515	193110	4	513.84	514.16	-0.32	0.003
2346	2836267	193164	4	513.27	510.22	3.05	0.025
MW035A	2836289	196354	4	534.32	534.99	-0.67	0.005
MW047A	2835260	195981	4	516.61	522.73	-6.12	0.049
MW084A	2836702	195669	4	547.99	548.61	-0.62	0.005
MW086A	2836882	196067	4	552.91	551.14	1.77	0.014
270-1	2839203	195930	5	552.45	559.39	-6.94	0.056
270-2	2839849	194334	5	530.81	535.87	-5.05	0.041
270-3	2841138	195318	5	516.43	514.59	1.83	0.015

**Table 8-3 Computed versus Observed Heads (continued)**

Name	Easting (feet)	Northing (feet)	Layer	Observed Head (feet amsl)	Computed Head (feet amsl)	Residual (feet)	Absolute Residual Error (feet/feet)
FTP-2B	2835812	193434	5	504.84	507.95	-3.11	0.025
MW037A	2836077	196436	5	512.00	526.92	-14.92	0.121
MW039A	2835948	196208	5	521.68	529.27	-7.59	0.061
MW062A	2836178	194789	5	516.94	523.78	-6.83	0.055
MW063A	2836724	194863	5	526.15	532.02	-5.87	0.047
MW083A	2837302	196290	5	557.16	553.92	3.25	0.026
MW087A	2836464	196681	5	533.24	535.74	-2.50	0.020
MW093A	2835012	194930	5	495.41	503.78	-8.37	0.068
MW095A	2834525	195116	5	478.59	476.64	1.95	0.016
MW096A	2835695	197304	5	502.65	507.18	-4.54	0.037
MW097A	2834512	195412	5	473.48	472.57	0.91	0.007
MW099A	2836045	197278	5	510.55	512.81	-2.26	0.018
MW110	2838430	194760	5	533.19	546.40	-13.21	0.107
MW112	2833800	192631	5	465.77	470.36	-4.59	0.037
MW113	2836075	192811	5	498.80	499.60	-0.80	0.006
MW114A	2833831	193680	5	465.03	466.77	-1.74	0.014
MW007B	2837559	195868	6	532.01	532.49	-0.49	0.004
MW012B	2836966	195878	6	505.06	525.88	-20.82	0.168
MW050B	2836143	196938	6	510.47	499.08	11.38	0.092
MW059B	2835347	195048	6	501.98	495.12	6.86	0.055
MW062B	2836191	194790	6	511.34	511.65	-0.31	0.003
MW072B	2837569	196445	6	538.40	528.74	9.65	0.078
MW090B	2834977	194201	6	487.68	489.05	-1.37	0.011
MW098B	2834822	195723	6	476.13	476.93	-0.80	0.006
MW100B	2835549	196687	6	485.18	484.30	0.88	0.007
MW104B	2836343	193537	6	507.41	511.39	-3.98	0.032
MW105B	2834997	193754	6	484.70	489.69	-5.00	0.040
Mean Residual (MR)						-1.51	
Mean Absolute Residual (MAR)						3.48	
Standard Deviation (SD)						5.00	
Sum of Squares						1884	
Minimum Residual						-20.82	
Maximum Residual						11.38	
Range						123.74	
MAR/Range						0.028	
SD/Range						0.040	

**Table 8-4      Calibrated Uranium  $K_d$  Table**

Unit	New $K_d$
Surf deposit	0.92
SH1	0.33
SH2	0.16
SH3	0.33
SH4/5	0.23

**Table 8-5a Summary of Surface Water Modeling Results – Stream Concentrations and Mass Loading**

Time (years)	005		007		Total
	Concentration (mg/L)	Mass Loading (kg/day)	Concentration (mg/L)	Mass Loading (kg/day)	Mass Loading (kg/day)
<b>Nitrate</b>					
1.4	8.6838	6.37E-01	0	0	6.37E-01
1.8	8.40079	6.16E-01	0	0	6.16E-01
2.2	8.04953	5.90E-01	0	0	5.90E-01
2.8	7.60445	5.58E-01	0	0	5.58E-01
3.6	7.05494	5.17E-01	0	0	5.17E-01
4.5	6.38541	4.68E-01	0	0	4.68E-01
5.6	5.73758	4.21E-01	0	0	4.21E-01
7.1	4.9472	3.63E-01	0	0	3.63E-01
8.9	4.12697	3.03E-01	0	0	3.03E-01
11.2	3.37321	2.47E-01	0	0	2.47E-01
14.2	2.63187	1.93E-01	0	0	1.93E-01
17.8	1.95244	1.43E-01	0	0	1.43E-01
22.4	1.37969	1.01E-01	0	0	1.01E-01
28.1	0.969339	7.11E-02	0	0	7.11E-02
35.5	0.68531	5.03E-02	0	0	5.03E-02
44.8	0.489104	3.59E-02	0	0	3.59E-02
56.2	0.332159	2.44E-02	0	0	2.44E-02
70.9	0.170159	1.25E-02	0	0	1.25E-02
89.3	5.28E-02	3.87E-03	0	0	3.87E-03
112.3	9.56E-03	7.01E-04	0	0	7.01E-04
<b>Uranium</b>					
0.0	3.49E+00	2.56E-04	1.17E-15	8.72E-21	2.56E-04
0.3	4.34E+00	3.19E-04	1.17E-03	8.76E-09	3.19E-04
0.4	4.36E+00	3.20E-04	2.24E-03	1.67E-08	3.20E-04
0.5	4.34E+00	3.18E-04	4.07E-03	3.04E-08	3.18E-04
0.6	4.26E+00	3.13E-04	7.11E-03	5.32E-08	3.13E-04
0.8	4.10E+00	3.01E-04	1.21E-02	9.06E-08	3.01E-04
1.0	3.82E+00	2.80E-04	2.10E-02	1.57E-07	2.80E-04
1.3	3.43E+00	2.52E-04	3.66E-02	2.74E-07	2.52E-04
1.6	2.95E+00	2.17E-04	6.69E-02	5.00E-07	2.17E-04
2.0	2.45E+00	1.79E-04	1.27E-01	9.48E-07	1.80E-04
2.5	1.94E+00	1.42E-04	2.49E-01	1.86E-06	1.44E-04
3.1	1.47E+00	1.08E-04	4.98E-01	3.73E-06	1.12E-04
4.0	1.08E+00	7.91E-05	9.81E-01	7.34E-06	8.64E-05
5.0	7.81E-01	5.73E-05	2.04E+00	1.53E-05	7.26E-05
6.2	5.88E-01	4.31E-05	3.80E+00	2.84E-05	7.15E-05
7.9	4.57E-01	3.35E-05	6.44E+00	4.82E-05	8.17E-05
9.9	3.69E-01	2.70E-05	8.11E+00	6.06E-05	8.76E-05

**Table 8-5a Summary of Surface Water Modeling Results – Stream Concentrations and Mass Loading (continued)**

Time (years)	005		007		Total
	Concentration (mg/L)	Mass Loading (kg/day)	Concentration (mg/L)	Mass Loading (kg/day)	Mass Loading (kg/day)
<b>Uranium (continued)</b>					
12.5	3.08E-01	2.26E-05	9.18E+00	6.86E-05	9.13E-05
15.7	2.80E-01	2.05E-05	1.34E+01	9.99E-05	1.20E-04
19.8	2.83E-01	2.08E-05	2.30E+01	1.72E-04	1.93E-04
24.9	3.32E-01	2.43E-05	2.85E+01	2.13E-04	2.37E-04
31.3	6.42E-01	4.71E-05	2.13E+01	1.60E-04	2.07E-04
39.4	2.28E+00	1.67E-04	9.56E+00	7.15E-05	2.39E-04
49.6	6.53E+00	4.79E-04	3.71E+00	2.77E-05	5.07E-04
62.2	1.09E+01	7.98E-04	1.38E+00	1.03E-05	8.08E-04
74.6	1.17E+01	8.55E-04	4.73E-01	3.54E-06	8.59E-04
87.0	1.03E+01	7.55E-04	1.35E-01	1.01E-06	7.56E-04
99.5	8.14E+00	5.97E-04	3.21E-02	2.40E-07	5.97E-04
111.9	5.91E+00	4.34E-04	6.50E-03	4.86E-08	4.34E-04
124.4	3.99E+00	2.93E-04	1.18E-03	8.81E-09	2.93E-04
136.8	2.55E+00	1.87E-04	1.99E-04	1.49E-09	1.87E-04
149.3	1.58E+00	1.16E-04	3.28E-05	2.45E-10	1.16E-04
161.7	9.60E-01	7.04E-05	5.69E-06	4.25E-11	7.04E-05
174.2	5.85E-01	4.29E-05	1.03E-06	7.68E-12	4.29E-05
186.6	3.59E-01	2.63E-05	1.64E-07	1.22E-12	2.63E-05
199.0	2.22E-01	1.63E-05	0.00E+00	0.00E+00	1.63E-05
211.4	1.38E-01	1.01E-05	0.00E+00	0.00E+00	1.01E-05
223.8	8.62E-02	6.32E-06	0.00E+00	0.00E+00	6.32E-06
236.2	5.36E-02	3.93E-06	0.00E+00	0.00E+00	3.93E-06
248.6	3.32E-02	2.43E-06	0.00E+00	0.00E+00	2.43E-06
<b>Arsenic</b>					
1.7	1.42E+00	1.04E-04	7.94E-04	5.93E-09	1.04E-04
2.1	1.38E+00	1.01E-04	2.83E-03	2.11E-08	1.01E-04
2.7	1.34E+00	9.80E-05	9.17E-03	6.86E-08	9.81E-05
3.4	1.29E+00	9.49E-05	2.62E-02	1.96E-07	9.51E-05
4.2	1.25E+00	9.17E-05	6.40E-02	4.78E-07	9.21E-05
5.3	1.22E+00	8.93E-05	1.31E-01	9.82E-07	9.03E-05
6.7	1.19E+00	8.75E-05	2.23E-01	1.67E-06	8.91E-05
8.4	1.17E+00	8.58E-05	3.33E-01	2.49E-06	8.83E-05
10.6	1.14E+00	8.35E-05	4.29E-01	3.21E-06	8.67E-05
13.4	1.06E+00	7.74E-05	4.73E-01	3.54E-06	8.10E-05
16.8	8.89E-01	6.52E-05	4.35E-01	3.25E-06	6.85E-05
21.2	6.43E-01	4.72E-05	3.22E-01	2.41E-06	4.96E-05
26.7	3.99E-01	2.93E-05	1.78E-01	1.33E-06	3.06E-05
33.4	2.25E-01	1.65E-05	7.93E-02	5.93E-07	1.71E-05

**Table 8-5a Summary of Surface Water Modeling Results – Stream Concentrations and Mass Loading (continued)**

Time (years)	005		007		Total
	Concentration (mg/L)	Mass Loading (kg/day)	Concentration (mg/L)	Mass Loading (kg/day)	Mass Loading (kg/day)
<b>Arsenic (continued)</b>					
42.2	1.27E-01	9.34E-06	2.50E-02	1.87E-07	9.52E-06
53.2	8.81E-02	6.46E-06	5.46E-03	4.08E-08	6.51E-06
66.8	6.93E-02	5.09E-06	6.62E-04	4.95E-09	5.09E-06
84.3	4.98E-02	3.65E-06	3.23E-05	2.41E-10	3.65E-06
106.1	2.46E-02	1.81E-06	4.29E-07	3.21E-12	1.81E-06
133.6	5.84E-03	4.29E-07	1.23E-08	9.23E-14	4.29E-07
168.1	5.88E-04	4.31E-08	3.61E-08	2.70E-13	4.31E-08
211.6	3.17E-05	2.33E-09	3.82E-09	2.86E-14	2.33E-09
266.3	8.94E-07	6.56E-11	4.08E-11	3.05E-16	6.56E-11
266.9	8.58E-07	6.29E-11	3.85E-11	2.88E-16	6.29E-11

**Table 8-5b Summary of Groundwater Modeling Results – Stream Concentrations and Mass Loading**

Nitrate		Uranium		Arsenic	
Time (years)	Mass Loading (kg/day)	Time (years)	Mass Loading (kg/day)	Time (years)	Mass Loading (kg/day)
1.3	5.30E+00	50.0	3.45E-06	1.3	3.23E-04
5	5.99E+00	100	5.60E-05	5	1.11E-03
10	9.19E+00	158.5	2.03E-04	10	2.82E-03
15.8	1.04E+01	200	2.69E-04	25	1.62E-03
20	8.78E+00	250	3.55E-04	50	4.16E-04
25	6.38E+00	300	3.42E-04	100	8.03E-05
50	1.68E+00	350	2.44E-04	158	4.79E-06
100	3.74E-01	400	2.22E-04	200	3.07E-07
125	2.53E-01	450	0.00031165		
		500	0.000437215		
		550	0.000514372		
		650	0.000453078		
		750	0.000293538		
		1000	0.000102996		

**Table 8-6 Flow Model Sensitivity Parameters**

Parameter	Parameter Type	Area
Kx15	Hydraulic Conductivity	Colluvium
Kx13	Hydraulic Conductivity	Terrace/Shale1/Shale2
Kx18	Hydraulic Conductivity	Alluvium
Kx12	Hydraulic Conductivity	Simulated Vertical Conduits
Kx11	Hydraulic Conductivity	Shale3/Shale4
Kx14	Hydraulic Conductivity	Shale5/Shale6
Kx16	Hydraulic Conductivity	Gravel Fill
R6	Recharge	Process Area
R3	Recharge	Prairie Grassland
R4	Recharge	Oak/Hickory Forrest
R5	Recharge	Agland
ET2	Evapotranspiration	Agland
ET5	Evapotranspiration	Prairie Grassland
ET3	Evapotranspiration	Oak/Hickory Forrest

**Table 8-7 Transport Model Sensitivity Parameters**

Parameter	Parameter Type	Area
Po2	Porosity	Shales
Po3	Porosity	Unconsolidated Deposits
Al1	Longitudinal Dispersion	All Areas/All Layers
Kd32	Linear Adsorption	Shale 4/ Shale 5
Kd33	Linear Adsorption	Simulated Vertical Conduits
Kd34	Linear Adsorption	Shale 2
Kd35	Linear Adsorption	Shale 1
Kd36	Linear Adsorption	Shale 3
Kd37	Linear Adsorption	Terrace
Kd38	Linear Adsorption	Gravel Deposits
Kd39	Linear Adsorption	Alluvium/Colluvium



**Table 9-1 Safe and Toxic Concentrations of Uranium in Water**

Species	U(ppm)	Effect	Ref
<b>FISH-IN WATER</b>			
Most fish	0.005	No effect	Mitchum and Moore (1966)
Bonytail	0.033	Max acceptable	Stephens et al. (1988)
Colorado squawfish	0.033	Max acceptable	Stephens et al. (1988)
Razorback sucker	0.033	Max acceptable	Stephens et al. (1988)
Razorback sucker	0.073	Max acceptable	Stephens et al. (1988)
Colorado squawfish	0.073	Max acceptable	Stephens et al. (1988)
Bonytail	0.073	Max acceptable	Stephens et al. (1988)
Trout	0.060	Toxic	Mitchum and Moore (1966)
Australian fish	2.34	96-hr LC 50	Holdway (1992); (hardness 3.2 mg/L)
Fathead minnow	Uranyl	96-hr LC 50	Tarzwel and Henderson (1960); hardness 20mg/L
Fathead minnow	Uranyl nitrate	96-hr LC 50	Tarzwel and Henderson (1960); hardness 20mg/L
Fathead minnow	Uranyl	96-hr LC 50	Tarzwel and Henderson (1960); hardness 20mg/L
Brook trout	5.5	96-hr LC 50	Parkhurst et al. (1984); hardness 35 mg/L
Brook trout	23	96-hr LC 50	Parkhurst et al. (1984); hardness 208 mg/L
Bonytail 31d, 115d, 207d	Uranyl nitrate	96-hr LC 50	Hamilton (1995), hardness 233-330mg/L
Razorback sucker 31d, 115d, 207d	Uranyl nitrate	96-hr LC 50	Hamilton (1995), hardness 233-330mg/L
Colorado squawfish 31d, 115d, 207d	Uranyl nitrate	96-hr LC 50	Hamilton (1995); hardness 233-330mg/L
Fathead minnow	135	96-hr LC 50	Tarzwel and Henderson (1960); hardness 400mg/L

Not Shaded: No observed effects; Shaded: Observed Effects

**Table 9-2 Safe and Toxic Concentrations of Nitrate in Water**

Species	Common name	Nitrate (nm)	Effect	Reference
<b>Amphibian- water</b>				
<i>Pseudacris triseriata</i>	Chorus frog	5	NOAEL	Hecnar 1991
<i>Rana pipiens</i>	Leopard frog	5	NOAEL	Hecnar 1991
<i>Rana clamitans</i>	Green frog	10	NOAEL	Hecnar 1991
<i>Bufo americanus</i>	American toad	13.6-39.3	LC50	Hecnar 1991
<i>Pseudacris triseriata</i>	Chorus frog	17	LC50	Hecnar 1991
<i>Rana pipiens</i>	Leopard frog	22.6	LC50	Hecnar 1991
<i>Rana clamitans</i>	Green frog	32.4	LC50	Hecnar 1991
<b>Invertebrate- water</b>				
<i>Hydropsyche occidentalis</i>	Caddisfly	1.4-2.2	NOAEL	Camargo and Ward 1995
<i>Cheumatopsyche pettiti</i>	Caddisfly	2.4-3.5	NOAEL	Camargo and Ward 1995
<i>Hydropsyche occidentalis</i>	Caddisfly	65.5-183.5	LC50	Camargo and Ward 1992
<i>Cheumatopsyche pettiti</i>	Caddisfly	106.5-210	LC50	Camargo and Ward 1992
<b>Fish- water</b>				
Salmonids	Trout and salmon	100	No effect	Meade 1974
<i>Monacanthus hispidus</i>	planehead filefish	573	NOAEL	Pierce et al. 1993
<i>Raja eglanteria</i>	clearnose skate	>960	NOAEL	Pierce et al. 1993
<i>Trachinotus carolinus</i>	Florida pompano	1000	NOAEL	Pierce et al. 1993
<i>Centropristis striata</i>	black sea bass	2400	NOAEL	Pierce et al. 1993
<i>Pomacentrus leucostriatus</i>	beaugregory	>3000	NOAEL	Pierce et al. 1993
<i>Oncorhynchus tshawytscha</i>	Chinook salmon	5000	LC50	Westin (1973) in Meade (1974)

Not Shaded. No observed effects; Shaded. Observed Effects

**Table 9-3 ARARs and Established Protective Values**

	MCL	Acute NRWQ CNR WQC	Chronic NRWQ CNR WQC	OK raw water criteria	OK ANC	OK CNC	Protective criteria for humans	Protective criteria for aquatic biota
Arsenic	10 ppb	340 ppb	150 ppb	40 ppb	340 ppb	150 ppb	10 ppb	150 ppb
Uranium	30 ppb	NA	NA	NA	NA	NA	30 ppb	1000 ppb
Nitrate	10 ppm	NA	NA	10 ppm	NA	NA	10 ppm	10 ppm